

Cite this: *J. Mater. Chem. B*,  
2024, 12, 9111Received 8th April 2024,  
Accepted 11th August 2024

DOI: 10.1039/d4tb00769g

rsc.li/materials-b

## Nanozymes in cancer immunotherapy: metabolic disruption and therapeutic synergy

Xiangrui Xu,<sup>a</sup> Yaowen Zhang,<sup>a</sup> Chijun Meng,<sup>a</sup> Wenzhuo Zheng,<sup>a</sup> Lingfeng Wang,<sup>a</sup> Chenyi Zhao<sup>a</sup> and Feng Luo<sup>a,b\*</sup>

Over the past decade, there has been a growing emphasis on investigating the role of immunotherapy in cancer treatment. However, it faces challenges such as limited efficacy, a diminished response rate, and serious adverse effects. Nanozymes, a subset of nanomaterials, demonstrate boundless potential in cancer catalytic therapy for their tunable activity, enhanced stability, and cost-effectiveness. By selectively targeting the metabolic vulnerabilities of tumors, they can effectively intensify the destruction of tumor cells and promote the release of antigenic substances, thereby eliciting immune clearance responses and impeding tumor progression. Combined with other therapies, they synergistically enhance the efficacy of immunotherapy. Hence, a large number of metabolism-regulating nanozymes with synergistic immunotherapeutic effects have been developed. This review summarizes recent advancements in cancer immunotherapy facilitated by nanozymes, focusing on engineering nanozymes to potentiate antitumor immune responses by disturbing tumor metabolism and performing synergistic treatment. The challenges and prospects in this field are outlined. We aim to provide guidance for nanozyme-mediated immunotherapy and pave the way for achieving durable tumor eradication.

### 1. Introduction

As one of the primary causes of mortality, cancer persists as a prominent global public health concern and places a significant burden on social finance. Therefore, tumor treatment remains a challenging and critical focus of medical research. Common treatment methods for cancer include surgery, radiotherapy (RT), and chemotherapy (CT), which exhibit a favorable

<sup>a</sup> State Key Laboratory of Oral Diseases & National Center for Stomatology & National Clinical Research Center for Oral Diseases, West China Hospital of Stomatology, Sichuan University, Chengdu 610041, Sichuan, China

<sup>b</sup> Department of Prosthodontics, West China School of Stomatology, Sichuan University, No. 14, Section 3, Renmin Nanlu, Chengdu 610041, China.  
E-mail: luofeng0122@scu.edu.cn; Fax: 86-28-85503474;  
Tel: +86 28 85503671/13488904276



Xiangrui Xu

Xiangrui Xu is pursuing his undergraduate degree at the West China School of Stomatology, Sichuan University. As a member of the State Key Laboratory of Oral Diseases, his current research interests focus on biomaterials regulating tumor metabolism and nanotechnology-based cancer immunotherapy.



Feng Luo

Dr Feng Luo works at the West China School of Stomatology, Sichuan University. Dr Luo received two doctorates from West China School of Stomatology, Sichuan University, and Tohoku University, Japan, respectively, and completed postdoctoral research at West China School of Stomatology, Sichuan University. Currently, his research is to explore the role and mechanism of NPs in treating neuroinflammation, investigate the role and mechanism of drug delivery systems in bone tissue engineering, and elucidate the properties and development of the functionality of new dental materials.



direct cytotoxic effect on tumors. However, they continue to face significant challenges posed by high tumor recurrence and metastasis rates. As such, it is necessary to explore alternative and more effective approaches to impede tumor progression.

In recent years, immunotherapy has garnered significant attention as a novel cancer treatment strategy due to its unique approach of harnessing the body's immune system to target and destroy cancer cells.<sup>1</sup> Unlike traditional cancer treatment which directly targets cancer cells, immunotherapy works by stimulating the patient's immune system to recognize and attack cancer cells while sparing normal, healthy cells, reducing the risk of side effects. Besides, immunotherapy can create a sustained immune response, providing long-term protection against cancer recurrence. Moreover, emerging cancer immunotherapies, such as cytokine therapy, immune checkpoint blockade (ICB), and adoptive cell transfer (ACT), have exhibited favorable therapeutic effects in clinical trials.<sup>2,3</sup> However, there are still some obstacles on the way to their clinical application. For example, the efficacy of cytokine therapy remains limited for "cold" tumors characterized by insufficient immunogenicity, which may limit immunotherapy to an adjuvant treatment option rather than a first-line therapy.<sup>4</sup> ICB can lead to immune-related adverse events (irAEs), and the clinical response rate of monomodal ICB is relatively low.<sup>5,6</sup> Therefore, it is of great importance to combine other treatment modalities to further enhance immunotherapeutic efficacy and minimize the occurrence of side effects.

The integration of nanotechnology and immunotherapy represents a current research trend in cancer treatment due to the potential synergistic benefits and reduced side effects.<sup>7</sup> Nanotechnology facilitates precise design and delivery of immunotherapeutic agents, enhancing their pharmacokinetics and bioavailability for efficient targeting of cancer cells. It also enables the development of multifunctional nanocarriers, allowing for combination therapies that address multiple facets of cancer progression simultaneously. This personalized and targeted approach holds promise in advancing cancer treatment by improving overall treatment outcomes.<sup>8</sup> Tumor cells undergo metabolic reprogramming to adapt to the dynamic metabolic microenvironment, which involves the regulation of substances such as glucose and amino acids. These metabolic processes affect the immunogenicity of tumor cells, thus impacting the effectiveness of immunotherapy. However, they also represent vulnerable targets for cancer treatment. Therefore, based on the metabolic variances between tumor cells and normal cells, employing efficient nanomaterials to target tumor metabolism emerges as a promising anticancer strategy.<sup>9</sup>

Nanozymes are a subset of nanomaterials that exhibit catalytic properties. In comparison to natural enzymes, they offer simplified preparation processes, heightened catalytic activity, and enhanced enzyme stability.<sup>10</sup> They primarily mimic oxidoreductases and hydrolases, exhibiting responsiveness to the tumor microenvironment (TME) and the ability to precisely modulate sensitive metabolic targets at the tumor site.<sup>11</sup> For instance, nanozymes mimicking oxidoreductases induce oxidative stress within tumor cells and trigger the generation of

reactive metabolites.<sup>12</sup> Conversely, nanozymes mimicking hydrolase activities can hydrolyze  $\text{H}_2\text{O}_2$  to produce  $\text{O}_2$ , alleviating the hypoxic conditions in tumor tissues.<sup>13</sup> Both catalytic products further influence tumor metabolism. Additionally, certain nanozymes can undergo surface modifications incorporating bioactive compounds for therapeutic drug delivery. They can synergistically interact with photosensitizers, sonosensitizers, immunomodulatory agents, and initiate combination therapies upon external stimuli, thus surpassing the constraints of immunotherapy and fundamentally transforming cancer treatment. For example, nanoparticles formed by encapsulating polyethylene glycol (PEG) derivatives can release drugs in a responsive manner in the acidic TME.<sup>14</sup> Similarly, metal-organic framework (MOF)-based nanozymes are utilized for therapeutic interventions due to their inherent drug-loading capabilities.<sup>15</sup> This showcases the tremendous potential of nanozymes as next-generation immunotherapeutic agents. Nanozymes are typically engineered to integrate with tumor-targeting molecules or designed to be responsive to the TME. This approach enhances the specificity and targeting capabilities towards cancer cells. Moreover, imaging techniques are utilized to guide the precise localization of nanozymes *in vivo*, minimizing potential side effects on normal cells. Consequently, nanozymes efficiently kill tumor cells through metabolic intervention and reprogram the levels of bioactive metabolites in TME, thus activating immune cells in the TME. Although these treatment methods have achieved considerable results, there are few reports on the multiple roles of nanozymes in cancer immunotherapy and their synergistic therapeutic mechanisms by intervening in tumor metabolism and mediating combination therapies.

In this review, we present a comprehensive summary of the recent research progress in utilizing nanozymes to achieve synergistic cancer immunotherapy strategies (Fig. 1). We commence with the mechanisms of cancer immunotherapy and the roles played by nanozymes in it. Subsequently, the latest advancements in utilizing nanozymes for immune modulation are critically reviewed, with a particular stress on their applications in targeting tumor metabolism and enabling combination immunotherapy. Furthermore, the prospects and challenges associated with employing nanozymes for metabolic immunotherapy are deliberated upon. The primary objective of this review is to deepen the understanding of cancer metabolic therapy mediated by nanozymes, impart novel insights to the readers, and promote further innovations and clinical applications of immunomodulatory nanozymes.

## 2. Mechanisms of cancer immunotherapy

Compared to conventional cancer therapies, immunotherapy has the capability to reshape the tumor immune microenvironment, thereby achieving durable tumor clearance. Below, we introduce the current three main types of immunotherapies



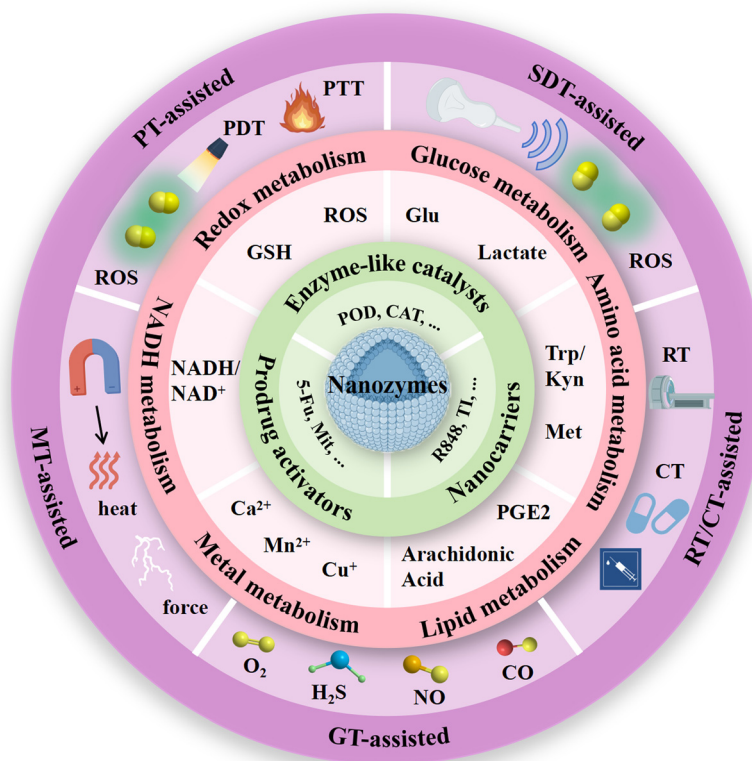


Fig. 1 Mechanisms of nanozyme-based treatment strategies for enhanced cancer immunotherapy (By Figdraw). PT, phototherapy; PTT, photothermal therapy; PDT, photodynamic therapy; SDT, sonodynamic therapy; RT, radiotherapy; CT, chemotherapy; GT, gas therapy; MT, magnetic therapy.

and their mechanisms, including immunogenic cell death (ICD), macrophage reprogramming, and ICB.

### 2.1. ICD

ICD represents a novel mode of cell death characterized by the expression or release of DAMPs from deceased cancer cells to induce antitumor immune responses. During ICD, early surface exposure of calreticulin (CRT) serves as a “eat me” signal promoting dendritic cell (DC) maturation. Then, late-stage release of HMGB1 specifically binds Toll-like receptor 4 on DC surfaces to optimally present antigens from dying tumor cells.<sup>16–18</sup> Subsequently, DCs mediate enhanced recruitment of immune cells and antigen presentation, initiating immune cells such as natural killer cells (NKs) and cytotoxic T lymphocytes (CTLs) to disrupt tumor cells.<sup>19–24</sup> Recent studies indicate a close association between endoplasmic reticulum (ER) stress and highly immunogenic ICD induction.<sup>25</sup> ER stress occurs due to disruptions in normal protein folding within the ER lumen caused by external disturbances such as fluctuations in  $\text{Ca}^{2+}$  levels, changes in redox status and nutrient deficiencies.<sup>26,27</sup> The increased immunogenicity resulting from ICD is primarily attributed to the surface exposure of CRT protein from the ER, which is a direct consequence of ER stress. The process of ICD can alter the TME, diminish the influence of immunosuppressive cells like regulatory T cells (Tregs), myeloid-derived suppressor cells (MDSCs), etc., thereby rendering tumors more

susceptible to immunotherapeutic interventions.<sup>20,28</sup> Additionally, it enhances T cell infiltration into tumor tissues, facilitating the activation of tumor-specific T cell-mediated immune responses.<sup>29</sup> ICD can be triggered by various inducers, including certain nanomaterials, chemotherapeutic drugs, RT, photodynamic therapy (PDT), and specific biologic agents, etc.<sup>30</sup> These strategies not only directly participate in specific catalytic reactions to promote tumor cell death but also enhance ICD to activate and bolster immune responses within the TME, offering a novel strategy for cancer therapy.

### 2.2. Macrophage reprogramming

Tumor-associated macrophages (TAMs) exhibit M1 and M2 phenotypes within the TME. TAMs exist in a sustained transitional state between M1 and M2 types, with the proportion of each cell type dependent on signaling types and concentrations in the TME.<sup>31,32</sup> M1 macrophages are typically considered immunostimulatory, secreting inflammatory cytokines such as interleukin-6 (IL-6), interleukin-12 (IL-12), and tumor necrosis factor- $\alpha$  (TNF- $\alpha$ ) upon activation. These mechanisms not only contribute to enhanced phagocytic activity for identifying and eliminating malignant tumor cells, but also promoting recruitment and activation of other immune cells such as CTLs through antigen presentation, thereby initiating both innate and adaptive immunity. Conversely, during tumor progression, M2 macrophages predominantly promote tumorigenesis. They



achieve this by secreting immunosuppressive factors like IL-10 and TGF- $\beta$ , inhibiting T cell activation and function, thereby facilitating immune escape within the TME and suppressing effective antitumor immunotherapy.<sup>33</sup> The activation-induced secretion of immunosuppressive molecules by M2-TAMs can further promote metabolic alterations within tumor cells.<sup>34</sup> Imbalance in the M1/M2 phenotype ratio of TAMs within tumors often correlates with tumor deterioration and poor prognosis. Therefore, strategies aimed at reprogramming TAMs from a tumor-promoting M2 phenotype to a tumor-inhibiting M1 phenotype through pharmacological or other interventions could potentially serve as therapeutic avenues to modulate the tumor immune microenvironment.<sup>35,36</sup> Utilizing the endocytic properties of macrophages, employing nanoparticles containing toll-like receptor (TLR) agonists or tumor peptides can promote macrophage re-education and enhance antitumor immunity.<sup>37</sup> Recent evidence also suggests that nanozymes capable of generating reactive oxygen species (ROS) and/or producing O<sub>2</sub> can serve as effective immune response initiators and enhancers, facilitating the reprogramming of M2-TAMs towards an M1 phenotype within tumors to attack cancer cells, while sparing normal cells' functions.<sup>38</sup> What's more, emerging evidence indicates metabolic changes within TAMs themselves, including glucose metabolism.<sup>39</sup> Metabolic alterations serve as the primary driving force for macrophage modulation in the TME and hold promising potential for immunotherapeutic strategies in cancer treatment.<sup>40</sup> Therefore, using nanomaterials with catalytic properties to regulate the metabolic reactions in TME may hold potential in effectively achieving macrophage reprogramming.

### 2.3. ICB

ICBs represent a prominent class of immunotherapeutic agents in oncology.<sup>41</sup> They operate by blocking the interaction between immune checkpoints and their ligands, thereby releasing immune cell suppression and enhancing the body's immune response against tumors. ICB primarily includes antibody therapies targeting cytotoxic T-lymphocyte antigen-4 (CTLA-4) and programmed death-ligand 1 (PD-L1)/programmed death-1(PD-1). CTLA-4, predominantly expressed on activated T cell surfaces, competitively binds with the B7 molecule against CD28, thereby inhibiting T cell activation. PD-1, an inhibitory receptor expressed on T cell surfaces, reduces T cell proliferation and function upon binding with its ligand PD-L1. By disrupting these inhibitory signals, ICB restores antitumor activity in T cells. The efficacy of ICB therapy has been notably demonstrated in various malignancies such as melanoma and non-small cell lung cancer.<sup>42</sup> In clinical settings, inhibitors targeting CTLA-4, PD-1, and PD-L1 have proven successful, with several ICIs currently under preclinical or clinical investigation. Despite bringing new hope to many cancer patients, ICB therapy is constrained by limitations and potential adverse effects. For instance, it is effective in only a subset of patients and may lead to irAEs, necessitating treatment interruption.<sup>43</sup> The characteristics and mechanisms of these adverse reactions remain incompletely understood but are likely associated with

aberrant T cell activity, humoral immune systems, and B cells. To enhance the therapeutic efficacy of ICB and mitigate toxicity, researchers are exploring various combination therapeutic strategies. Among them, the coupling of nanomaterials with ICB offers a novel perspective and approach to cancer treatment, aiming to activate and enhance immune responses, thereby potentially improving the efficiency and selectivity of cancer therapy.<sup>44</sup>

## 3. Roles of nanozymes in cancer immunotherapy

A substantial body of research has elucidated the distinctive roles of nanozymes in cancer immunotherapy. As multifunctional nanomaterials, nanozymes not only exhibit the enzymatic catalytic activity, but also serve as nanocarriers and prodrug activators to develop a more efficient enzyme-catalytic treatment strategy. This section systematically discusses the mechanisms of nanozymes in cancer immunotherapy from three perspectives: the role of nanozymes as enzyme-like catalysts, nanocarriers and prodrug activators.

### 3.1. Enzyme-like catalysts

The mechanisms by which nanozymes exert their roles in antitumor therapy are largely determined by their enzyme-like activities. Nanozymes can manipulate the redox reactions within the tumor cells, thereby eliciting localized therapeutic effects.<sup>45</sup> This property is conducive to targeted tumor treatment. By modulating the redox state of the TME, nanozymes can influence the levels of active metabolites and induce tumor cell ICD, thereby further affecting T cell infiltration and macrophage phenotypes, promoting activation of the endogenous immune system against tumors.<sup>46</sup> The enzymatic activity of nanozymes can be regulated not only by controlling their composition, morphology, and surface properties but also by adjusting parameters such as pH, temperature, light, magnetic fields, or other external stimuli.<sup>47</sup> This capability enhances their effectiveness in cancer therapy. The oxidoreductase-mimicking nanozymes, including peroxidases (PODs), oxidases (OXDs), catalases (CATs), and superoxide dismutases (SODs), have been investigated for their potential applications in cancer immunotherapy.

**3.1.1. POD-like properties.** PODs catalyze the oxidation of substrates in the existence of H<sub>2</sub>O<sub>2</sub> or organic peroxides. Typically, nanomaterials containing transition metals such as Fe, Cu, Zn, Co, Mo, Pt, and Pd can function as POD-like nanozymes.<sup>48</sup> Non-metallic elemental-based nanostructures, particularly carbon-based nanomaterials, can also serve as POD mimics.<sup>49,50</sup> Nanozymes exhibiting POD-like activity can mediate chemodynamic therapy (CDT). They utilize Fenton/Fenton-like reactions to enhance the production of  $\bullet$ OH radicals at tumor sites, through which H<sub>2</sub>O<sub>2</sub> is converted into highly toxic  $\bullet$ OH, triggering oxidative stress in cancer cells. This could potentially cause damage to organelles such as mitochondria, as well as macromolecules like proteins and lipids, thereby





influencing the biological metabolic processes such as tricarboxylic acid (TCA) cycle and oxidative phosphorylation (OXPHOS), consequently instigating tumor cell ICD and fostering cancer immunotherapy. Furthermore, ROS play an indispensable role in regulating the M2/M1 ratio towards the M1 phenotype by initiating signaling pathways in M1 macrophages. Researchers designed 1T2H-MoS<sub>2</sub> nanozymes through phase transformation *via* a molten sodium reduction reaction.<sup>51</sup> The significant electronegativity difference between Na and S sites, facilitated by embedded Na atoms, enhanced electron transfer and induced sulfur vacancies (SV) and the 1T phase formation, thus inducing up-regulation of POD-like activity. Nanozymes accumulated at the tumor site, generating extracellular •OH that facilitate the conversion of M2-like TAMs to M1 phenotype within the tumor, thereby inhibiting tumor growth. This resulted in the reprogramming of the immunosuppressive TME.

Glutathione peroxidase (GPX)-like nanozymes are employed in cancer therapy as auxiliary tools to deplete glutathione (GSH), thereby mitigating the loss of reactive oxygen species (ROS). Based on their active centers, prevalent GPX-like nanozymes can be categorized into selenium-based, copper-based, vanadium-based, and manganese-based nanozymes, *etc.*<sup>52</sup> Atom doping represents an effective strategy for modulating the enzymatic activity of nanozymes, enhancing their catalytic performance by altering their electronic structure and catalytic properties. The impact on activity varies with different types of doped atoms.<sup>53</sup> For example, Mei *et al.* innovatively developed a copper-doped PPy synthesis method using copper chloride as a replacement for ferric chloride.<sup>54</sup> Upon laser irradiation, CuP exhibited significant thermal-enhanced enzymatic activity, including CAT, POD, and GPX, to specifically promote O<sub>2</sub> and •OH amplification but GSH reduction in TME, thereby causing irreversible oxidative stress damage to cancer cells and reversing the immunosuppressive microenvironment. Apart from doping metal ions to alter enzyme activity, catalytic reactions primarily occur on the surface of nanomaterials, where nanozymes of different sizes and shapes often exhibit varied catalytic activities. Nanozymes with smaller dimensions demonstrate excellent catalytic performance due to their higher surface area-to-volume ratio, tending to expose more enzymatically active sites.<sup>55</sup> Recent literature also highlights the use of various nanozyme morphologies such as nanospheres, nanoflowers, nanoplates, and nanorods.<sup>56–58</sup> For instance, the POD-like activity of Fe<sub>3</sub>O<sub>4</sub> nanocrystals varies across spherical, octahedral, and triangular plate morphologies, reflecting the dependency of the enzymatic activity on the distinct exposures of hematite nanocrystal facets.<sup>59</sup>

**3.1.2. OXD-like properties.** OXDs are a family of enzymes that catalyze the substrate oxidation using O<sub>2</sub> as the electron acceptor, which is then reduced to H<sub>2</sub>O<sub>2</sub> or H<sub>2</sub>O. As an OXD is more active at low pHs, the weakly acidic TME enables it to better exert its catalytic activity.<sup>60</sup> Nanoceria is a commonly used OXD-like nanozyme. Its OXD-like activity is attributed to the redox transformation between Ce<sup>3+</sup> and Ce<sup>4+</sup> oxidation states, along with the generation of associated superoxide

radicals.<sup>61</sup> Similarly, various ultrafine nanomaterials based on noble metals also exhibit OXD-like activity.<sup>62</sup> The OXD-like activity of a nanozyme is frequently utilized to supplement endogenous H<sub>2</sub>O<sub>2</sub>, thereby promoting POD-mediated Fenton/Fenton-like reactions. For example, Yang *et al.* wrapped multienzyme-like MnO<sub>x</sub> with tumor cell membranes to obtain a tumor-targeted nanozyme.<sup>63</sup> Due to the presence of mixed-valence states of Mn<sup>2+</sup> and Mn<sup>3+</sup>, MnO<sub>x</sub> exhibited diverse enzyme-like activities (CAT, POD, OXD), thus generating a large amount of ROS and alleviating tumor hypoxia, reshaping tumor immune microenvironment. Glucose oxidase (GOx)-like nanozymes facilitate the conversion of glucose into endogenous H<sub>2</sub>O<sub>2</sub>, serving not only as a method to sever the nutrient supply to tumors but also as an efficient auxiliary measure for Fenton therapy.<sup>64</sup> Additionally, glutathione peroxidase (GSHOx)-like nanozymes induce toxic accumulation of ROS within tumor cells by depleting endogenous GSH, potentially leading to ferroptosis. Apart from the above, certain nanozymes also exhibit NADH oxidase (NOX)-like activity, demonstrating the potential to inhibit ATP generation within tumor cells and thereby promote cell death.

What's more, lactate oxidase (LOx)-like nanozymes reverse the acidic environment of the TME by consuming lactate, thereby reshaping the immunosuppressive TME.<sup>65</sup> However, current research on nanozymes with LOx-like activity is relatively sparse. Coordination engineering is regarded as an effective approach to modulate the local electronic structure by precisely controlling the number or types of ligand atoms.<sup>66</sup> Recent studies indicate that coordinating heterocyclic N with metals enhances the catalytic activity of carbon-supported metal *x*-N<sub>y</sub> (M<sub>x</sub>N<sub>y</sub>) materials.<sup>67,68</sup> Various strategies primarily focus on manipulating the charge density of metal centers by controlling the N coordination number, akin to active sites in natural metalloenzymes.<sup>69</sup> Understanding the impact of metal stoichiometry on N-active site environments and local coordination electronic configurations is crucial. Liu *et al.* recently reported a new LOx-like nanozyme (Co<sub>4</sub>N/C NE).<sup>70</sup> By modulating the coordination number of metal atoms, they achieved an optimal electronic configuration between the nitrogen atoms in the active center and their ligands, endowing Co<sub>4</sub>N/C NE with superior LOx mimic activity.

**3.1.3. CAT-like properties.** CATs are typical antioxidant enzymes that exist in almost all organisms exposed to oxygen and accelerate the decomposition of H<sub>2</sub>O<sub>2</sub> into H<sub>2</sub>O and O<sub>2</sub>. As a protective mechanism against ROS-induced oxidative damage, CATs may effectively counteract hypoxia during cancer treatment, thus allowing activation of immune defense mechanisms within tumors. Nanozymes with CAT-like activity have been utilized as sensitizers for cancer treatment through RT, CT, PDT and sonodynamic therapy (SDT).<sup>71–76</sup> Major CAT-mimic nanozymes for cancer therapy these years are principally derived from metallic materials, encompassing metal-based, metal oxide-based, and metal sulfide-based nanozymes.<sup>77</sup> For example, a chiral nanozyme (MoS<sub>2</sub>/CoS<sub>2</sub>) with both POD-like and CAT-like activities that possess better pharmacokinetics and tumor-specific targeting ability has been designed



recently.<sup>78</sup> According to extensive research, surface modifications, including surface coatings and modifications *via* macromolecules or small molecules, also impact the catalytic capabilities of nanozymes.<sup>79,80</sup> MoS<sub>2</sub>/CoS<sub>2</sub> nanozymes modified with chiral ligands exhibit enhanced dispersion stability, thereby promoting their POD-like and CAT-like activities. The substantial generation of ROS in conjunction with amplified supply of oxygen, significantly augmented the reprogramming of TAMs for cancer immunotherapy. In addition, certain non-metallic materials may also exhibit CAT-like activity. In another study, bubbles were observed when incubating graphene oxide quantum dots with H<sub>2</sub>O<sub>2</sub>, indicating that graphene oxide quantum dots also exhibit catalytic decomposition of H<sub>2</sub>O<sub>2</sub> to generate O<sub>2</sub> similar to CATs.<sup>81</sup>

**3.1.4. SOD-like properties.** Oxygen metabolism produces superoxide radicals, which cause severe oxidative damage to normal cells when they build up. Therefore, normal cells need to be regularly protected from damage caused by superoxide radicals. SODs are important antioxidant enzymes that convert superoxide radicals into O<sub>2</sub> and H<sub>2</sub>O<sub>2</sub>, thereby preventing oxidative stress in the body. At present, cerium oxide nanoparticles are the most commonly employed nanozymes exhibiting SOD-like activity.<sup>82</sup> It has been substantiated that SOD-like nanozymes can augment their catalytic activity in collaboration with POD-like nanozymes through the generation of H<sub>2</sub>O<sub>2</sub>.<sup>83</sup> However, research on the anticancer effects of SOD-like nanozymes through the clearance of ROS is relatively scarce. As we know, ROS can not only mediate immunosuppression induced by MDSCs, but also trigger the differentiation and polarization of M2-TAMs.<sup>84,85</sup> Based on these findings, Guo *et al.* composed a Zr–CeO nanozyme with an enhanced ratio of Ce<sup>3+</sup>/Ce<sup>4+</sup> *via* Zr<sup>4+</sup> doping, leading to its enhanced SOD-like and CAT-like activities.<sup>86</sup> Induction of intracellular ROS clearance by Zr–CeO reduced the levels of arginase 1 and iNOS within MDSCs, thereby promoting T cell proliferation. Additionally, it hindered M2 polarization by inhibiting the ERK and STAT3 pathways.

### 3.2. Nanocarriers

Due to their excellent controllable surface modification potential, nanozymes may also act as nanocarriers in cancer therapy. Through rational design, nanozymes can achieve targeted delivery of therapeutic agents, while concurrently enabling controlled release of the therapeutic agents, thereby enhancing treatment efficacy.<sup>87</sup>

Nanozymes can serve as carriers for immunomodulators to regulate the function of immune cells, such as activating T cells and inhibiting Tregs, which enhance the recognition and clearance abilities of immune system against tumor cells.<sup>88</sup> For instance, TLR agonists, such as resiquimod (R848) and imiquimod (R837), as well as inhibitory molecules, including TGF- $\beta$  inhibitors (TI) and indoleamine 2,3-dioxygenase (IDO) inhibitors, have been utilized.<sup>89–91</sup> The design of these nanozyme-based nanoplatfoms typically involves the use of highly biocompatible carrier materials, such as MOFs, which encapsulate the therapeutic payloads within their structure or on their surface. These materials exhibit unique characteristics

that are highly beneficial for therapeutic applications, such as high surface area and tunable surface properties, enabling uniform dispersion and loading of active antitumor drugs, as well as stimulus-responsive behavior. For instance, a photo-triggered nanozyme (Fe-MOF-RP) was constructed as both a core catalytic component for tumor ablation and a biocompatible delivery vehicle for immune stimulants.<sup>92</sup> On one hand, it catalyzed the decomposition of H<sub>2</sub>O<sub>2</sub> within tumors, generating O<sub>2</sub> to enhance PDT. The induced ferroptosis synergized with PDT, prompting tumor cells to release tumor-associated antigens (TAAs) and inducing ICD. On the other hand, light-triggered R848 adjuvant released on demand stimulated DC maturation and promoted the conversion of the tumor's M2 phenotype to effector M1 macrophages. Auxiliary materials such as serum albumin (SA) and phase-change materials may be employed to modify nanozymes, preventing cargo leakage and selectively activating immunomodulation in the desired environment.<sup>93,94</sup> These kinds of nanozymes can effectively shield therapeutic agents from external environmental influences and can be engineered to respond to specific stimuli (*e.g.*, pH, temperature, chemical substances) for drug release.<sup>95,96</sup> Furthermore, by loading chemotherapeutic agents or photosensitizers/sonosensitizers, nanozyme-based catalytic therapy can be synergized with other modalities for multimodal integrated cancer treatment.<sup>97,98</sup> The loading of imaging agents also contributes to guiding nano-based drug delivery, enabling the monitoring of site-specific drug accumulation, thereby achieving therapeutic visualization and significantly enhancing the accuracy of cancer treatment.<sup>99</sup>

The surface of nanozymes can be functionalized with specific molecules,<sup>100</sup> such as antibodies, oligonucleotides, or ligands, which can bind to target molecules (*e.g.*, specific proteins on the surface of tumor cells), thereby preventing off-target effects and enhancing the accumulation of nanozymes in the targeted area. For instance, mannose (Man) can bind with mannose receptors highly expressed on the surface of M2 macrophages to achieve precise immunomodulation targeting TAMs.<sup>101</sup> Apart from above, subcellular targeting in cancer therapy has become a hot topic of current research.<sup>102–104</sup> For instance, loading subcellular targeting molecules for the ER or mitochondria on nanozymes can precisely accumulate therapeutic drugs in organelles, greatly reducing the threshold dosage of therapeutic drugs and significantly promoting precise tumor therapy mediated by endogenous stimuli. Additionally, because of their internal characters, nanozymes can also be under precise control of external force fields such as magnetic fields to improve the treatment accuracy and efficiency.<sup>105</sup>

### 3.3. Prodrug activators

The enzyme-like activities of nanozymes not only directly mediate damage to cancer cells, but also can be utilized in the activation strategy of chemotherapeutic prodrugs. By activating non-toxic prodrugs to release cytotoxic metabolites, indirect cancer treatment is achieved. Compared to natural enzymes, nanozymes integrate the unique properties of both



natural enzymes and nanomaterials, thus the prodrug activation strategy mediated by nanozymes holds better prospects. In 2020, researchers initially introduced a prodrug activation system predicated on nanozymes, harnessing the POD-like activity of the nanozyme to proficiently initiate the prodrug IAA, thereby instigating ROS storms and inducing mitochondrial apoptosis in tumor cells.<sup>106</sup> In recent years, the rise of bioorthogonal chemistry has greatly propelled the evolution of prodrug strategies.<sup>107</sup> Bioorthogonal chemistry refers to chemical reactions that occur within complex biological environments without interfering with endogenous biochemical reactions. In contrast to biomimetic nanozymes directly activating substrates present in the TME, bioorthogonal nanozymes selectively activate exogenously added prodrugs in the tumor region, achieving one-to-one reactions and improving the precision of cancer treatment while significantly reducing off-target effects.<sup>108–110</sup> Currently, the activation capabilities of bioorthogonal nanozymes on a range of chemotherapeutic agents, including 5-fluorouracil (5-FU),<sup>111,112</sup> and mitoxantrone (Mit),<sup>113</sup> have been investigated. *In vivo* experiments have demonstrated their favorable antitumor properties. Furthermore, bioorthogonal nanozymes can be employed to locally activate immunomodulatory drugs, holding significant potential in cancer immunotherapy. Researchers have developed a palladium (Pd)-based bioorthogonal nanozyme (MoS<sub>2</sub>@Pd-Man) capable of catalyzing the synthesis of the FDA-approved TAM repolarizing drug vorinostat.<sup>114</sup> Surface modification with Man conferred targeting ability to M2 macrophages that overexpress the mannose receptor (CD206). The polarization of macrophages from M2 to M1 led to enhanced

catalytic Fenton reaction by MoS<sub>2</sub>@Pd, generating H<sub>2</sub>O<sub>2</sub> that promote ROS-mediated cancer cell eradication. This marked the inaugural application of bioorthogonal nanozymes in cancer immunotherapy. In another study, Pd nanozymes were encapsulated within a monolayer of gold nanoparticles to generate bioorthogonal nanozymes, which avoided nonspecific immunogenicity induced by hydrophobic catalysts.<sup>115</sup> These nanozymes are internalized by macrophages *via* endocytosis and subsequently activate R837 *in situ* near lysosomal TLR7/8 receptors, promoting the reprogramming of macrophages from an M2-like phenotype to an M1-like phenotype. This type of design offered a biocompatible method for future cancer immunotherapy applications.

#### 4. Nanozymes for tumor metabolic disruption

Cancer is considered a genomic disease, but it can also be viewed as a metabolic or immune disorder.<sup>116,117</sup> It is worth noting that tumor cells not only go through metabolic reprogramming, but also shape the metabolically hostile TME and modulate the survival and functions of immune cells through metabolic crosstalk.<sup>118</sup> Ultimately, this favors immune evasion and tumor progression. Continuous increase in ROS within the TME is implicated in promoting tumor growth, dissemination, and metastasis, whereas excessive ROS levels exert cytotoxic effects through non-specific protein oxidation, altered reaction patterns, and biomolecular damage, leading to malignant cell apoptosis and necrosis.<sup>119</sup> Typically, cells possess various anti-oxidant systems to defend against ROS damage (Fig. 2). For

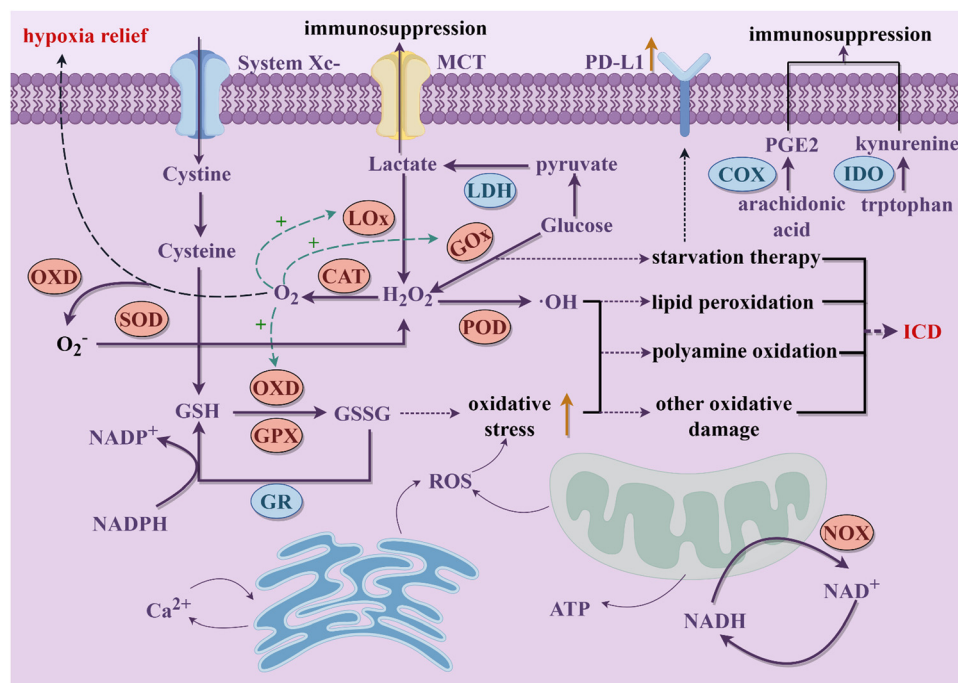


Fig. 2 The schematic diagram of the potential interference of nanozymes on the main metabolic processes in tumor cells discussed in this review to activate immune responses (By Figdraw).



instance, SODs convert  $O_2^-$  to  $H_2O_2$ , subsequently metabolized to water by enzymes including CAT and GPX. GSH, another crucial intracellular antioxidant, modulates redox homeostasis by controlling ROS levels in metabolic reactions, thereby attenuating ROS-induced oxidative stress.<sup>120</sup> Additionally, the unique aerobic glycolysis effect of tumor cells enhances their dependency on glucose, leading to lactate accumulation in the TME, thereby augmenting immune suppression. Tumor cells also disrupt cellular immunity by competitively consuming glucose and certain amino acids like methionine (Met), thereby impairing immune cell function. Metabolites of specific amino acids and lipid molecules, such as tryptophan (Trp) and prostaglandin  $E_2$  ( $PGE_2$ ), also have been shown to activate tumor immune evasion pathways.<sup>121,122</sup> Through the combined actions of numerous metabolic pathways, immune suppression within the tumor tissue intensifies, fostering tumor growth and metastasis.

Cellular metabolic pathways are primarily regulated through interconnected enzymatic reactions. Due to their excellent chemical stability, nanozymes can maintain high catalytic efficiency in harsh environments. Therefore, they hold promise as potential tools for disrupting tumor cell metabolism (Fig. 2). Excessive  $H_2O_2$  within tumor cells, under the actions of nanozymes mimicking CATs and PODs respectively, generates oxygen and highly reactive  $\cdot OH$ . The former not only further promotes enzymatic reactions mediated by other OXDs within tumor cells but also mitigates hypoxia in tumor tissues. The latter mediates a series of oxidative damages to proteins, lipids, and other molecules, ultimately causing tumor cell rupture, releasing intracellular substances, and triggering robust immune clearance responses.<sup>68</sup> Nanozymes simulating OXD and GPX activities catalyze the reduction of intracellular GSH concentration in tumor cells, leading to a relative increase in ROS levels and thereby inducing oxidative stress damage, which synergistically achieves a dual effect with the amplification of ROS.<sup>123</sup> OXD-like nanozymes also disrupt the NADH/NAD<sup>+</sup> cycle equilibrium, suppress ATP production, and lead to

energy depletion and cell death in tumor cells.<sup>124</sup> What's more, nanozymes with LOx and GOx-like activities target tumor cell glucose metabolism, depleting intracellular glucose and reducing lactate accumulation in the TME, thereby enhancing immune responses.<sup>125</sup> Beyond enzyme-like activities, some nanozymes are able to carry inhibitory molecules to suppress related metabolic pathways and restoring immune mechanisms.<sup>126</sup> During catalytic processes, certain nanozymes also exhibit efficient metal ion release capabilities, disrupting tumor cell metabolism by promoting intracellular metal ions overload and thereby inducing immune activation effects. Therapies targeting tumor metabolism mediated by nanozymes can induce ICD of tumor cells and achieve macrophage reprogramming, further increasing infiltration of cytotoxic immune cells and alleviating the immunosuppressive microenvironment in combination with ICB therapy.<sup>127</sup> This section provides a summary of the latest advancements in nanozyme strategies targeting the disruption of redox metabolism, glucose metabolism, amino acid metabolism, lipid metabolism, metal metabolism and NADH metabolism. These strategies synergistically promote innate or acquired antitumor immunity to achieve effective antitumor outcomes.

#### 4.1. Targeting redox metabolism

The metabolic reprogramming of tumor cells induces alterations in their redox metabolism. Nanozymes can intervene and disrupt the redox balance within tumor cells by mimicking various oxidoreductases, thereby eliciting robust immune clearance responses in the body. This section provides a comprehensive review of the application of nanozymes in modulating redox metabolism to induce immune responses (Table 1).

**4.1.1. ROS amplification.** ROS are intrinsic derivatives of molecular oxygen within cells and play a pivotal role in maintaining cellular homeostasis through a cascade of redox reactions within the biological system.<sup>136–138</sup> Due to the accumulation of mutations, metabolic dysregulation, and intricate microenvironmental factors, ROS, particularly  $H_2O_2$ , tends to

Table 1 Representative redox metabolism-regulating nanozymes for cancer immunotherapy

	Nanozyme components	Cargos	Antitumor effects	Models	Ref.
ROS amplification	IMSN	SB-505124	Hypoxia relieving, ROS amplification to promote ferroptosis, and macrophage polarization from M1 to M2	CT26 tumor-bearing Balb/c mice	128
	DA-CQD@Pd	CpGODN	ROS production to induce ICD, TLR 9 activation	Balb/C mice bearing CT26 tumors	129
	HCS-FeCu	—	Mild photothermal amplification and oxidative stress-induced pyroptosis combined with ICB therapy	4T1-Luc breast tumor-bearing mice	130
GSH consumption	ChA CQDs	—	Inducing ferroptosis through consumption of GSH	BALB/c nude mice with HepG2 cells; ICR mice with H22 cells	131
Dual effect	Cu NPs	UCNPs, GOx	Consuming glucose, augmenting ROS accumulation to induce ferroptosis	Bilateral 4T1-tumor-bearing Balb/c mice	132
	Cu-alanine NPs	Cin, GOx	Consuming glucose and inducing ferroptosis	4T1 breast tumor-bearing mice	133
	<i>E. coli</i> -Au@Pt	—	Immune activation effects, ferroptosis induction, in conjunction with CBI therapy	B16-F10 cells implanted nude Balb/C mice; HepG2 cells implanted nude Balb/C mice	134
	$Bi_2Fe_4O_9$ NSs	—	Hypoxia relieving, tumor cell apoptosis and ferroptosis induction	BALB/c mice with 4T1 tumors	135





aberrantly accumulate in tumor tissues at mild to moderate levels to stimulate tumor development.<sup>139</sup> High levels of ROS can inflict irreversible damage on cellular biomolecules, ultimately culminating in cell demise. For example, ROS have been demonstrated to induce mitochondrial damage and ER stress by amplifying intracellular oxidative stress, thereby impeding ATP synthesis and normal functions of intracellular proteins.<sup>140,141</sup> It is widely acknowledged that oxidative stress induced by ROS in the ER is a critical prerequisite for ICD.<sup>25,142</sup> Therefore, promoting ROS generation to specifically kill cancer cells is a promising anticancer treatment strategy.

Various therapeutic strategies for amplifying ROS production have been extensively investigated in current research. For example, Liu *et al.* constructed polyethylene glycolated iron-manganese silicate nanoparticles (IMSN) loaded with TI to achieve cancer catalytic therapy.<sup>128</sup> IMSN exhibited intrinsic POD-like and CAT-like activities that indirectly reprogrammed the tumor immunosuppressive microenvironment by increasing ROS levels in the TME and relieving tumor hypoxia. The addition of TI induced macrophage polarization from M2 to M1 and further enhanced the therapeutic effect of IMSN. Significant improvement was observed in both *in vitro* three-dimensional tumor models (MTCS) and *in vivo* models that demonstrated immunosuppression within the TME. Single-atom nanozymes (SANs) leverage atomic dispersed metal centers to maximize their intrinsic enzyme-like activity. Carbon quantum dots (CQDs) have demonstrated their exceptional suitability as supports for SANs, owing to their diminutive size and abundant surface anchoring points.<sup>143</sup> Therefore, Lu *et al.* utilized dopamine-hybridized carbon quantum dots (DA-CQDs) for surface anchoring of Pd single atoms, resulting in the formation of DA-CQD@Pd nanozymes capable of catalyzing the *in situ* polymerization of poly (ethylene glycol) diacrylate (PEGDA) into a hydrogel, thereby enhancing its stability.<sup>129</sup> Simultaneously, both the Pd NPs and the quinone/hydroquinone redox pair on the DA-CQDs exhibited catalytic activity towards the generation of  $\cdot\text{OH}$  from  $\text{H}_2\text{O}_2$ . The hydrogel functioned as a localized ecological niche, providing sustained release of the immune adjuvant CpGODN to further promote antitumor immune responses.

The intrinsic relationship between tumor oxidative stress and cellular pyroptosis underscores the appeal of disturbing the intracellular oxidative balance as a means to induce pyroptosis.<sup>144</sup> Hollow carbon-structured nanomaterials exhibit mild high-temperature properties under safe radiation energy, rendering them suitable for mild hyperthermia to elicit immune responses.<sup>145</sup> In pursuit of elucidating the targeted amplification of oxidative stress-induced tumor pyroptosis under mild hyperthermia, Liu *et al.* devised hollow carbon spheres adorned with iron and copper atoms (HCS-FeCu) to emulate the functionality of diverse enzymes.<sup>130</sup> The mild photothermal amplification facilitated by hollow carbon spheres augmented intracellular nanozyme-mediated oxidative stress, prompting the generation of ROS that instigated tumor cell pyroptosis *via* the ROS-Tom20-Bax-Caspase 3-GSDME signaling pathway, thereby releasing DAMPs such as ATP and

lactate dehydrogenase (LDH) (Fig. 3a). Theoretical calculations suggested that mild photothermal stimulation engendered high-energy electrons, heightening the interaction between the HCS-FeCu surface and adsorbed oxygen, thereby enhancing the efficiency of ROS generation (Fig. 3b). When combined with ICB therapy, hyperthermia-mediated pyroptosis immunotherapy significantly augmented the therapeutic efficacy of  $\alpha\text{PD-1}$  (Fig. 3c).

**4.1.2. GSH consumption.** The detrimental impacts imposed by ROS on cellular structures are not solely contingent on their intracellular abundance, but also encompass the intricate interplay between ROS and endogenous antioxidant entities.<sup>146</sup> Disruption of the delicate equilibrium between prooxidants and antioxidants culminates in oxidative stress. As the most important endogenous antioxidant in cells, GSH has been shown to limit the production of excessive ROS to maintain tumor redox homeostasis.<sup>147</sup> Selectively targeting GSH metabolism in cancer cells is an effective measure to promote oxidation.

Ferroptosis is a cellular demise mechanism which primarily arises from inadequate elimination of ROS and has garnered significant interest in recent years. The diminishment of GSH results in the incapacitation of GPX4, culminating in the buildup of ROS generated through lipid peroxidation and consequentially giving rise to ferroptosis.<sup>148–150</sup> Additionally, it has been reported that cancer cells undergoing ferroptosis exhibit immunogenic behavior such as promoting the recognition and phagocytosis of tumor antigens by DCs, thereby activating CTLs and enhancing tumor immunotherapy.<sup>151–153</sup> Research has also shown that ferroptosis may induce tumoral PD-L1 expression through both membrane damage-independent mechanisms (NF- $\kappa\text{B}$  pathway) and membrane damage-dependent mechanisms (calcium influx).<sup>154</sup> The utilization of current nanozymes is limited by their intricate syntheses, high production expenditures, and lack of biocompatibility. Given its low toxicity and facile synthesis, CQDs present an attractive material option for the fabrication of nanozymes.<sup>155,156</sup> Nevertheless, limited studies have explored the use of CQDs-based nanozymes for inducing ferroptosis in tumors and subsequently triggering immune responses against cancer. In pursuit of this objective, Zeng *et al.* synthesized a CQDs-based nanozyme through simple hydrothermal treatment of chlorogenic acid (ChA), a cheap and easily accessible bioactive component in coffee.<sup>131</sup> Surprisingly, the ChA CQDs exhibited significant GSHox-like activity (Fig. 3d), thus inducing ferroptosis in HepG2 cells by disrupting the lipid repair systems catalyzed by GPX4 (Fig. 3e). *In vivo*, the ChA CQDs were found to recruit a large number of immune cells into tumor tissues with minimal toxicity, which included T cells, NK cells, and macrophages, effectively transforming “cold” tumors into “hot” tumors (Fig. 3f). Therefore, the advancement of ferroptosis-targeted therapy may potentially increase tumor sensitivity to ICBs, including  $\alpha\text{PD-L1}/\alpha\text{PD-1}$  and  $\alpha\text{CTLA-4}$ .

**4.1.3. Dual effect.** Due to the existence of intracellular redox balance mechanisms, the single effect of GSH depletion or ROS amplification is constrained in its ability to increase



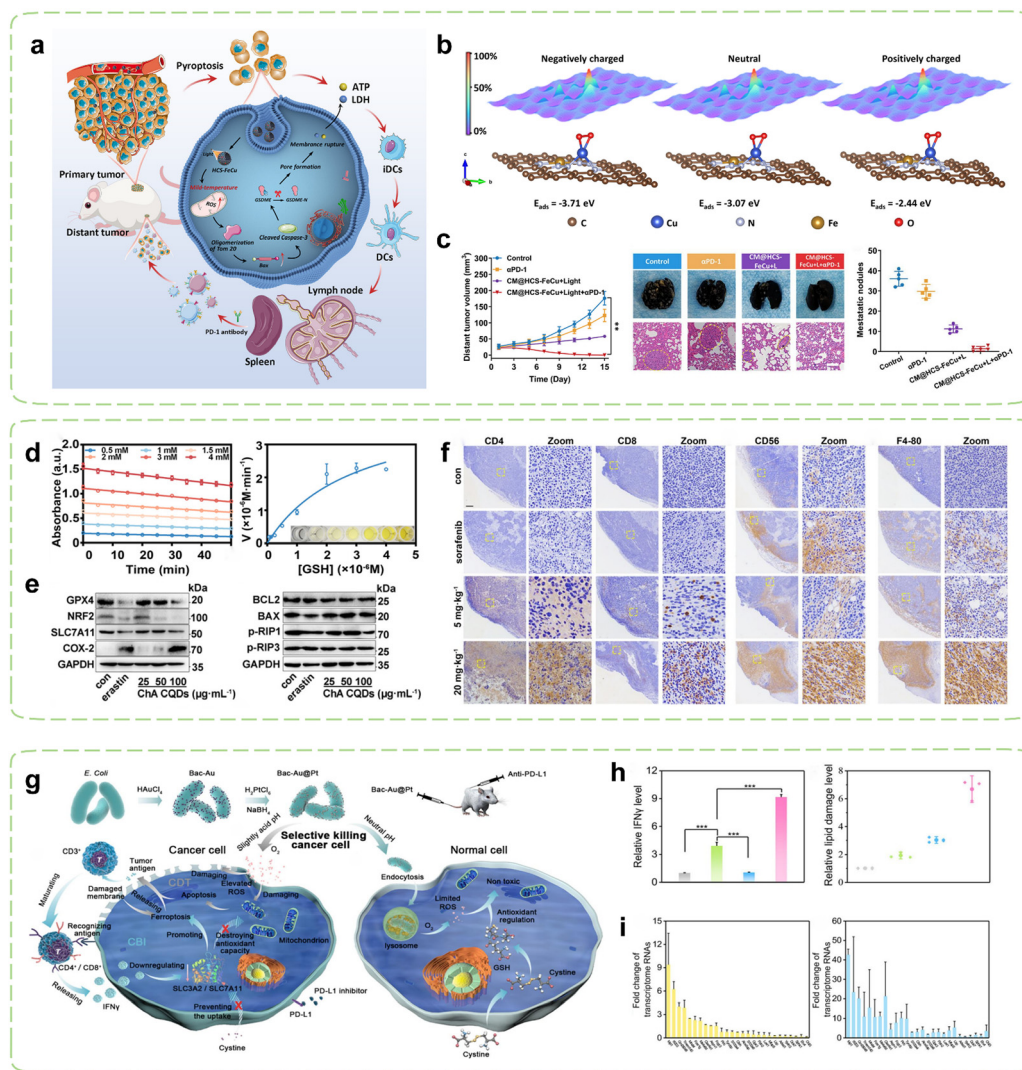


**Fig. 3** Nanozyme strategies for targeted intervention in redox metabolism. (a) Schematic diagram of HCS-FeCu Nanozyme enhancing cancer immunotherapy by mediating pyroptosis-induced ICD. (b) Adsorption energies ( $E_{\text{ads}}$ ) of  $\text{O}_2$  on HCS-FeCu surface with different electron energies. (c) Tumor suppression effects after combined treatment with  $\alpha\text{PD-1}$ . Reproduced with permission.<sup>130</sup> Copyright 2023, American Chemical Society. (d) Evaluation of GSHOx-like activity of ChA CQDs. (e) Expression of Ferroptosis-related biomarkers and apoptosis and necrosis-associated proteins induced by ChA-CQDs treatment in HepG2 cells. (f) Infiltration status of immune cells in H22 tumors after treatment with ChA CQDs. Reproduced with permission.<sup>131</sup> Copyright 2022, American Chemical Society. (g) Schematic diagram of Immunotherapy mediated by Bac-Au@Pt nanozyme inducing oxidative stress in tumor cells. (h) Expression of  $\text{IFN}\gamma$  and lipid ROS levels in tumor tissues of mice post-treatment. (i) Fold changes of transcriptome RNAs predominantly influenced by CDT in the Bac-Au@Pt group and the Bac-Au@Pt +  $\alpha\text{PD-1}$  group. Reproduced with permission.<sup>134</sup> Copyright 2021, American Chemical Society.

intracellular oxidative stress. Recently, the dual strategy of synergistically increasing endogenous ROS and specifically promoting antioxidant GSH consumption has attracted widespread attention.<sup>157</sup> Research indicates that this strategy, which concurrently utilize open-source approaches while minimizing expenditures, can induce a dual effect. This involves enhancing intracellular oxidative stress while diminishing the antioxidant capacity of tumor cells. Consequently, this amplifies the detrimental effects on tumor cells, thereby boosting tumor clearance efficacy and immune response. Diverse nanozymes exhibiting both GSH consumption activity and ROS generation activity have also been subject to extensive study.<sup>158–160</sup> Among

the multitude of nanomaterials, copper stands out due to its cost-effectiveness, abundant availability, and scalability for large-scale production.<sup>161</sup> Researchers have discovered that Cu<sup>I</sup>-based nanozymes can efficiently generate  $\cdot\text{OH}$  under weakly acidic conditions, exhibiting a reaction rate approximately 160 times higher than Fe<sup>II</sup>-based nanozymes due to the low redox potential of  $\text{Cu}^{\text{I}}/\text{Cu}^{\text{II}}$ .<sup>162</sup> Furthermore,  $\text{Cu}^{\text{II}}$  effectively depletes GSH through the redox reaction. The resulting product  $\text{Cu}^{\text{I}}$  initiates the Fenton reaction through its binding with  $\text{H}_2\text{O}_2$ , thereby facilitating cyclic amplification of oxidative stress.<sup>163</sup> On this basis, Lin *et al.* designed a TME-responsive smart nanoplatform.<sup>132</sup> As an *in vivo* upconversion luminescence



(UCL) imaging tool, UCNPs were activated specifically after the reaction between UCCG and GSH. Consequently, the luminous intensity of UCNPs core could be utilized to monitor real-time ROS amplification therapy. With both POD-like and GSHOx-like activity, this nanoplatfrom augmented the production of ROS through a cost-effective approach, causing ferroptosis of tumor cells, thereby promoting the transition from M2 phenotype to M1 phenotype and the local infiltration of CD4<sup>+</sup>T cells and CD8<sup>+</sup>T cells. In another study, Zhang *et al.* incorporated cinnamaldehyde (Cin) into copper alanine nanoparticles (CAC).<sup>133</sup> Within the acidic TME, Cin was released through the cleavage of hydrazone bonds, leading to the rapid consumption of GSH and an elevation in ROS levels. By integrating the natural enzyme GOx with the nanozyme Cu, the nanoparticles demonstrated high efficiency in both GSH consumption and ROS production, thus promoting the exposure of CRT and enhancing ICD.

Microbial synthesis of metal nanoparticles is recognized as a simple and environmentally friendly method. The resulting nanoparticles exhibit high catalytic activity due to their clean surface, large specific surface area, and good colloidal stability.<sup>164–166</sup> Furthermore, microorganisms can also act as immune adjuvants to activate the immune system.<sup>167</sup> Based on this concept, Han *et al.* fabricated a POD-like Au@Pt core-shell nanozyme decorated on the surface of bacteria (Fig. 3g).<sup>134</sup> With the help of PD-L1 inhibitors, mature T cells recognized tumor cells and subsequently released interferon  $\gamma$  (IFN- $\gamma$ ), which led to a reduction in the uptake of cystine by tumor cells, subsequently decreasing the level of GSH within the tumor cells. As a result, the antioxidant capacity of the tumor cells was more profoundly compromised, leading to their enhanced destruction (Fig. 3h). Combining bacterium-induced immunotherapy with augmented CDT (Fig. 3i), T cells were further activated and transformed into CD4<sup>+</sup> or CD8<sup>+</sup>T cells to recognized tumor cells. Temperature regulation can precisely control the catalytic activity of nanozymes by affecting their enzymatic kinetics. Currently, nanozymes are mainly controlled at high temperature (37–42 °C) for catalytic purposes, but this approach has a small safety window and may cause damage to the human body.<sup>168,169</sup> In contrast, low-temperature activation (4–37 °C) of nanozymes results in less adverse effects and holds promising prospects. Liu *et al.* created a cold-activated nanozyme based on Bi<sub>2</sub>Fe<sub>4</sub>O<sub>9</sub> nanosheets (NSs).<sup>135</sup> A smartphone-operated intervention device was also designed to remotely manage its cold catalysis. Within the temperature range of 4–37 °C, the thermoelectric properties of the device enabled it to exhibit GSHOx-like activity. Combining its pH-dependent POD and CAT activities, this nanozyme induced apoptosis and ferroptosis in tumor cells, exposing TAAs and achieving repolarization of macrophages through the IKK/NF- $\kappa$ B signaling pathway for precise targeted immunotherapy.

#### 4.2. Targeting glucose metabolism

Under hypoxic conditions, rapidly proliferating tumor cells tend to transition their aerobic respiration from OXPHOS to

aerobic glycolysis (also referred to as the Warburg effect), a less efficient but expedient mechanism for fermenting glucose to obtain energy.<sup>170,171</sup> This metabolic adaptation aligns with the heightened proliferation rate of malignant cells. Consequently, cancer cells exhibit a greater reliance on glucose metabolism compared to normal cells and are more vulnerable to glucose deficiency.<sup>172–174</sup> Extensive research has revealed a substantial association between PD-L1 expression and glycolytic activity.<sup>175–177</sup> Moreover, cancer cells exhibiting heightened glycolytic activity stimulate the production of substantial quantities of lactic acid within the TME, subsequently leading to TME acidification and consequent suppression of infiltrating immune cell functionality.<sup>178</sup> Building upon these findings, cancer immunotherapy strategies aimed at inhibiting tumor glucose metabolism and eliminating lactate from the TME have been developed and extensively implemented. Nanozymes demonstrate immense regulatory potential in these contexts. On one hand, nanozymes can exert effects in starvation therapy (ST) through their catalytic activity. On the other hand, meticulously designed nanozymes can further disrupt glucose metabolism within tumor cells by delivering pathway-specific modulators.

Inhibiting PD-L1 expression represents an emerging alternative immunotherapy approach, alongside PD-L1 blockade. Increasing glucose consumption to enhance tumor glycolysis has been demonstrated to induce upregulation of intracellular PD-L1 expression in tumor cells. Further research has revealed that the key glycolytic enzyme HK2 phosphorylates I $\kappa$ B $\alpha$ , promoting its degradation and thereby activating the NF- $\kappa$ B pathway, which subsequently enhances PD-L1 expression.<sup>179</sup> On the contrary, inhibition of PD-L1 substantiates curtailed tumor glycolysis and fortifies the proficiency of T cells.<sup>180</sup> Tumor cells with high PD-L1 expression may be more sensitive to PD-1/PD-L1 inhibitors, making ICB a potential effective therapeutic approach.<sup>181</sup> Therefore, leveraging the nanozyme-catalyzed glucose consumption to induce a low-glucose environment within tumor cells can enhance PD-L1 expression, thereby promoting  $\alpha$ PD-L1 immunotherapy. GOx exhibits remarkable efficiency in catalyzing the oxidation of glucose, generating gluconic acid and H<sub>2</sub>O<sub>2</sub> as products. This outcome effectively reduces acidity while concurrently augmenting oxidative stress, thereby establishing a microenvironment conducive to enhanced catalytic reactions instigated by nanozymes. However, the aforementioned catalytic reaction entails the participation of oxygen, which is impeded by the hypoxic TME. This issue can be resolved by combining GOx with CAT, which work in union to overcome the deficiency of oxygen. Tian *et al.* employed a biomimetic approach to fabricate a hybrid nanozyme Mn-GOx with dual enzyme-like activity, which was the first study that nanozymes and GOx had been hybridized together through the biomineralization-like method (Fig. 4a).<sup>182</sup> The fusion of GOx with Mn-based nanozymes possessing CAT-like activity, enabled the cascade of two catalytic reactions, leading to periodic amplification of glucose consumption. Simultaneously, the GOx-induced low glucose microenvironment within tumor cells not only synergistically promoted ICB





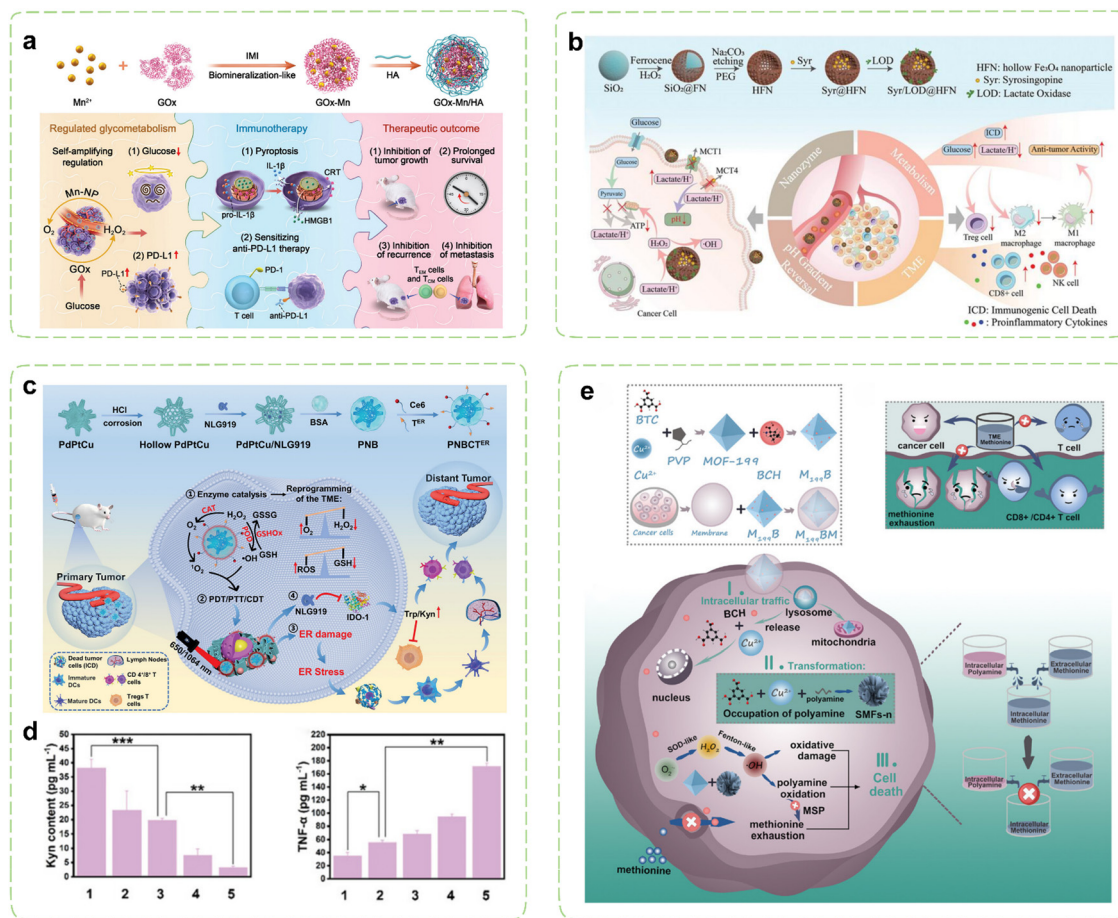


**Fig. 4** Nanozyme strategies for targeted intervention in glucose metabolism and amino acid metabolism. (a) Schematic illustration of hybrid nanozymes regulating tumor glycometabolism to induce tumor cell pyroptosis and enhance antitumor immunotherapy. Reproduced with permission.<sup>182</sup> Copyright 2022, Wiley-VCH. (b) Schematic diagram of the multifunctional nanoplatform for enhanced synergistic cancer immunotherapy through augmented self-replenishing catalytic reactions and integrated ST. Reproduced with permission.<sup>183</sup> Copyright 2023, Wiley-VCH. (c) Schematic illustration of cancer immunotherapy mediated by PdPtCu nanozymes reprogramming TME and relieving immunosuppression. (d) Assessment of the alleviating effect of nanozyme treatment on antitumor immunosuppressive effects *in vivo*. Reproduced with permission.<sup>184</sup> Copyright 2023, Wiley-VCH. (e) Schematic diagram of selective exhaustion of the methionine pool of tumor cells by sequential-positioned MOF nanotransformers for boosted antitumor immunity. Reproduced with permission.<sup>185</sup> Copyright 2023, Wiley-VCH.

therapy by inducing the expression of PD-L1 on tumor cells, but also induced potent tumor cell apoptosis thus triggering a robust antitumor immune response. By combining Mn-GOx with hyaluronic acid (HA), targeted delivery *via* intravenous administration was sped in breast cancer mice. Experimental results demonstrated significantly prolonged survival in cancer mice, along with the induction of strong immune memory effects through combination therapies. Additionally, favorable treatment outcomes were observed in both B16F10 and orthotopic 4T1 tumor models. Thus, the integration of tumor glucose metabolism regulation with immunotherapy effectively suppressed tumor growth, recurrence, and metastasis.

Owing to the heightened Warburg effect in cancer cells, there is a significant buildup of lactate in the TME, leading to metabolic acidosis. Research suggests that lactate derived from tumors serves as a key regulatory factor in promoting tumor growth. Additionally, lactate plays a crucial role in the polarization and metabolic reprogramming of TAMs, leading to the

induction of an immunosuppressive TME that facilitates tumor immune evasion.<sup>186</sup> Current research on inhibiting glucose metabolism of tumor cells primarily focuses on glucose-deprivation therapies that aim to limit glucose utilization. However, considering the relatively lower glucose concentration observed within tumors ( $1\text{--}2\ \mu\text{Mol g}^{-1}$ ) compared to the higher intratumoral lactate levels (LA,  $5\text{--}20\ \mu\text{Mol g}^{-1}$ ), there is a greater potential for effective tumor therapy by targeting the endogenous generation and utilization of intratumoral lactate with nanodrugs.<sup>187</sup> Therefore, the clearance of lactate in the TME is crucial for enhancing cancer therapy efficacy. Contemporary lactate clearance strategies predominantly rely on three approaches: natural enzymes that metabolize lactate, small molecule inhibitors targeting these enzymes, and inhibitors blocking lactate transport.<sup>188</sup> Natural enzymes involved in lactate metabolism, such as LDH and LOx, exhibit low activity and stability under harsh TME conditions. In contrast, nanozymes as substitutes for natural enzymes possess resistance to





adverse conditions, prolonged efficacy, and targeted delivery advantages. Thus, they can efficiently consume lactate generated by aerobic glycolysis in tumors, remodel the TME, alleviate immune suppression effects, and inhibit tumor progression. Repolarizing TAMs is a significant target in immunotherapy. M1 and M2 macrophages display metabolic differences, with M1 relying primarily on glycolysis for energy acquisition, while M2 macrophages rely on oxidative phosphorylation. These metabolic distinctions form the basis for their diverse functions within the immune system.<sup>189,190</sup> Chen *et al.* developed a strategy to enhance TAMs-centered anticancer immunotherapy by loading carbonic anhydrase IX (CAIX) inhibitors onto LDH-mimicking SnSe NSs.<sup>191</sup> By leveraging the catalytic properties of SnSe NSs, lactate depletion within the TME was induced. Sustained lactate consumption facilitated the repolarization of TAMs towards the M1 phenotype, which led to the restoration of M1's tumor-killing activity and triggered a metabolic shift from oxidative phosphorylation to glycolysis, which in turn synergistically regulated TAMs. Inhibitors of CAIX restrained the efflux of H<sup>+</sup>, leading to a synergistic reduction in tumor acidification, consequently mitigating acidosis and immunosuppression. Along with the photothermal activity of SnSe NSs, the immune response was significantly induced to ablate tumors and inhibit lung metastasis of tumor cells.

To prevent intracellular acidification, excessive lactate produced by tumor glycolysis is transported extracellularly *via* monocarboxylate transporters (MCTs).<sup>192</sup> Extracellular lactate contributes to malignant progression of tumors and evasion of immune responses. The most crucial MCTs in cancer are MCT1 and MCT4, which are significantly overexpressed and play pivotal roles in cancer development and invasiveness.<sup>193</sup> Consequently, Therefore, MCT1/4 has been commonly downregulated as a target for nanocarrier-based tumor treatment to reduce lactate efflux, reverse tumor pH gradients associated with hypoxia, and phenotype heterogeneity. As a clinically utilized antihypertensive medication, syrosingopine (Syr) exerts its effects by inhibiting the functionality of monocarboxylate transporters MCT1 and MCT4, thereby suppressing lactate efflux and reversing the pH gradient within tumors.<sup>194</sup> However, the efficacy of individual small molecule inhibitors is limited and prone to off-target effects.<sup>195</sup> Therefore, it is crucial to develop combination treatment strategies that exploit synergistic antitumor effects to achieve effective therapeutic outcomes. In this context, Wang *et al.* reported a nanozyme platform for co-delivery of Syr and lactate oxidase (LOD) (Fig. 4b).<sup>183</sup> The intracellular accumulation of lactate in tumor cells reciprocally inhibits their glycolytic pathway and provides ample substrate for the LOD-catalyzed production of H<sub>2</sub>O<sub>2</sub>. Following the conversion of accumulated lactate to abundant H<sub>2</sub>O<sub>2</sub> within the cells, hollow iron oxide (HFe<sub>3</sub>O<sub>4</sub>) nanoparticles with POD-like activity catalyze the generation of ROS, leading to mitochondrial dysfunction and inhibition of OXPHOS pathway. Dual inhibition of aerobic glycolysis and OXPHOS effectively disrupts cellular ATP supply, demonstrating therapeutic potential. Significant reduction in lactate concentration within the TME and induction of ICD in tumor cells facilitated by LOD

lead to increased concentrations of pro-inflammatory cytokines (TNF- $\alpha$  and IFN- $\gamma$ ) in serum, thereby greatly reactivating integrated antitumor immune activity, including reactivation of effector T cells and NK cells, suppression of Treg cells, polarization of macrophages to M1 phenotype, and promotion of DC maturation.

What's more, lactate is traditionally regarded as a metabolic waste product that must be excreted by cancer cells. However, recent studies have shown that lactate is also capable of serving as an energy substrate across various conditions.<sup>196,197</sup> Following significant glucose consumption, tumor cells can uptake and oxidize lactate to sustain cellular energy demands. Recent studies have also shown that lactate functions not only as an intermediary in TCA cycle metabolism but also as a metabolic regulator, promoting tumorigenesis by acting as an energy source.<sup>198–200</sup> Hence, leveraging the enzyme-like activity of nanozymes to catalyze lactate consumption can disrupt the energy supply of the cancer cells, thereby facilitating lactate-based ST. In pursuit of this objective, Li *et al.* developed a nanotherapeutic agent (PNDPL) comprising a PtBi nanozyme, LOx, and the IDO inhibitor NLG919.<sup>201</sup> This study represented the first investigation into the synergistic antitumor effects of regulating lactate metabolism and IDO-associated immunotherapy. CAT-like PtBi nanozymes established a positive feedback loop with LOx and drove the continual consumption of lactate, thereby achieving the desired effect of ST. Under 1064 nm irradiation, PNDPL induced ICD and inhibited immune escape through the synergistic immunotherapy.

### 4.3. Targeting amino acid metabolism

The metabolic reprogramming of amino acids within tumor cells promotes tumor survival. Simultaneously, there is extensive crosstalk between amino acid metabolism and T cell immunity, resulting in immune evasion by the tumor.<sup>202</sup> Throughout the activation, differentiation, and functionality of T cells, amino acids and their metabolites can function as energy reservoirs and substrates for protein synthesis and modification.<sup>203</sup> Tumor cells can dampen T cell immunity by depriving amino acids within the TME, and the toxic byproducts of amino acids can also impede T cell functions.<sup>204</sup> Consequently, strategies focusing on targeting amino acid metabolism have emerged as an efficient approach for modulating the immunosuppressive TME. By loading pathway-specific modulators, nanozymes can alter amino acid concentrations in the TME, thereby restricting metabolic demands of tumor cells. Concurrently utilizing their intrinsic catalytic activity, they can mediate metabolic disruptions in tumor cells, inhibiting their growth and alleviating immune suppression effects.

Numerous enzymes implicated in amino acid metabolism are markedly upregulated in tumor cells, thereby aiding in the evasion of immune surveillance within the TME. IDO catalyzes the conversion of Trp to kynurenine (Kyn), resulting in Trp depletion in the TME, which leads to growth arrest and apoptosis of effector T cells. Simultaneously, Kyn, functioning as an immunosuppressive agent, directly fosters



immunosuppression mediated by Tregs.<sup>205,206</sup> Thus, inhibiting IDO can reverse immunosuppression, while activating T cells to elicit immune responses. Li *et al.* reported an ER-targeted nanozyme loaded with the IDO inhibitor to reshape the immune microenvironment (Fig. 4c).<sup>184</sup> Under the influence of triple enzyme-like activities (CAT, GSHOx, and POD) of PdPtCu nanozyme, cellular oxidative stress was enhanced and the tumor hypoxia was relieved. Then, the synergistic therapeutic effects transformed immunosuppressive TME into immunogenic TME, which was further enhanced *via* ER stress-induced strong ICD. During the treatment, the IDO-mediated Trp/Kyn immune escape pathway in TME was disturbed by the NLG919, which profoundly promoted the activity of effector T cells (Fig. 4d). In another study, Wang *et al.* investigated the synergistic anticancer effects of ceria nanozymes and PDT.<sup>207</sup> ER-targeted PDT performed by erythrocyte membrane-camouflaged ceria nanozymes amplified the induction of ICD through ER stress, while its payload, 1-MT, acted as an IDO inhibitor to inhibit Trp catabolism. Meanwhile, ceria nanozymes possessed multienzyme-like properties, promoting oxidation under acidic TME conditions and antioxidation under neutral or alkaline conditions. The tumor-targeted prooxidation property of ceria nanozymes enhanced the PDT efficacy and antioxidative behavior in healthy tissues such as the kidney. In organotypic brain slices of glioblastoma, the upregulation of the surface markers and maturation markers of DCs indicated that a robust immune response was induced.

Among essential amino acids, Met assumes a paramount role in both survival and functions of T cells.<sup>208</sup> Recent investigations have unveiled that cancer cells, particularly tumor-initiating cells, display prominently heightened activity within the Met cycle and demonstrate reliance on exogenous Met. Tam *et al.* reported a case that upon discontinuation of Met supplementation, tumor-initiating cells lost their tumorigenic capability upon reintroduction into a normal environment, which resulted in a remarkable decrease in tumor load, reaching up to 94%.<sup>209</sup> In order to alleviate the metabolic burden in the face of elevated Met cycle flux, malignant cells can replenish their Met pool through a Met salvage pathway by utilizing polyamine metabolism.<sup>210</sup> Cancer cells possess the capability to mitigate functions of T cells through direct competition for Met.<sup>211</sup> Deficiency in Met may lead to functional impairments and even death in the majority of T cells. To deal with this problem, Qu *et al.* constructed a sequential positioned MOF nanotransformer to restrain the open source and reduce the reflux of Met to exhaust the Met pool (Fig. 4e).<sup>185</sup> The cancer cell membrane coating endowed M<sub>199</sub>BM NPs with the ability to target the homotypic tumor site. Endocytosed M<sub>199</sub>BM NPs were capable of subsequent degradation within the cytoplasm and liberation of system L transporter inhibitors, thus impeding Met uptake. Moreover, M<sub>199</sub>BM exhibited SOD-like activity, generating •OH that oxidized polyamines, thereby depleting the Met pool in a dual-action approach. It is noteworthy that the metal ions and ligands released by M<sub>199</sub>BM underwent time-dependent reorganization with spermine/spermidine within both the cytoplasm and nucleus, effectuating continuous localization of

the M<sub>199</sub>BM. This intracellular trafficking route aligned well with polyamine distribution, facilitating polyamine oxidation and intracellular Met depletion. The deprivation of Met in cancer cells bolstered the infiltration of CTLs and helper T cells (Th), thereby realizing enhanced cancer immunotherapy.

#### 4.4. Targeting lipid metabolism

Certain lipid metabolites, including PGE<sub>2</sub>, possess the capacity to function as immunosuppressive agents and modulate immune responses. Under pathological conditions, arachidonic acid (AA) originating from membrane phospholipids have the potential to disturb intracellular oxidative stress.<sup>212</sup> Consequently, Therapies targeting lipid metabolism are emerging as groundbreaking approaches in cancer treatment, offering unprecedented opportunities for effective cancer management. Strategically designed nanozymes can mediate cascade reactions to disrupt lipid metabolism processes by delivering metabolic modulators and leveraging their inherent enzyme-like activity, which paves new directions for restoring antitumor immunity.

Cyclooxygenase-2 (COX-2) has been validated as an important factor in immunosuppression by facilitating the metabolism of AA and elevating PGE<sub>2</sub> levels within tumor cells. Elevated COX-2 expression impedes the migration of DCs while promoting the accumulation of MDSCs and inducing M2 polarization.<sup>213–215</sup> Consequently, cancer immunotherapy strategies centered around COX-2 inhibitors hold substantial therapeutic potential.<sup>216</sup> Building upon previous research, Wang *et al.* introduced aspirin (ASA) and doxorubicin (DOX) onto Au@HMnMSNs, enabling the combination of CT and CDT within nanozymes (Fig. 5a).<sup>217</sup> Elevated intracellular levels of GSH instigated the degradation process within nanoreactors, resulting in the prompt liberation of Mn<sup>2+</sup> specifically within cancer cells. Prior investigations have demonstrated that Au NPs exhibit catalytic GOx-like activity, facilitating the breakdown of glucose and generating H<sub>2</sub>O<sub>2</sub>, thereby intensifying the Fenton-like reaction mediated by released Mn<sup>2+</sup>. Simultaneously, the utilization of GSH promoted the generation of ROS. Additionally, the elliptical structure of tadpole-shaped Au@HMnMSNs avoided the deactivation of Au NPs caused by robust protein adsorption. Concurrently, the incorporation of ASA synergistically augmented CDT and CT by suppressing PGE<sub>2</sub> expression and inducing ICD, which amplified the efficacy of antitumor immunotherapy.

Lipid peroxidation stands as the primary hallmark of ferroptosis, with particular emphasis on the role of polyunsaturated fatty acids binding to the cytoplasmic membrane.<sup>221</sup> Recent investigations have highlighted the release of IFN- $\gamma$  by T cells, which, when joining up with arachidonic acid, synergistically activates ACSL4, thereby inducing ferroptosis in tumor cells.<sup>222</sup> ACSL4 assumes the responsibility of converting AA into AA CoA, participating in the synthesis of membrane phospholipids. Augmenting the content of AA in tumor tissue can effectively trigger ACSL4-mediated IFN- $\gamma$ -induced immunogenic ferroptosis.<sup>223–225</sup> In pursuit of this goal, Wang *et al.* reported a novel six-enzyme co-expressed composite



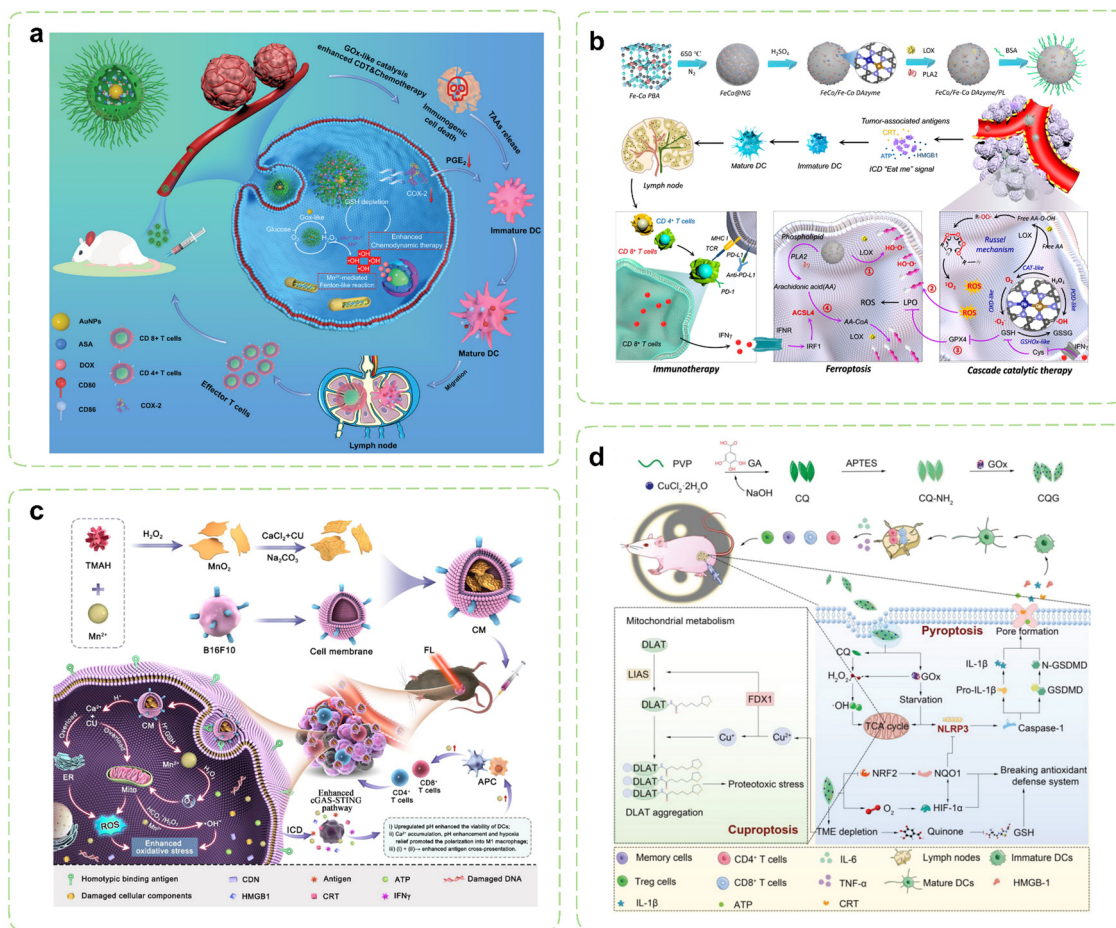


Fig. 5 Nanozyme strategies for targeted intervention in lipid metabolism and metal metabolism. (a) Schematic illustration of Au@HMnMSNs nanozymes for reinforcing the induction of ICD via multiple metabolic regulations. Reproduced with permission.<sup>217</sup> Copyright 2021, Wiley-VCH. (b) Schematic diagram of the synthesis of a multi-enzyme co-expression nanozyme platform (FeCo/Fe-Co DAzyme/PL) and the induction of cascade immunogenic ferroptosis. Reproduced with permission.<sup>218</sup> Copyright 2023, American Chemical Society. (c) Schematic illustration of the immunotherapeutic mechanisms of the pH-responsive dual-ion nanomodulator. Reproduced with permission.<sup>219</sup> Copyright 2023, American Chemical Society. (d) Schematic diagram of the pyroptosis-cuproptosis synergistic immunotherapy of CQG nanozymes in cancer treatment. Reproduced with permission.<sup>220</sup> Copyright 2023, Wiley-VCH.

nanoplatfrom that could not only induce initial immunogenic tumor ferroptosis through its own multienzyme-like activities, but also upregulate AA expression to synergize with CD8<sup>+</sup> T cell-derived IFN- $\gamma$  to induce ACSL4-mediated immunogenic tumor ferroptosis (Fig. 5b).<sup>218</sup> Phospholipase A2 (PLA2) and lipoxygenase (LOX) were loaded on FeCo/Fe-Co dual-metal atom nanozyme (FeCo/Fe-Co DAzyme) with intrinsic multienzyme-like activities similar to natural OXDs, GSHOxs, CATs, and PODs to form the ultimate nanocomposites. During the treatment procedure, the liberated O<sub>2</sub> triggered by the nanoreactor subsequently reacted with free AA derived from phospholipids catalyzed by PLA2, leading to the generation of AA hydroperoxides (AA OOH), which would be ultimately produced into a substantial quantity of singlet oxygen (<sup>1</sup>O<sub>2</sub>) through the Russell mechanism. Combining with the multiple ROS storms, GSH/GPX4 depletion, LOX catalysis, and IFN- $\gamma$ -mediated ACSL4 activation, irreversible cascade immunogenic tumor ferroptosis was achieved. *In vivo*, the percentage of mature DCs and

secretion levels of pro-inflammatory cytokines were obviously increased in the FeCo/Fe-Co DAzyme/PL +  $\alpha$ PD-L1 group, thus revealing the effectiveness of the immunotherapy.

#### 4.5. Targeting metal metabolism

Metal ions, encompassing Ca<sup>2+</sup>, Mn<sup>2+</sup>, Fe<sup>2+/3+</sup>, and others, play indispensable roles in diverse biological processes, including metabolism and immune homeostasis relevant to tumor occurrence and treatment.<sup>226,227</sup> Nanozymes typically dissolve during catalytic processes, releasing their metallic components. These ions not only participate in critical redox reactions essential for catalytic activity but also disrupt the homeostasis of endogenous metal ions, thereby mediating cellular damage and triggering immune responses.<sup>228</sup> The rate and extent of dissolution may be influenced by factors such as pH, temperature, and the presence of biological ligands or ROS in the microenvironment.<sup>229</sup>





Throughout the onset and progression of cancer, malignant cells demonstrate heightened susceptibility to the modulation of  $\text{Ca}^{2+}$  when compared to their normal counterparts. The induction of calcium overload may instigate mitochondrial dysfunction, elevated levels of ROS, impairment of cell membranes and organelles, as well as disruption of the cytoskeleton, thereby culminating in tumor cell death while triggering immune responses.<sup>230</sup> Notably, certain investigations have also indicated that  $\text{Mn}^{2+}$  can stimulate DCs' maturation and polarization of macrophages towards the M1 phenotype by serving as an activator of the cyclic GMP-AMP synthase/stimulator of interferon genes (cGAS-STING) pathway.<sup>231</sup> Hence, the prospect of employing a dual-ion therapy involving  $\text{Ca}^{2+}$  and  $\text{Mn}^{2+}$  holds great promise for tumor treatment. Tang *et al.* wrapped  $\text{CaCO}_3$ -loaded  $\text{MnO}_2$  NSs with B16F10 cell membranes to create a "dual-ion overloading nanoregulator" (Fig. 5c).<sup>219</sup> The degradation rates in PBS solutions showed the low pH-responsive and -dissociable characteristics, which was in line with the weakly acidic TME.  $\text{MnO}_2$  served not only to elevate cytoplasmic  $\text{Mn}^{2+}$  levels and deplete GSH but also enhanced activation of the cGAS-STING pathway by mitigating tumor hypoxia and engendering ROS through its inherent enzyme-like activities. Meanwhile,  $\text{CaCO}_3$  mitigated acidification of the TME by neutralizing protons within tumor cells, thereby reshaping the TME and fostering intracellular oxidative stress. The mitochondria and ER represented the primary reservoirs of intracellular calcium and the principal loci for ROS production. Under the enhanced influence of loaded curcumin (CU), released  $\text{Ca}^{2+}$  disrupted calcium homeostasis within both mitochondria and the ER. This disruption led to reduced ATP generation within mitochondria and ER stress, ultimately causing severe oxidative damage to tumor cells. This process strongly induced ICD and prompted macrophages to shift from an M2 to an M1 phenotype, activating sustained immune clearance responses *in vivo*.

As an essential micronutrient within the human body, copper is intimately associated with a multitude of signaling pathways and tumor-related biological behaviors. Researchers have unveiled a novel copper-dependent form of programmed cell death, termed "cuproptosis",<sup>232</sup> which has been demonstrated to be reliant on mitochondrial respiration and exists independently of apoptosis, ferroptosis, and necroptotic death. Cuproptosis is initiated by the direct binding of surplus copper ions to lipoylated constituents of the TCA cycle within mitochondria. This binding event promotes the aggregation of dihydrolipoamide S acetyltransferase (DLAT), leading to the subsequent degradation of iron-sulfur cluster proteins and triggering a toxic response that culminates in cellular death. The utilization of copper chelators to reduce copper bioavailability, and the employment of copper ion carriers for the facilitation of copper delivery into cells both can augment intracellular copper levels to induce cuproptosis.<sup>233</sup> The clinical applications of copper carriers are presently limited due to their comparably lower biocompatibility and stability. Consequently, it is imperative to develop copper ion carriers possessing favorable safety, stability, and selectivity. Li *et al.* designed

enzyme-like self-destructive copper-quinone-GOx nanoparticles (CQG NPs) to induce the first proposal and verification of the synergistic effect arising from pyroptosis and cuproptosis in cancer immunotherapy (Fig. 5d).<sup>220</sup> Due to the instability of the copper-quinone coordination bonds in nanozymes, they could be destroyed and degraded by GSH, releasing a large amount of copper ions in the process. CQG NPs inhibited the expression of NQO1 and NRF2 proteins by depleting GSH and generating abundant oxygen. Additionally, their SOD-like activities facilitated the conversion of endogenous ROS into plentiful  $\text{H}_2\text{O}_2$ . Under the dual stimulation of a weakly acidic TME and elevated levels of  $\text{H}_2\text{O}_2$ , the CQG NPs exhibited heightened POD-like activities, ultimately triggering robust ferroptosis by inhibiting the NRF2-NQO1 antioxidant signaling pathway. Simultaneously, the degradation of the CQG NPs within the TME released copper ions, which further depleted endogenous copper chelators GSH and enhanced cuproptosis synergistically with enzyme-like activities. The synergistic therapy effectively converted M2 into M1 and inhibited Tregs within the TME. Importantly, the number of effector memory T cells (Tem) and central memory T cells (Tcm) significantly increased, indicating that the nanozymes induced long-term immune memory effects.

#### 4.6. Targeting NADH metabolism

In tumor cells, the NADH/NAD<sup>+</sup> redox pairs play a more pivotal role as vital coenzymes in cellular metabolism, contributing to the maintenance of energy equilibrium and the regulation of diverse biochemical reactions.<sup>234</sup> During the glycolysis process in tumor cells, glucose is metabolized into two molecules of pyruvate, generating 2 molecules of NADH in this process. These NADH molecules subsequently participate in mitochondrial oxidative phosphorylation, where they serve as electron carriers in the electron transport chain. These electrons are ultimately used to reduce oxygen to water, while ATP synthase utilizes the proton gradient to generate ATP.<sup>235</sup> Consequently, the disruption of NADH metabolism and the perturbation of NADH/NAD<sup>+</sup> homeostasis can effectively impair ATP production, representing a viable strategy for combating cancer.<sup>236</sup>

Nanozymes exhibiting NOX-like activity may disturb intracellular NADH/NAD<sup>+</sup> cycling, consequently interfering with ATP synthesis and destabilizing cancer cells. Oxygen vacancies (OVs) is a novel and effective tool for regulating the highly reactive free radicals in the TME.<sup>237</sup> Research has shown that defect engineering methods can organize and enrich activated catalytic sites in nanomaterials, thus simulating artificial enzymes in a biological environment.<sup>238</sup> The coexistence of defects and OVs can serve as synergistic active sites, promoting the efficient production of nanozymes. To this end, Zhao *et al.* employed an oxygen-deficient molybdenum oxide (MoOx) nanostructure to deliberately induce substitutional defects *via* Cu doping, resulting in the formation of a Cu-doped MoOx (Cu-MoOx) nanozyme with a concurrent abundance of OVs and copper substitutions.<sup>239</sup> The defect-engineered nanozyme demonstrated high catalytic performance through the simulation of multiple enzyme activities, including POD, OXD, and





NOX. Subsequently, R848 was incorporated into tumor cell membrane-coated CMO nanozymes to construct engineered nanosystems (CMO-R@4T1). This CMO nanozyme-mediated photodynamic immunotherapy cascaded ROS generation and disrupted the balance of NADH/NAD<sup>+</sup> through utilizing NOX-like activity to induce ATP synthesis inhibition, thereby promoting apoptosis of tumor cells to facilitate ICD and DC maturation. This, in turn, facilitated the accumulation of CTLs and helper T cells in primary and metastatic tumors with the help of R848, thereby augmenting systemic primary tumor ablation and impeding cancer metastasis to distant sites.

## 5. Nanozymes for combination cancer immunotherapy

In recent years, nearly 90% of cancer-related deaths have been attributed to metastasis rather than primary tumor growth.<sup>240</sup> Immunotherapy has shown promising prospects in treating metastatic tumors by enhancing the immune defense mechanism against tumors and modifying the immunosuppression in the TME. However, the response rate of single-mode immunotherapy is low. Nanozyme mediated metabolic disruption of tumor cells has been shown to induce immune responses, however, its intensity and magnitude remain limited for effective tumor eradication.<sup>241</sup> Therefore, the pursuit of multimodal synergistic treatment strategies to enhance antitumor immunotherapy is of great significance. Various external stimulus therapies, such as phototherapy (PT), SDT, RT, CT, gas therapy (GT), and magnetic therapy (MT), have been demonstrated to assist in the metabolic disruption of tumor cells by nanozymes.<sup>242,243</sup> Furthermore, they synergistically promote the eradication of cancer cells and enhance the efficiency of subsequent immune response activation. This section aims to elucidate the role and mechanisms of external therapy-assisted

nanozyme-mediated combination immunotherapy in cancer treatment.

### 5.1. PT-assisted nanozymes

As a potent strategy for achieving tumor ablation, PT has garnered considerable attention in recent years owing to its exceptional targeting specificity, non-invasiveness, and spatio-temporal controllability. Nonetheless, PT, such as photothermal therapy (PTT), has demonstrated inherent limitations as a standalone intervention, including restricted therapeutic efficacy against deep-seated tumors, an inability to eradicate multiple tumor lesions simultaneously, and the potential for drug resistance following prolonged use.<sup>244</sup> PT and nanozyme therapy are considered complementary, as the light modality demonstrates outstanding tunability and sensitivity in precisely targeting tumors, while nanozymes can overcome inherent light penetration deficiencies of deep-seated tumors through drug delivery and disrupting tumor metabolism internally. In recent years, diversified collaborative therapeutic strategies which integrates PT with nanozymes has been extensively investigated and has exhibited a remarkable capacity to augment the efficiency of immunotherapy. They culminate in a “1 + 1 > 2” synergistic therapeutic effect. This section furnishes a comprehensive synthesis of the fusion of PT with nanozymes in cancer immunotherapy (Table 2).

**5.1.1. Combination immunotherapy of nanozymes and PTT.** PTT harnesses photothermal agents to generate elevated temperature upon laser irradiation, facilitating the ablation of tumor cells, thereby activating the immune system.<sup>253</sup> Furthermore, the generated localized heat not only induces elevated temperatures but also enhances the catalytic reactions of nanozymes, thereby further contributing to the destruction of tumor cells and stimulating immune responses.<sup>254</sup> In contrast to individual PTT, the combination therapy of PTT and nanozymes typically necessitates lower temperature, as elevated temperature resulting from the approach bolster immune

**Table 2** Representative PT-assisted nanozymes for combination cancer immunotherapy

	Nanozyme components	Cargos	Synergistic effects	Models	Ref.
PTT-assisted nanozymes	Cu@Fe <sub>2</sub> C@mSiO <sub>2</sub>	R848, ICG	Immune activation, photothermal catalytic treatment	Subcutaneous 4T1 tumor-bearing Balb/c mice; metastatic 4T1/B16F10 tumor-bearing Balb/c mice; metastatic 4T1/B16F10 tumor-bearing C57BL/6j mice	245
	Fe <sub>3</sub> O <sub>4</sub> @Cu <sub>1.77</sub> Se	—	M2 polarization to M1, ICD induction	4T1 tumor-bearing BALB/c mice	246
	AuPtAg	GOx	αPD-L1 combination, hypoxia relief, heat resistance reduction to enhance PTT	Bilateral 4T1 tumor-bearing Balb/c mice	247
	AuNR@CeO <sub>2</sub> /AuNP	JQ1, Rhb	Enhanced hyperthermia accompanied by a large amount of ROS generation leading to pyroptosis, ICB combination	4T1 xenograft tumor-bearing BALB/c mice	248
	RuTe <sub>2</sub>	GOx, TMB	Trimodal synergistic induction of ICD	4T1 tumor-bearing mice	249
PDT-assisted nanozymes	CMZM	Ce6	Hypoxia relief, multimodal guided enhanced immunotherapy	BALB/c mice with 4T1 cells	250
	CNPs	CPBA	Ferroptosis, PD-L1 inactivation, suppression of immunosuppressive factors and M2-TAMs	MB49 tumor-bearing C57BL/6 mice	251
	AuP-nPt	ATO, IR780	Blocking oxygen metabolism and enhancing PTT-induced ICD	C57 mice with LLC cells	252



defenses by recruiting a greater number of immune cells and augmenting the permeability of tumor cell membranes.

Currently, the catalytic reactions of the majority of nanozymes predominantly rely on Fenton-like reactions. For example, iron carbide, characterized by its exceptional magnetic properties, photothermal conversion capabilities, and POD-like activity, can serve as a contrast agent for MRI, as well as a therapeutic agent for PTT and CDT. An iron carbide based immunomodulatory system has been devised for real-time visualization and synergistic cancer therapy.<sup>245</sup> Phase change materials [PEG/lauric acid (LA)] exhibited dual-responsive behavior to temperature and pH, enabling more effective and controllable release of R848. Guided by MRI/NIR-II dual-mode imaging, the system achieved active targeting to tumor sites through AS1411, promoting DCs maturation and enhancing the functionality of CD8<sup>+</sup> T cells while suppressing the proportion of MDSCs. Furthermore, preliminary evidence suggested that this nanosystem may stimulate the ROS signaling pathway STAT3. The overexpression of matrix metalloproteinases (MMPs) in tumor tissues offers a promising avenue for augmenting the specificity of cancer therapy.<sup>255</sup> Accordingly, a metal nanozyme assembled using gelatin as a template was engineered (Fig. 6a).<sup>246</sup> Upon magnetic targeting and transport to the tumor site, gelatin could undergo degradation by abundant MMPs in the TME, leading to the conversion of nanozymes into small fragments. This process significantly enhanced the permeability of treatment and MRI. Subsequent NIR-II light irradiation not only induced effective PTT and enabled photoacoustic (PA) imaging, but also significantly amplified the Fenton reaction, thus inducing more lipid peroxidation and promoting ferroptosis in tumor cells by generating  $\cdot\text{OH}$  and depleting GSH. The expression of CD80 and CD86 in the experimental group was significantly enhanced, while the expression of CD206 was significantly reduced, indicating that this synergistic effect polarized TAMs from the M2 type to the M1 type. In animal experiments, the polarization of M2 to M1 in tumors treated with the nanozyme under illumination increased by 2.2-fold, 1.5-fold, and 2.7-fold, respectively, while TNF- $\alpha$  increased by 1.4-fold and 1.2-fold, respectively (Fig. 6b).

The heat generated by photothermal conversion can also enhance the catalytic activity of GOx-like nanozymes, providing a basis for enhanced nanozyme-mediated ST.<sup>256</sup> Moreover, enhanced ST accelerates the depletion of intracellular ATP in tumor cells, significantly reducing ATP levels and thereby suppressing the expression of protective heat shock proteins (HSPs) during thermal stress in cancer cells, decreasing their thermotolerance.<sup>257,258</sup> In summary, combining PTT with nanozyme-based ST helps reduce the required therapeutic temperature for PTT to below 50 °C, achieving mild PTT (mPTT), thus avoiding off-target effects and side effects on normal tissues and optimizing tumor ablation.<sup>259</sup> Li *et al.* developed an AuPtAg-GOx nanozyme that exhibited mild photothermal properties through the integration of ST, thereby reducing the heat resistance of tumor cells and promoting the antitumor immune response.<sup>247</sup> AuPtAg Gox with CAT-like activity exhibited a significant consumption of glucose in

tumor cells, which further promoted ST and enhanced the therapeutic effect of mPTT. The western blot results of the treated 4T1 cells indicated that mPTT led to an increase in the expression of HSPs in the control group, while the expression of HSP70 and HSP90 in the AuPtAg-GOx group significantly decreased. Meanwhile, the nanozyme resulted in an intensified recruitment of TILs and a sensitized ICB therapy. As we know, glucose consumption not only helps reduce intracellular ATP levels but also mediates ICB based on decreased PD-L1 expression levels. Recently, bromodomain and extra-terminal (BET) inhibitors like JQ1 also have garnered significant attention for their same ICB function.<sup>260</sup> They disrupt the aberrant binding of BET proteins (BRD2, BRD3, BRD4, and BDRT) with acetylated histones, halting the transcriptional activity of cancer-promoting genes such as c-Myc.<sup>261,262</sup> Emerging evidence indicates that JQ1 mediates ICB therapy by directly downregulating PD-L1 levels through reduced c-Myc transcription.<sup>263,264</sup> This underscores its potential in modulating the tumor immune microenvironment. Therefore, Tang *et al.* encapsulated JQ1 inside a biomimetic mesoporous nanozyme that utilized PTT to achieve enhanced immunotherapy by inducing pyroptosis and suppressing immune resistance simultaneously (Fig. 6c).<sup>248</sup> In the presence of homologous cancer cell membranes and RhB, this nanozyme enabled precise tumor targeting for FLI. CeO<sub>2</sub> catalyzed the *in situ* generation of H<sub>2</sub>O<sub>2</sub> to induce glucose oxidation and ROS production within the hypoxic TME, while GOx-like AuNPs induced high temperature upon NIR irradiation *via* photothermal effects. By depleting glucose, they amplified the thermotherapeutic effect under hypoxic conditions, consequently inhibiting HSP70. The enhanced thermotherapy, accompanied by abundant ROS generation, led to the release of cyt c and activation of caspase 3, thereby inducing pyroptosis.

Furthermore, increasing evidence supports the notion that a rational combination of PTT with multiple treatment modalities can significantly enhance the therapeutic efficacy of immunotherapy. For example, thermal energy generated by PTT enhances the enzyme-like activity, thereby augmenting the efficacy of ST and CDT. ST generates H<sub>2</sub>O<sub>2</sub> and gluconic acid, and with the increase in H<sub>2</sub>O<sub>2</sub> concentration and acidity in the TME, the efficiency of the Fenton-like reaction is developed. Therefore, the combination of PTT with nanozymes capable of mediating CT and ST simultaneously holds the potential to induce a cascading amplification effect. Conventional photothermal agents often exhibit side effects on normal tissues due to their “always-on” capability. Zhu *et al.* utilized RuTe<sub>2</sub> nanozymes as a platform to load GOx and TMB molecules (RGT NRs).<sup>249</sup> Oxidized TMB (oxTMB) exhibited robust NIR photothermal properties when oxidized by  $\cdot\text{OH}$ , resulting in tumor-specific activation of PTT. PTT enhanced the consumption of glucose and the production of ROS in tumors by enhancing CDT, resulting in a large release of antigens and triggering a systemic immune response. Following treatment with oxTMB plus RGT and 808 nm laser irradiation, no evidence of tumor metastasis was observed in the lungs of mouse models, indicating that oxTMB in combination with NIR



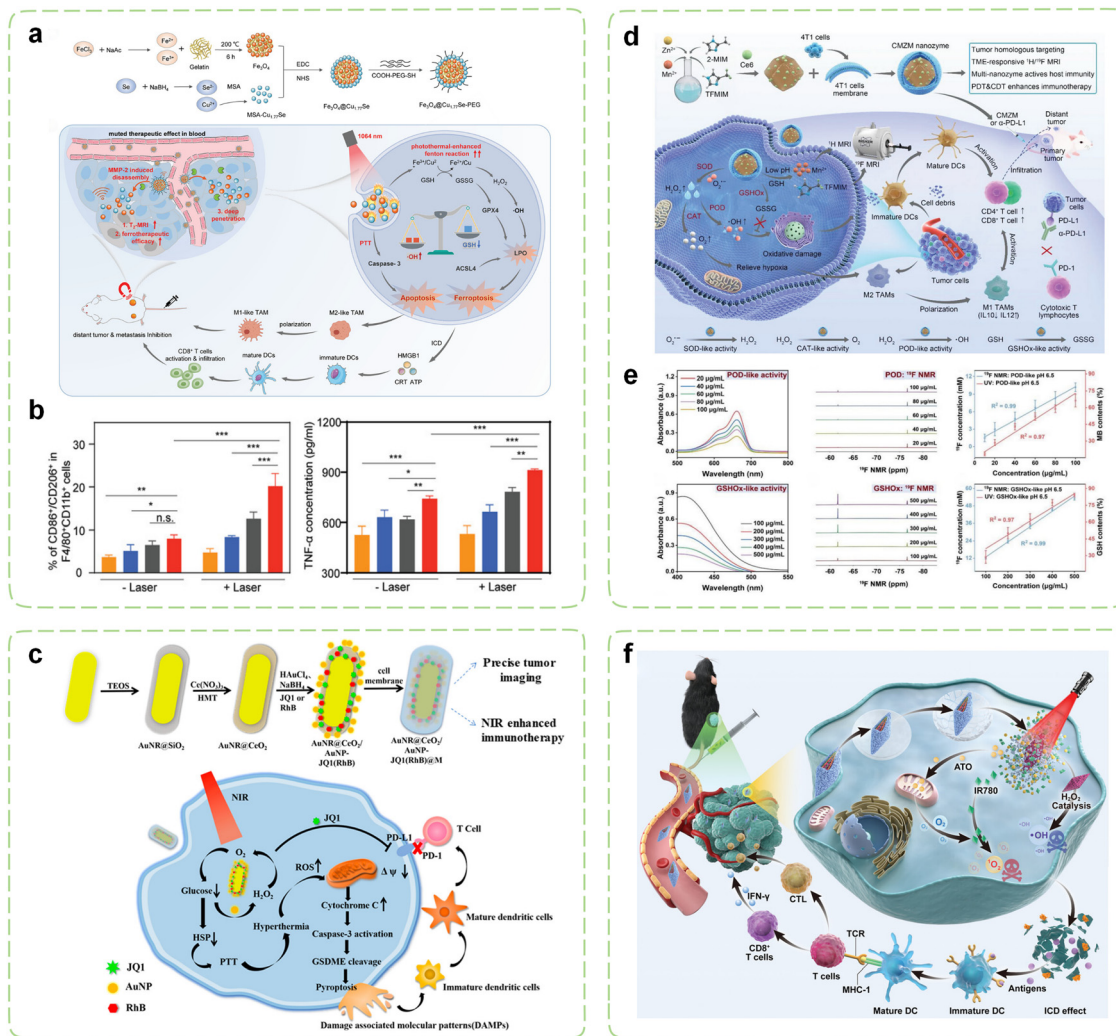


**Fig. 6** Combination cancer immunotherapy initiated by PT-assisted nanozymes. (a) Schematic diagram of visualized combination photothermal immunotherapy mediated by MMP-2-activatable  $\text{Fe}_3\text{O}_4@_{\text{Cu}_{1.77}}\text{Se}$  nanozymes and its synthesis route. (b) The ratio of M1 to M2-TAMs ( $n = 3$ ) and the secretion of TNF- $\alpha$  in serum after treatment ( $n = 3$ ). From left to right are the PBS group,  $\text{Fe}_3\text{O}_4$  group,  $\text{Cu}_{1.77}\text{Se}$  group, and  $\text{Fe}_3\text{O}_4@_{\text{Cu}_{1.77}}\text{Se}$  group. Reproduced with permission.<sup>246</sup> Copyright 2022, Wiley-VCH. (c) Schematic diagram of synergistic induction of pyroptosis to assist the ICB therapy. Reproduced with permission.<sup>248</sup> Copyright 2023, American Chemical Society. (d) Schematic diagram of the reversal of immunosuppressive TME through ROS storms induced by CMZM with the multienzyme-like activity. (e) Determination of enzymatic activity of CMZM using the UV vis NIR method and the <sup>19</sup>F NMR method. Reproduced with permission.<sup>250</sup> Copyright 2023, Wiley-VCH. (f) Schematic diagram of enhanced lung cancer immunotherapy through the integration of PTT, PDT, CDT using AP-HAI nanozyme probe under NIR imaging guidance. Reproduced with permission.<sup>252</sup> Copyright 2023, Wiley-VCH.

stimulation profoundly inhibited the growth of metastatic tumors.

**5.1.2. Combination immunotherapy of nanozymes and PDT.** As another form of PT, PDT depends on photosensitizers to convert adjacent  $\text{O}_2$  and  $\text{H}_2\text{O}$  into cytotoxic ROS, thereby inducing aberrant tumor cell death and augmenting the immunogenicity of the TME.<sup>265</sup> PDT and POD-like nanozymes can synergistically induce ROS storms and doubly activate immune responses in TME. However, the activation effect of this combination therapy on DCs appears to be insufficient due to the inadequate  $\text{H}_2\text{O}_2$  levels ( $50\text{--}100 \times 10^{-6}$  M) and the overexpression of GSH ( $1\text{--}10$  mM) in the TME.<sup>266</sup> To deal with this problem, Zhou *et al.* synthesized a multienzyme-like (SOD,

CAT, POD, GSHOx) nano-immunomodulator (CMZM) to enhance the disruption of ROS homeostasis in all aspects (Fig. 6d).<sup>250</sup> Under the overexpression of GSH and acidic conditions in the TME, CMZM expedited the release of manganese ions and chlorin e6 (Ce6), facilitating the disruption of  $\text{H}_2\text{O}_2$  equilibrium within the TME and the redox metabolism within tumor cells. Simultaneously, it strengthened the  $19\text{F}/1\text{H}$  T1-weighted MRI and fluorescence imaging (FLI) of the tumor, enabling precise tumor localization for real-time monitoring of tumor growth during immunotherapy. In the 4T1 tumor-bearing mice models, the polarization efficiency of M1 macrophages significantly increased in the CMZM + laser group. Upon combination with  $\alpha\text{PD-L1}$ , the tumor growth inhibition





rates of primary and distant tumors were considerably higher in the CMZM + laser group compared to the control group, which indicated this approach overcame the limitations of ICB therapy caused by insufficient immune response in “cold” tumors, achieving a significant leap in the suppression of metastatic tumors. It is worth noting that 19F NMR can also determine the POD-like activity and GSHOx-like activity of CMZM (Fig. 6e), which represented a novel *in vivo* application for monitoring the enzyme-like activities of nanozymes.

Lowering PD-L1 expression may reduce immune inhibitory signals for T cells, promoting recruitment and activation of T cells, thereby enhancing immune response against tumors.<sup>267</sup> The combination immunotherapy of nanozymes and PDT has demonstrated significant impact by inducing PD-L1 deactivation to reverse and reshape the tumor immune microenvironment into an immunostimulatory milieu. Liao *et al.* devised a facile one-pot coprecipitation method for synthesizing cluster-structured nanoparticles (CNPs) composed of Fe<sub>3</sub>O<sub>4</sub> and iron chlorophyll (Chl/Fe) photosensitizers to treat bladder cancer.<sup>251</sup> CPBA was then utilized to modified CNPs to enhance targeted delivery through biorecognition of highly expressed glycoprotein receptors on cancer cells, thereby boosting the Fenton reaction rate for CDT and lowering cancer cells' antioxidant capacity to sensitize them to subsequent PDT treatment. Inspired by the transurethral BCG treatment procedure, nano-photosensitizer intravesical instillation was employed instead of systemic circulation *via* intravenous injection. These locally delivered photosensitizers can directly interact with bladder tumors, minimizing systemic dosing-related adverse effects. CDT-PDT therapy significantly suppressed tumor growth, elevating the survival rate of MB49-bearing mice from 0% to 91.7%. Moreover, CDT-PDT exhibited potential in reducing immune suppressive factors including PD-L1, IDO-1, and TGF- $\beta$ , thereby reshaping the immune microenvironment to prevent tumor recurrence.

What's more, the integration of PDT-based multimodal treatment strategy has also been demonstrated to possess superior performance in tumor immunotherapy. Cui *et al.* innovatively fabricated theragnostic photo-enhanced nanozymes probes (AP-HAI), which could be utilized for effective treatment of lung cancer under NIR imaging guidance (Fig. 6f).<sup>252</sup> The abundant amino groups in HAS not only conferred biocompatibility to the probe but also enhanced the affinity of ultra-small nPt nanozymes with H<sub>2</sub>O<sub>2</sub> by hydrogen bonding, hence further boosting the catalytic therapy with increased POD-like activity. The loaded ATO impaired tumor respiratory metabolism, causing oxygen retention and thereby enhancing the effectiveness of IR780-mediated PDT. Catalytic therapy and PDT synergistically promoted the production of a large amount of ROS in tumor cells, leading to severe disruption of redox balance and inducing ICD. Utilizing the photothermal properties of AuP and ATO for photothermal surgery at the tumor site enhanced blood perfusion, facilitated aggregation of

endogenous immune cells and nanozyme probes, therefore accelerating the ablation of lung tumors.

## 5.2. SDT- assisted nanozymes

SDT is an emerging cancer treatment modality that involves the activation of low-intensity ultrasound (US) *via* sonosensitizers, which generate toxic ROS and induce apoptosis in tumor cells. Several studies have demonstrated that US-triggered SDT can significantly activate immune responses through releasing TAAs from the cells. Currently, SDT has demonstrated its superior performance in exhibiting minimal invasiveness and maximal tissue penetration depth.<sup>268</sup> The multimodal imaging capability of nanozymes, combined with US imaging, provides a robust tool for precise tumor localization and treatment. Also, US serves as an activation trigger for precise initiation of therapeutic responses for its high penetrative power and flexible controllability. Consequently, there is a growing focus on collaborative treatment strategies that combine SDT with nanozyme technology.

Optimizing ROS production *via* TME regulation is imperative to augment the effectiveness of SDT even further. On this basis, the synergistic combination of CDT and SDT holds the potential to yield enhanced ICD outcomes. Xue *et al.* synthesized CoFe<sub>2</sub>O<sub>4</sub> nanoflowers (CFP) with multienzyme-like activities using conventional solvothermal techniques.<sup>269</sup> CFP, acting as a highly efficient sound sensitizer, possessed a narrower band gap, facilitating the separation of US-triggered electron (e<sup>-</sup>)/hole (h<sup>+</sup>) pair from the energy band and thereby mitigating the challenges posed by widespread hypoxia within the TME (Fig. 7a). This characteristic also contributed to partially overcoming treatment resistance. Additionally, the inherent redox properties of CFP, including Co<sup>2+</sup>/Co<sup>3+</sup> and Fe<sup>2+</sup>/Fe<sup>3+</sup>, exhibited robust Fenton-like and CAT-like activities. Consequently, this combination enabled the generation of abundant ROS while simultaneously relieving hypoxia. The amplified cytotoxic ROS produced by the combination therapy effectively induced ICD and repolarized M2 macrophages into M1 phenotypes, synergistically inhibiting detrimental tumor metastasis with ICB therapy (Fig. 7b).

The thermal effect plays an important role in the clinical field of medicine for disease treatment. In addition to the photothermal impact that is induced by light, various external stimulators, such as US, can also elicit the generation of free radicals for thermodynamic therapy (TDT) by activating diverse substances.<sup>272</sup> Xue *et al.* incorporated AIPH onto the surface of a ZrO<sub>2-x</sub>@Pt Schottky junction to optimize the band structure of it and enhance the efficient production of ROS under US activation (Fig. 7c).<sup>270</sup> AIPH could be activated by US-induced transient hyperthermia, leading to the self-decomposition and the generation of alkyl radicals (Fig. 7d). Together with the ROS generated during the US sensing process, this synergistic effect augmented the oxidative stress level in tumor cells. Additionally, Pt nanozymes with CAT-like activity sustainably produced <sup>1</sup>O<sub>2</sub> during SDT by mitigating hypoxia in the TME. Significantly, the nanotherapeutic system triggered the release of diverse DAMPs through SDT-TDT combination therapy, which





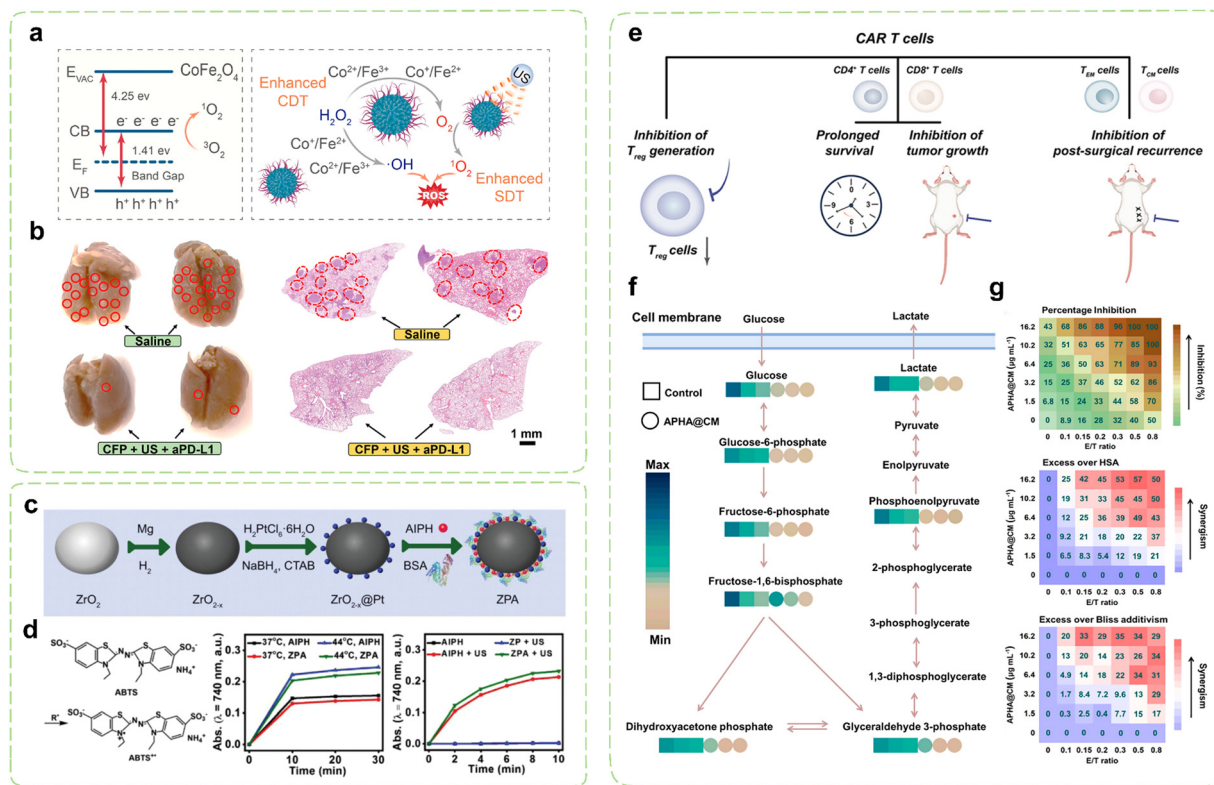


Fig. 7 Combination cancer immunotherapy initiated by SDT-assisted nanozymes. (a) Energy level diagram of CFP and its mechanism diagram for activating synergistic immunotherapy. (b) Histological slices of lung metastases in the 4T1 mice model, with metastatic nodules highlighted by red circles. Reproduced with permission.<sup>269</sup> Copyright 2021, American Chemical Society. (c) The synthesis route of  $ZrO_{2-x}@Pt/AIPH$  (ZPA) nanozyme. (d) Illustration and testing of alkyl radical generation characteristics for ZPA-mediated TDT. Reproduced with permission.<sup>270</sup> Copyright 2022, Wiley-VCH. (e) Immune activation effects of CAR T cell therapy. (f) Metabolomics analysis of tumor glycolysis to evaluate the GOx-like performance of APHA@CM. (g) Evaluation of the enhanced antitumor effect of combination therapy mediated by APHA@CM on CAR T cell therapy using the HSA and Bliss additive models. Reproduced with permission.<sup>271</sup> Copyright 2023, American Chemical Society.

demonstrated its potential as a potent inducer of ICD in immunotherapy.

In recent years, extensive research has been conducted on multimodal treatment strategies that synergistically combine SDT with diverse therapeutic modalities. These approaches have demonstrated remarkable synergistic effects in inducing ICD. For example, Xue *et al.* immobilized GOx and the US sensitizer IR780 onto the surface of PdPt NPs *via* covalent bonding and electrostatic interaction respectively, to facilitate PTT-enhanced SDT-ST combination therapy.<sup>273</sup> The CAT-like activity promoted SDT sensitization while exacerbating glucose consumption. Simultaneously, its exceptional photothermal conversion capability facilitated the thermal ablation of tumors and elicited robust ICD under the synergistic influence of the trimodal treatment. In another study, Liu *et al.* prepared a HA-modified multienzyme-like nanoplatform based on Au NPs and a hollow black  $TiO_2$  nanosphere modified by carbon dots (HABT-C@HA), which combined ST, CDT and SDT together.<sup>274</sup> The trienzyme-like (CAT, GOx, and POD) HABT-C generated adequate oxygen to relieve hypoxia and facilitate ROS production. Moreover, theoretical calculations and experimental results indicated that the electron-rich sites present in the  $TiO_2$  lattice significantly enhanced electron-hole

separation, reduced the surface adsorption energy of  $H_2O$  and  $O_2$ , and improved ROS production efficiency under US irradiation. This led to extraordinary oxidative damage to cancer cells. Furthermore, immunohistochemistry, flow cytometry, and qPCR analyses revealed a reduction in immunosuppressive mediators and an augmentation in the infiltration of CTLs after the treatment. These findings indicated that antitumor immunity was effectively stimulated by the combination therapy.

Moreover, SDT-assisted TME reprogramming can pave the way for other immunotherapies. Chimeric antigen receptor (CAR) T cell therapy is a groundbreaking cancer immunotherapy that utilizes genetic modification and transformation of T cells extracted from patients *in vitro* in order to achieve specific recognition and effective eradication of tumor cells (Fig. 7e).<sup>275</sup> Despite its remarkable success, the immunosuppressive micro-environment of solid tumors hinders the efficacy of CAR-T cells. Several approaches have been proposed to enhance the anti-tumor efficacy of CAR-T cell therapy, including combining it with other anticancer therapies to expand its clinical effectiveness. Jiang *et al.* developed a CAR T cell membrane-camouflaged multifunctional nanocatalyst (APHA@CM) to improve it.<sup>271</sup> The CAR T cell membrane modified with



$\alpha$ -CD19 single-chain variable fragment established an environment conducive to the specific elimination of NALM 6 tumor cells by the nanozyme. PDA-coated AuNPs directly deprived glucose, thereby suppressing the glycolytic metabolic pathway and significantly reducing lactate efflux into the extracellular environment (Fig. 7f), thus creating favorable conditions for the proliferation and differentiation of CAR-T cells, while the photothermal properties extended from the visible light region to the NIR-II region, offering advantages for treating deep-seated tumors. Furthermore, the incorporation of HRP enabled hypoxia relief and enhanced the synergistic SDT-PTT induced by Au/PDA NPs, thereby promoting ICD and establishing an immunogenic TME. The findings suggest that APHA@CM could augment the effectiveness of CAR T cell therapy for solid tumors by reprogramming immune suppression and regulating

the metabolic microenvironment (Fig. 7g). Moreover, multi-modal imaging capabilities such as PA and NIR-II “turn on” fluorescence facilitated precise regulation of the TME and CAR T cell therapy.

### 5.3. RT/CT-assisted nanozymes

Currently, RT and CT are mainstream clinical interventions for tumors. Besides their direct killing effects, both modalities can trigger ICD *via* direct cytotoxicity.<sup>29,276</sup> When combining them with nanozyme technology, they can enhance the effectiveness of nanozyme-mediated cancer immunotherapy by altering tumor tissue vascular permeability, increasing H<sub>2</sub>O<sub>2</sub> levels in the TME, and modulating the composition of immune cells within the TME. In return, nanozymes effectively leverage their unique physicochemical properties to engage in a series of

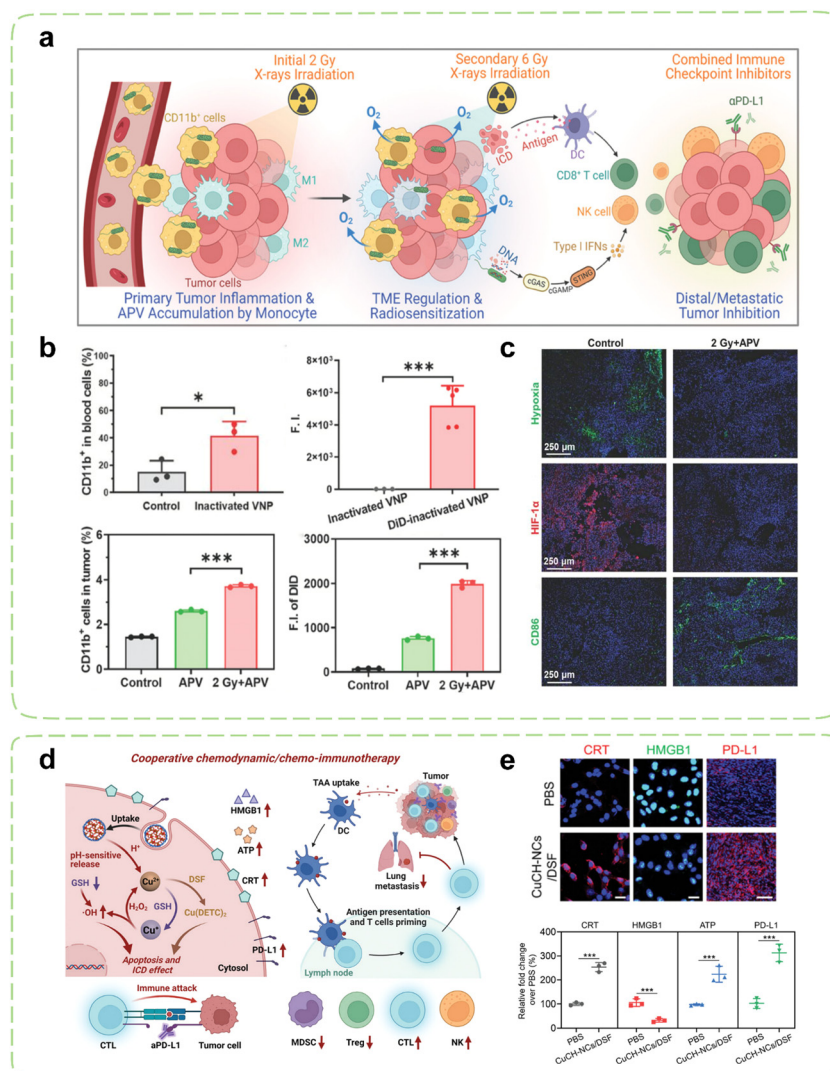


**Fig. 8** Combination cancer immunotherapy initiated by RT/CT-assisted nanozymes. (a) Schematic diagram illustrating the alleviation of hypoxic microenvironment by APV and its promotion of antitumor radioimmunotherapy. (b) Tumor-specific delivery of APVs by monocytes and the influence of X-rays on the delivery efficiency. (c) Comparison of immunofluorescent staining of the B16-F10 tumors microenvironment following initial X-rays irradiation with the control group without X-rays irradiation. Reproduced with permission.<sup>279</sup> Copyright 2023, Wiley-VCH. (d) Schematic diagram of the collaborative chemodynamic/chemo-immunotherapy mediated by CuCH NCs. (e) Analysis of ICD biomarkers induced by the CuCH-NCs/DSF combination in 4T1 cells. Reproduced with permission.<sup>280</sup> Copyright 2022, Wiley-VCH.



biochemical reactions with active substances in the TME, thereby modulating the TME and achieving biochemical sensitization within tumors.<sup>77</sup> The foremost challenge confronting RT and CT is tumor hypoxia, which not only hampers the treatment efficacy but also indirectly fosters immunosuppression in cancer, thereby impacting therapeutic outcomes.<sup>73</sup> Thus, *in situ* oxygen-generating nanozyme system for synergistic RT/CT may offer a promising avenue to overcome this hurdle.

Bacteria-mediated drug delivery strategies is a prominent research focus within the field of drug delivery.<sup>277</sup> Significantly, bacterial carriers have the capacity to stimulate the immune system and augment the synergistic therapeutic impact on tumors when combined with other treatment modalities such as immunotherapy and RT.<sup>278</sup> Yang *et al.* developed a special bacterial carrier by coating the surface of VNP20009 with AuPt bimetallic nanozymes (APV).<sup>279</sup> The hybrid nanozymes possessed high CAT-like activity and demonstrated excellent radiosensitizer effects (Fig. 8a). The resultant activation of the cGAS-STING pathway and subsequent production of inflammatory cytokines enhanced the antitumor immune activity. Upon injection into the bloodstream, inactive VNP20009 bacteria were primarily engulfed by CD11b<sup>+</sup> immune cells and subsequently accumulated in the tumor areas (Fig. 8b). Pre-irradiation of the tumor with low-dose X-rays (2Gy) after injection facilitated the efficient targeted transmission of APV by immune cells through tumor inflammation (Fig. 8b and c). Results demonstrated that the enhanced APV transmission could augment RT and ICB therapy. Moreover, it led to a significant increase in the proportion of infiltrating CD8<sup>+</sup> T cells in the TME.

The combination of chemotherapeutic drugs and nanozymes also has infinite potential in synergistic complementation towards antitumor effects.<sup>281</sup> Deng *et al.* reported a self-oxygenation/degradable inorganic nanozyme reactor (CDSMD NR) that can effectively alleviate tumor hypoxia for enhancing the sensitivity of chemo-immunotherapy.<sup>282</sup> CaO<sub>2</sub> underwent significant hydrolysis to produce H<sub>2</sub>O<sub>2</sub>, which acted as a “fuel” and decomposed through a shell to generate oxygen in the presence of MnO<sub>2</sub>. *In vivo* experiments substantiated the efficacy of CDSMD NRs in mitigating hypoxia in mice bearing B16F10 tumors. In combination with CTLA-4, these nanoparticles demonstrated the ability to enhance CTLA-4 mediated ICB and facilitated intratumoral expansion of CD8<sup>+</sup> T cells, while concurrently diminishing the population of Tregs. Simultaneously, it was observed that DOX fostered optimal maturation of DCs, thereby exerting a further reversal of the immunosuppressive TME. ICB has been clinically employed as an effective strategy for treating malignant tumors, yet it still faces challenges in achieving high response rates due to insufficient PD-L1 expression on certain tumor cells, such as triple-negative breast cancer (TNBC).<sup>283</sup> To deal with this problem, Chen *et al.* successfully synthesized individual albumin nanocages (CuCH NCs) through albumin template biomineralization using pH-activated POD-like proenzymes (Fig. 8d).<sup>280</sup> The acidic TME triggered the release of a substantial amount of

Cu<sup>2+</sup>, while non-toxic DSF formed chelates with Cu<sup>2+</sup> *in situ*, resulting in the synthesis of Cu (DETC)<sub>2</sub>. This led to a significant enhancement in cytotoxicity and subsequent CT-induced damage. Additionally, Cu<sup>2+</sup> was spontaneously reduced by GSH to Cu<sup>+</sup>, which acted as a catalyst for H<sub>2</sub>O<sub>2</sub> to generate •OH, thereby inducing chemodynamic damage to cells. The synergistic effect of CuCH-NCs/DSF promoted tumor cell apoptosis and cuproptosis, enhanced the ICD effect (Fig. 8e), and up-regulated PD-L1 expression in 4T1 breast tumor models, confirming the efficacy of combination therapy to enhance PD-L1 expression for *in vivo* ICB therapy, thereby enhancing the therapeutic efficacy against TNBC.

#### 5.4. GT- assisted nanozymes

GT utilizing gas molecules is an immensely promising treatment modality in the field of nanomedicine. The innate low toxicity of gas molecules obviates the possibility of systemic toxicity, thus rendering GT as a “green” selective cancer treatment approach.<sup>284</sup> Certain gas molecules, namely O<sub>2</sub>, can facilitate attenuation of cancer treatment resistance and amelioration of drug delivery efficacy. Other gas molecules, such as hydrogen sulfide (H<sub>2</sub>S), nitric oxide (NO), and carbon monoxide (CO), function as vital physiological signaling molecules responsible for homeostasis maintenance within the human body. This section elucidates the outcomes of GT-assisted nanozyme-mediated cancer immunotherapy.

Considered a fundamental aspect of the TME, hypoxia impairs the functionality of immune cells and severely curtails the effectiveness of certain cancer therapies. Yang *et al.* have evidenced that Hyperbaric oxygen (HBO) therapy can effectively surmount solid hypoxia in tumor tissue, not only augmenting the likelihood of drug penetration into tumors but also aiding PDT to induce ROS production in tumor cells.<sup>285,286</sup> To explore the enhancing effect of HBO on CDT, they utilized probiotic EcN and supplemented it with Na<sub>2</sub>SeO<sub>3</sub> during its cultivation process, prompting the bacteria to secrete Se NPs in the form of outer membrane vesicles (Se@OMV) (Fig. 9a).<sup>287</sup> Upon targeted delivery to tumor cells, Se@OMV acted as a nanozyme facilitating electron transfer from GSH to O<sub>2</sub>, resulting in the generation of •O<sub>2</sub><sup>-</sup>. HBO promoted the catalysis of GOx, thus inducing oxidative damage to tumor cells and triggering strong ICD. By synergistically leveraging the immune-stimulatory effects of EcN, the treatment substantially boosted the immunogenicity of tumor cells and significantly enhanced the infiltration of CTLs, thus facilitating ICB treatment and eliciting long-term immune memory (Fig. 9b).

As crucial gaseous signaling molecules in the human body, H<sub>2</sub>S possess distinctive therapeutic properties against cancer. Nonetheless, unregulated generation may result in deleterious cytotoxic effects.<sup>291</sup> The fabrication of responsive nanocarriers serves to enhance the targeted transportation of gas to tumor regions, thereby mitigating the potential hazards associated with gas toxicity. For example, Shen *et al.* devised a hybrid nanozyme that exhibited metalloprotein-like properties by inducing the *in situ* growth of iron sulfide in GOx (FeS@GOx).<sup>292</sup> GOx boosted the CDT induced by FeS, thereby





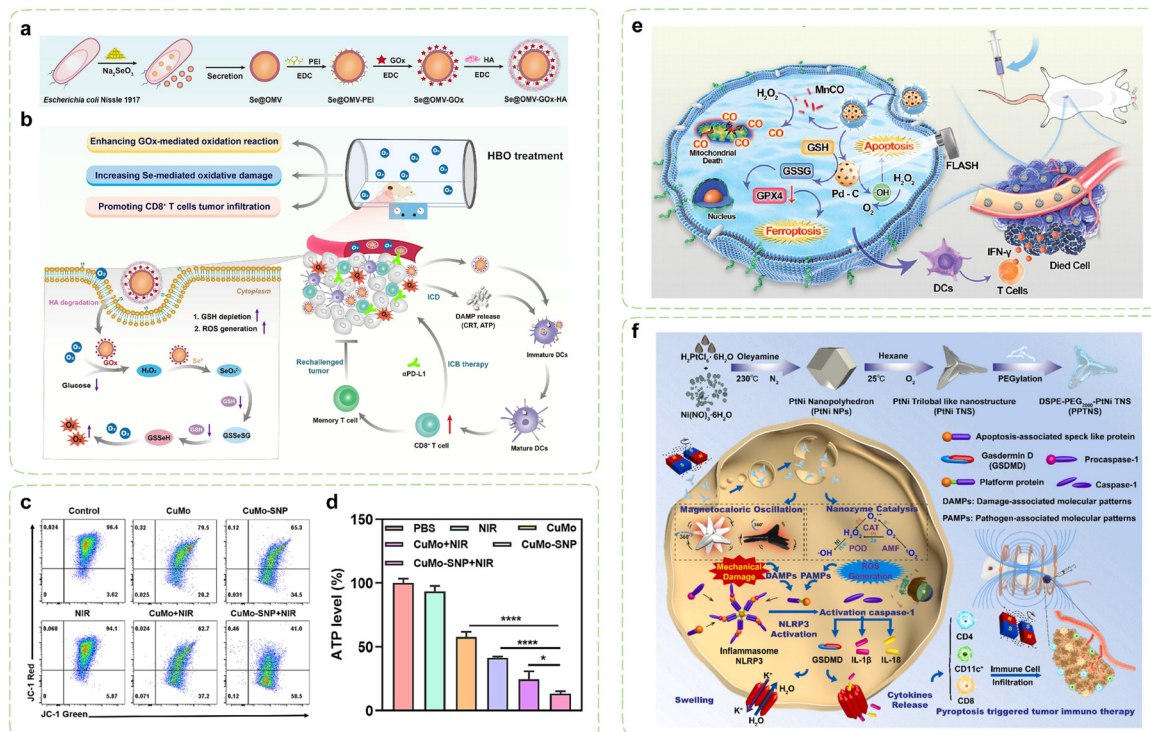


**Fig. 9** Combination cancer immunotherapy initiated by GT-assisted nanozymes and MT-assisted nanozymes. (a) Illustration of the synthesis of hybrid nanozymes secreted by probiotic EcN in the form of outer membrane vesicles (OMV). (b) Schematic diagram of the intracellular metabolic disruption and immune microenvironment remodeling induced by HBO-assisted nanozyme therapy. Reproduced with permission.<sup>287</sup> Copyright 2023, Elsevier. (c) Mitochondrial dysfunction examined through the evaluation of mitochondrial membrane potential (MMP). (d) Percentages of ATP concentration in different treatment groups compared to the control group. Reproduced with permission.<sup>288</sup> Copyright 2023, Elsevier. (e) Schematic diagram of the synergistic FLASH RT radiation immunotherapy with Pd-C SAzyme and CO gas therapy. Reproduced with permission.<sup>289</sup> Copyright 2023, Wiley-VCH. (f) Schematic diagram of the magnetic cancer immunotherapy induced by nanozyme-triggered pyroptosis under alternating magnetic field. Reproduced with permission.<sup>290</sup> Copyright 2023, Elsevier.

expediting the cascade generation of  $\cdot\text{OH}$ , while gluconic acid effectively lowered the intracellular pH, further facilitating the degradation of FeS and ensuing release of  $\text{H}_2\text{S}$ . The presence of  $\text{H}_2\text{S}$  repressed the activity of ROS scavenging enzymes (such as TrxR and CAT) and culminated in the accumulation of ROS in tumor cells, thus promoting ICD.

In addition to  $\text{H}_2\text{S}$ , NO also plays multiple roles as a signaling molecule in tumor therapy. Arginine functions as a prodrug which undergoes oxidation to generate NO. Liu *et al.* synthesized chiral Ru nanozymes *via* the coordination of Ru nanozymes and arginine.<sup>293</sup> Through simultaneous modulation of OXD and nitric oxide synthase (NOS) activity, these nanozymes, especially L-Arginine@Ru nanozymes, exhibited rapid generation of  $^1\text{O}_2$  and  $\text{O}_2$  and subsequently induced abundant production of NO, which effectively activated 5'-AMP sensitized protein kinases and the NF- $\kappa$ B pathway, thereby enhancing M1 phenotype polarization. The observed reduction in GPX4 levels and apoptotic protein (Bcl2) in tumor cells suggested that excessive  $^1\text{O}_2$  induced both tumor cell apoptosis and ferroptosis, thus achieving a synergistic "cocktail therapy" for antitumor treatment in conjunction with NO. Oxidative stress can induce mitochondrial protective autophagy, thereby reducing oxidative damage to mitochondria.<sup>294</sup> Fortunately,

studies have shown that NO can modulate protective autophagy induced by external stimuli by inhibiting autophagosome formation, thereby assisting in maximal inhibition of ATP production in response to intracellular oxidative damage.<sup>295</sup> In another study, sodium nitroprusside (SNP) as another prodrug of NO were encapsulated within a hollow Mo-doped Cu9S5 nanozyme (CuMo-SNP).<sup>288</sup> The variable metal pairs ( $\text{Cu}^{+2+}$ ,  $\text{Mo}^{4+/6+}$ ) imparted CuMo SNPs with POD and GSHox-like activities, which synergistically enhanced intracellular oxidative stress on mitochondria. As a GSH-responsive NO donors, the continuous production of NO by SNP hindered the formation of autophagosomes, leading to detrimental effects on the protective autophagy process of mitochondria (Fig. 9c), which contributed to reduced ATP levels in tumors (Fig. 9d), thereby inhibiting the synthesis of HSPs and amplifying the effectiveness of mPTT. Additionally, the ROS/NO-mediated mPTT demonstrated a significant increase in recruiting TILs and suppressed distant tumors in combination with  $\alpha$ PD-L1.

CO is a vital mitochondrial-associated neurotransmitter. CO treatment of cancer cells accelerates the second phase of mitochondrial respiration, which is the principal oxygen-consuming stage.<sup>296</sup> Consequently, cancer cells are compelled to consume more oxygen for energy production. This metabolic



process results in mitochondrial depletion and ROS generation, thereby imparting pro-apoptotic effects that lead to cancer cell death. Jiang *et al.* developed a MnCO-loaded porous Pd-C SAzyme covered by 4T1 cancer cell membrane which can sensitize FLASH radioimmunotherapy (Fig. 9e).<sup>289</sup> MnCO was triggered by the overexpression of H<sub>2</sub>O<sub>2</sub> within tumor cells, resulting in the generation of CO and the induction of mitochondrial apoptosis. The liberated Mn<sup>2+</sup> along with Pd-C SAzyme possessing trienzyme-like activities (CAT, POD and GSHOx) synergistically acted to induce ROS amplification and provoke tumor cell ferroptosis, converted immune-cold tumors into immune-hot tumors, substantially increased the level of CD8<sup>+</sup> T cells and impeded tumor recurrence.

### 5.5. MT- assisted nanozymes

The utilization of magnetic fields in cancer treatment has exhibited promising outcomes, demonstrating their potential as an adjuvant therapy. The application of an external magnetic field can impose a magnetic force on the magnetic materials and deliver them to the tumor areas.<sup>297</sup> When subjected to an alternating magnetic field (AMF), the magnetic materials generate heat, elevating the local temperature of the tumor tissue to over 43 °C, thereby eradicating heat-sensitive tumor cells and achieving targeted therapeutic effects, with minimal impact on adjacent normal tissues and cells.<sup>298</sup> Furthermore, in the last decade, scientists have made considerable progress in cancer treatment by utilizing magnetic fields to instigate a novel facet of “mechanical stimulation”.<sup>299</sup> Under an external magnetic field, the magnetic manipulation of magnetic materials can exert mechanical tension on the cancer cell membrane and organelles, stretching the cytoskeleton, activating ion channels or signal pathways, and transmitting signals to the target cell structure to induce apoptosis and necrosis of cancer cells. Because the cell contents liberated by destroyed tumor cells help to enhance the immune response, the efficacy of anti-tumor immunotherapy can be improved by utilizing magnetic nanozymes and their magnetic responses under an external magnetic field. Li *et al.* developed a versatile immunotherapeutic nanoplatform that achieved efficient tumor immunotherapy through pyroptosis induction (Fig. 9f).<sup>290</sup> PEGylated platinum nickel (PtNi) bimetallic nanomaterials (PPTNS) exhibited a unique “trilobal” structure capable of inducing irregular horizontal and vertical vibrations when subjected to an external AMF, resulting in mechanical force (MF). Furthermore, the magnetic hyperthermia therapy (MHT) triggered by AMF promoted the release of metal ions, effectively enhancing the POD/CAT-like activity, thereby generating a substantial amount of ROS. The dual effect successfully triggered pyroptosis, leading to immune cell recruitment and simultaneous activation. The increase in cytokine concentrations in serum further enhanced the immunoregulatory effects, such as the upregulation of TNF- $\alpha$  and IFN- $\gamma$ . Additionally, PPTNS also exhibited multimodal imaging characteristics such as multispectral photoacoustic tomography (MSOT) and MRI, which ensure both accuracy and efficacy of treatment.

## 6. Conclusions and perspectives

Among the numerous cancer treatment modalities, immunotherapy emerges as the most efficacious and auspicious strategy for impeding tumor recurrence and metastasis, while concurrently augmenting the likelihood of achieving complete tumor eradication. Nevertheless, the limitations of monotherapy seriously hinder the effectiveness of contemporary immunotherapy interventions. The metabolic reprogramming of tumor cells presents viable targets for the catalytic cancer therapy mediated by enzymes. However, most standard enzymes are globular proteins (with a small portion being RNA) and constrained by their natural functions and regulatory mechanisms, demanding high stability in catalytic environments and entailing costly extraction and storage. In contrast, as a promising class of enzyme mimetics, nanozymes exhibit catalytic activity akin to standard enzymes and can achieve specific multifunctional catalytic activities and targeting through design. They are able to maintain high stability in complex *in vivo* environments, which also represents their faster reaction rates and higher substrate conversion rates in tumor catalytic metabolic therapy, thereby yielding superior therapeutic efficacy. Furthermore, they are cost-effective to manufacture, and support scalable production. Consequently, nanozymes have emerged as reliable materials for the development of next-generation cancer nanotherapeutic approaches. This review delineates the particular mechanisms through which nanozymes improve the effectiveness of cancer immunotherapy by disrupting metabolic processes and facilitating synergistic therapy. Elaborate elucidation is provided regarding how nanozymes intervene in six metabolic pathways: redox metabolism, glucose metabolism, amino acid metabolism, lipid metabolism, metal metabolism, and NADH metabolism, which enables a potent reversal of the immunosuppressive TME. What's more, the practical application of multimodal immunotherapeutic approaches is explored. By taking advantage of the synergistic effects of these modalities, nanozymes not only reverse immunosuppressive TME, but also significantly enhances the therapeutic efficacy of current immunotherapy. Additionally, the integration of nanotechnology with multimodal imaging technologies has greatly improved the precision of treatment. The combination of nanozyme technology and cancer immunotherapy can not only break through the bottleneck of monomodal immunotherapy but also further deepen the understanding of nanotechnology in specific cancer immunotherapy.

Despite the notable progress made in this novel immunotherapy, there are still some challenges to be addressed before achieving clinical translation. These include:

(1) Tumor cells possess numerous metabolic pathways and exhibit a high degree of metabolic adaptability. In order to minimize stress-induced damage, tumor cells can promptly switch or activate alternative metabolic pathways when encountering obstacles. Currently, synthetic nanozymes exhibit a narrower range of metabolic regulatory functions compared to the standard enzymes, primarily focusing on



redox metabolic processes. Future efforts may involve the design or simulation of a diverse range of expanded enzyme-like activities to diversify the types of nanozymes, thereby coordinating and controlling more comprehensive metabolic pathways. For example, nucleotide metabolism dysregulation has a significant impact on almost all malignant cell activity across different cancer types.<sup>300</sup> In addition to its typical role as a substrate for nucleic acid biosynthesis, nucleotides also provide fuel for a highly active series of processes within cancer cells. Thus, nucleotide synthesis inhibitors have great potential as a component of yet-to-be-fully-realized combination therapy strategies.

(2) Currently, most nanozyme drugs target the substrates and products of metabolic pathways, while there is still insufficient research on the targeted effects of key enzymes or signaling pathway regulatory molecules in intermediate metabolic processes. Therefore, integrating multi-omics analyses such as genomics, transcriptomics, and proteomics can systematically uncover the tumor metabolic network and reveal potential targets. This will be a new direction for the future development of nanozyme drugs research.

(3) There is metabolic crosstalk between cancer cells and immune cells within the TME. For example, cancer cells compete with immune cells for essential nutrients, directly reducing the necessary nutrient supply to immune cells and impairing their functions. At the same time, immune cells in the TME also exhibit metabolic communication and cooperation. By studying the underlying mechanisms, we can develop regulatory nanozyme drugs that specifically target immune cell metabolism and open up a new chapter in nanozyme metabolic immunotherapy.

(4) Compared with standard enzymes, the toxicity and safety of nanozymes remain one of the main obstacles to their clinical use. Therefore, integrating relevant approaches to enhance the biocompatibility of nanozymes represents a future direction for development. Detailed studies on the *in vivo* stability, immunogenicity, and relevant pharmacokinetics of nanozyme drugs are necessary to better understand their fate in the body and assess their long-term *in vivo* toxicity. Meanwhile, research on the next generation of biodegradable nanozyme materials is also of great importance to enable the widespread clinical application of nanozymes.

## Declarations

### Ethics approval and consent to participate

Not applicable.

### Consent for publication

Not applicable.

## Author contributions

Xiangrui Xu: investigation, conceptualization, visualization, writing – original draft; Yaowen Zhang: writing – review &

editing; Chijun Meng: writing – review & editing; Wenzhuo Zheng: writing – review & editing; Lingfeng Wang: writing – review & editing; Chenyi Zhao: writing – review & editing; Feng Luo: conceptualization, supervision, writing – review & editing. All authors read and approved the final manuscript.

## Data availability

This is a review paper and no new data have been presented.

## Conflicts of interest

The authors declare that they have no known competing financial interests or personal relationships that could have appeared to influence the work reported in this paper.

## Acknowledgements

This study was supported by the National Natural Science Foundation of China Youth Science Fund Project (Grant number 82001107) and the Applied Basic Research Project of Sichuan province (Grant number 2022NSFSC1345). Thanks are given to the Figdraw platform for the assistance in drawing Fig. 1 and 2.

## References

- H. Wang and D. J. Mooney, *Nat. Mater.*, 2018, **17**, 761–772.
- S. Zhu, T. Zhang, L. Zheng, H. Liu, W. Song, D. Liu, Z. Li and C.-X. Pan, *J. Hematol. Oncol.*, 2021, **14**, 156.
- A. D. Waldman, J. M. Fritz and M. J. Lenardo, *Nat. Rev. Immunol.*, 2020, **20**, 651–668.
- P. Bonaventura, T. Shekarian, V. Alcazer, J. Valladeau-Guilemond, S. Valsesia-Wittmann, S. Amigorena, C. Caux and S. Depil, *Front. Immunol.*, 2019, **10**, 168.
- A. C. Huang and R. Zappasodi, *Nat. Immunol.*, 2022, **23**, 660–670.
- W. Ye, A. Olsson-Brown, R. A. Watson, V. T. F. Cheung, R. D. Morgan, I. Nassiri, R. Cooper, C. A. Taylor, U. Akbani, O. Brain, R. N. Matin, N. Coupe, M. R. Middleton, M. Coles, J. J. Sacco, M. J. Payne and B. P. Fairfax, *Br. J. Cancer*, 2021, **124**, 1661–1669.
- E. Bockamp, S. Rosigkeit, D. Siegl and D. Schuppan, *Cells*, 2020, **9**, 2102.
- L. Sun, H. Liu, Y. Ye, Y. Lei, R. Islam, S. Tan, R. Tong, Y.-B. Miao and L. Cai, *Signal Transduction Targeted Ther.*, 2023, **8**, 418.
- M. Cerezo and S. Rocchi, *Cell Death Dis.*, 2020, **11**, 964.
- R. Zhang, X. Yan and K. Fan, *Acc. Mater. Res.*, 2021, **2**, 534–547.
- Y. Wang, X. Jia, S. An, W. Yin, J. Huang and X. Jiang, *Adv. Mater.*, 2023, **36**, 2301810.
- S. Naveen Prasad, V. Bansal and R. Ramanathan, *TrAC, Trends Anal. Chem.*, 2021, **144**, 116429.
- Z. Wang, R. Zhang, X. Yan and K. Fan, *Mater. Today*, 2020, **41**, 81–119.





- 14 J. Wu, J. Chen, Y. Feng, S. Zhang, L. Lin, Z. Guo, P. Sun, C. Xu, H. Tian and X. Chen, *Sci. Adv.*, 2020, **6**, eabc7828.
- 15 L. Alvarado-Ramírez, G. Machorro-García, A. López-Legarrea, D. Trejo-Ayala, M. J. Rostro-Alanis, M. Sánchez-Sánchez, R. M. Blanco, J. Rodríguez-Rodríguez and R. Parra-Saldívar, *Biotechnol. Adv.*, 2024, **70**, 108299.
- 16 G. Kroemer, L. Galluzzi, O. Kepp and L. Zitvogel, *Annu. Rev. Immunol.*, 2013, **31**, 51–72.
- 17 M. Obeid, A. Tesniere, F. Ghiringhelli, G. M. Fimia, L. Apetoh, J. L. Perfettini, M. Castedo, G. Mignot, T. Panaretakis, N. Casares, D. Métivier, N. Larochette, P. van Endert, F. Ciccosanti, M. Piacentini, L. Zitvogel and G. Kroemer, *Nat. Med.*, 2007, **13**, 54–61.
- 18 D. V. Krysko, A. D. Garg, A. Kaczmarek, O. Krysko, P. Agostinis and P. Vandenabeele, *Nat. Rev. Cancer*, 2012, **12**, 860–875.
- 19 B. Decraene, Y. Yang, F. De Smet, A. D. Garg, P. Agostinis and S. De Vleeschouwer, *Genes Immun.*, 2022, **23**, 1–11.
- 20 J. Fucikova, O. Kepp, L. Kasikova, G. Petroni, T. Yamazaki, P. Liu, L. Zhao, R. Spisek, G. Kroemer and L. Galluzzi, *Cell Death Dis.*, 2020, **11**, 1013.
- 21 C. Cao, T. Zhang, N. Yang, X. Niu, Z. Zhou, J. Wang, D. Yang, P. Chen, L. Zhong, X. Dong and Y. Zhao, *Signal Transduction Targeted Ther.*, 2022, **7**, 86.
- 22 H. Dong, W. Du, J. Dong, R. Che, F. Kong, W. Cheng, M. Ma, N. Gu and Y. Zhang, *Nat. Commun.*, 2022, **13**, 5365.
- 23 J. Yang, H. Dai, Y. Sun, L. Wang, G. Qin, J. Zhou, Q. Chen and G. Sun, *Anal. Bioanal. Chem.*, 2022, **414**, 2971–2989.
- 24 Y. Dai, Y. Ding and L. Li, *Chin. Chem. Lett.*, 2021, **32**, 2715–2728.
- 25 W. Li, J. Yang, L. Luo, M. Jiang, B. Qin, H. Yin, C. Zhu, X. Yuan, J. Zhang, Z. Luo, Y. Du, Q. Li, Y. Lou, Y. Qiu and J. You, *Nat. Commun.*, 2019, **10**, 3349.
- 26 C. Guo, R. Ma, X. Liu, Y. Xia, P. Niu, J. Ma, X. Zhou, Y. Li and Z. Sun, *Chemosphere*, 2018, **210**, 183–192.
- 27 I. Kim, W. Xu and J. C. Reed, *Nat. Rev. Drug Discovery*, 2008, **7**, 1013–1030.
- 28 L. Galluzzi, A. Buqué, O. Kepp, L. Zitvogel and G. Kroemer, *Nat. Rev. Immunol.*, 2017, **17**, 97–111.
- 29 L. Galluzzi, I. Vitale, S. Warren, S. Adjemian, P. Agostinis, A. B. Martinez, T. A. Chan, G. Coukos, S. Demaria, E. Deutsch, D. Draganov, R. L. Edelson, S. C. Formenti, J. Fucikova, L. Gabriele, U. S. Gaipal, S. R. Gameiro, A. D. Garg, E. Golden, J. Han, K. J. Harrington, A. Hemminki, J. W. Hodge, D. M. S. Hossain, T. Illidge, M. Karin, H. L. Kaufman, O. Kepp, G. Kroemer, J. J. Lasarte, S. Loi, M. T. Lotze, G. Manic, T. Merghoub, A. A. Melcher, K. L. Mossman, F. Prosper, Ø. Rekdal, M. Rescigno, C. Riganti, A. Sistigu, M. J. Smyth, R. Spisek, J. Stagg, B. E. Strauss, D. Tang, K. Tatsuno, S. W. van Gool, P. Vandenabeele, T. Yamazaki, D. Zamarin, L. Zitvogel, A. Cesano and F. M. Marincola, *J. Immunother. Cancer*, 2020, **8**, e000337.
- 30 D. Ding and X. Jiang, *Small Methods*, 2023, **7**, 2300354.
- 31 C. B. Rodell, S. P. Arlauckas, M. F. Cuccarese, C. S. Garris, R. Li, M. S. Ahmed, R. H. Kohler, M. J. Pittet and R. Weissleder, *Nat. Biomed. Eng.*, 2018, **2**, 578–588.
- 32 S. Goswami, S. Anandhan, D. Raychaudhuri and P. Sharma, *Nat. Rev. Immunol.*, 2023, **23**, 106–120.
- 33 P. J. Murray, J. E. Allen, S. K. Biswas, E. A. Fisher, D. W. Gilroy, S. Goerdts, S. Gordon, J. A. Hamilton, L. B. Ivashkiv, T. Lawrence and M. Locati, *Immunity*, 2014, **41**, 14–20.
- 34 D. I. Gabrilovich and S. Nagaraj, *Nat. Rev. Immunol.*, 2009, **9**, 162–174.
- 35 N. R. Anderson, N. G. Minutolo, S. Gill and M. Klichinsky, *Cancer Res.*, 2021, **81**, 1201–1208.
- 36 L. Tang, Y. Yin, Y. Cao, C. Fu, H. Liu, J. Feng, W. Wang and X.-J. Liang, *Adv. Mater.*, 2023, **35**, 2303835.
- 37 X. Xiang, J. Wang, D. Lu and X. Xu, *Signal Transduction Targeted Ther.*, 2021, **6**, 75.
- 38 J. J. Xu, B. B. Zheng, S. H. Zhang, X. L. Liao, Q. L. Tong, G. G. Wei, S. Yu, G. X. Chen, A. H. Wu, S. Gao, Y. Y. Qian, Z. Y. Xiao and W. Lu, *Adv. Funct. Mater.*, 2021, **31**, 2008022.
- 39 S. J. Van Dyken and R. M. Locksley, *Annu. Rev. Immunol.*, 2013, **31**, 317–343.
- 40 K. Mehla and P. K. Singh, *Trends Cancer*, 2019, **5**, 822–834.
- 41 M. S. Carlino, J. Larkin and G. V. Long, *Lancet*, 2021, **398**, 1002–1014.
- 42 M. A. Curran, W. Montalvo, H. Yagita and J. P. Allison, *Proc. Natl. Acad. Sci. U. S. A.*, 2010, **107**, 4275–4280.
- 43 G. Morad, B. A. Helmink, P. Sharma and J. A. Wargo, *Cell*, 2021, **184**, 5309–5337.
- 44 S. H. Kiaie, H. Salehi-Shadkani, M. J. Sanaei, M. Azizi, M. Shokrollahi Barough, M. S. Nasr and M. Sheibani, *J. Nanobiotechnol.*, 2023, **21**, 339.
- 45 N. N. P, S. A.-O. Mehla, A. Begum, H. A.-O. Chaturvedi, R. Ojha, C. Hartinger, M. Plebanski and S. A.-O. Bhargava, *Adv. Healthcare Mater.*, 2023, **12**, 2192–2659.
- 46 G. S. R. Raju, E. Pavitra, G. L. Varaprasad, S. S. Bandaru, G. P. Nagaraju, B. Farran, Y. S. Huh and Y.-K. Han, *J. Nanobiotechnol.*, 2022, **20**, 274.
- 47 X. Ding, Z. Zhao, Y. Zhang, M. Duan, C. Liu and Y. Xu, *Small*, 2023, **19**, e2207142.
- 48 F. Attar, M. G. Shahpar, B. Rasti, M. Sharifi, A. A. Saboury, S. M. Rezayat and M. Falahati, *J. Mol. Liq.*, 2019, **278**, 130–144.
- 49 Q. Zhong, Y. Chen, A. Su and Y. Wang, *Sens. Actuators, B*, 2018, **273**, 1098–1102.
- 50 H. Wang, C. Liu, Z. Liu, J. Ren and X. Qu, *Small*, 2018, **14**, 1703710.
- 51 M. Cui, L. Qian, K. Lu, J. Liu, B. Chu, X. Wu, F. Dong, B. Song and Y. He, *Small*, 2024, 202402101.
- 52 Y. Lai, J. Wang, N. Yue, Q. Zhang, J. Wu, W. Qi and R. Su, *Biomater. Sci.*, 2023, **11**, 2292–2316.
- 53 Y. Yang, X. Tan, Y. Wang, B. Shen, Y. Yang and H. Huang, *Chem. Eng. J.*, 2023, **468**, 143703.
- 54 W. W. Zeng, M. A. Yu, T. Chen, Y. Q. Liu, Y. F. Yi, C. Y. Huang, J. Tang, H. Y. Li, M. T. Ou, T. Q. Wang, M. Y. Wu and L. Mei, *Adv. Sci.*, 2022, **9**, 2201703.
- 55 K. Jiang, D. A. Smith and A. Pinchuk, *J. Phys. Chem. C*, 2013, **117**, 27073–27080.
- 56 Z. Tian, J. Li, Z. Zhang, W. Gao, X. Zhou and Y. Qu, *Biomaterials*, 2015, **59**, 116–124.



- 57 X. Xia, J. Zhang, N. Lu, M. J. Kim, K. Ghale, Y. Xu, E. McKenzie, J. Liu and H. Ye, *ACS Nano*, 2015, **9**, 9994–10004.
- 58 X. Hu, F. Li, F. Xia, X. Guo, N. Wang, L. Liang, B. Yang, K. Fan, X. Yan and D. Ling, *J. Am. Chem. Soc.*, 2020, **142**, 1636–1644.
- 59 C. Li, J. Ye, X. Yang, S. Liu, Z. Zhang, J. Wang, K. Zhang, J. Xu, Y. Fu and P. Yang, *ACS Nano*, 2022, **16**, 18143–18156.
- 60 Y. Chong, Q. Liu and C. Ge, *Nano Today*, 2021, **37**, 101076.
- 61 G. Vinothkumar, P. Arunkumar, A. Mahesh, A. Dhayalan and K. Suresh Babu, *New J. Chem.*, 2018, **42**, 18810–18823.
- 62 J.-G. You, Y.-W. Liu, C.-Y. Lu, W.-L. Tseng and C.-J. Yu, *Biosens. Bioelectron.*, 2017, **92**, 442–448.
- 63 Z. Zhao, S. Dong, Y. Liu, J. Wang, L. Ba, C. Zhang, X. Cao, C. Wu and P. Yang, *ACS Nano*, 2022, **16**, 20400–20418.
- 64 L. H. Fu, C. Qi, J. Lin and P. Huang, *Chem. Soc. Rev.*, 2018, **47**, 6454–6472.
- 65 X. Li, Y. Yang, B. Zhang, X. Lin, X. Fu, Y. An, Y. Zou, J.-X. Wang, Z. Wang and T. Yu, *Signal Transduction Targeted Ther.*, 2022, **7**, 305.
- 66 X. Feng, Y. Song, J. S. Chen, Z. Xu, S. J. Dunn and W. Lin, *J. Am. Chem. Soc.*, 2021, **143**, 1107–1118.
- 67 S. Zhang, Y. Li, S. Sun, L. Liu, X. Mu, S. Liu, M. Jiao, X. Chen, K. Chen, H. Ma, T. Li, X. Liu, H. Wang, J. Zhang, J. Yang and X.-D. Zhang, *Nat. Commun.*, 2022, **13**, 4744.
- 68 K. Fan, J. Xi, L. Fan, P. Wang, C. Zhu, Y. Tang, X. Xu, M. Liang, B. Jiang, X. Yan and L. Gao, *Nat. Commun.*, 2018, **9**, 1440.
- 69 S. Ji, B. Jiang, H. Hao, Y. Chen, J. Dong, Y. Mao, Z. Zhang, R. Gao, W. Chen, R. Zhang, Q. Liang, H. Li, S. Liu, Y. Wang, Q. Zhang, L. Gu, D. Duan, M. Liang, D. Wang, X. Yan and Y. Li, *Nat. Catal.*, 2021, **4**, 407–417.
- 70 S. Zhao, H. Li, R. Liu, N. Tao, L. Deng, Q. Xu, J. Hou, J. Sheng, J. Zheng, L. Wang, W. Chen, S. Guo and Y.-N. Liu, *J. Am. Chem. Soc.*, 2023, **145**, 10322–10332.
- 71 N. Vasan, J. Baselga and D. M. Hyman, *Nature*, 2019, **575**, 299–309.
- 72 Z. Shen, Q. Ma, X. Zhou, G. Zhang, G. Hao, Y. Sun and J. Cao, *NPG Asia Mater.*, 2021, **13**, 39.
- 73 D. C. Singleton, A. Macann and W. R. Wilson, *Nat. Rev. Clin. Oncol.*, 2021, **18**, 751–772.
- 74 Y. Wu, Y. Song, R. Wang and T. Wang, *Mol. Cancer*, 2023, **22**, 96.
- 75 Z. Chen, F. Han, Y. Du, H. Shi and W. Zhou, *Signal Transduction Targeted Ther.*, 2023, **8**, 70.
- 76 C. Zhang, X. Wang, J. Du, Z. Gu and Y. Zhao, *Adv. Sci.*, 2021, **8**, 2002797.
- 77 Q. Wang, J. Liu, L. He, S. Liu and P. Yang, *Nanoscale*, 2023, **15**, 12455–12463.
- 78 Y. Zhang, T. Cui, J. Yang, Y. Huang, J. Ren and X. Qu, *Angew. Chem., Int. Ed.*, 2023, **62**, e202307076.
- 79 J. Li, N. Lu, S. Han, X. Li, M. Wang, M. Cai, Z. Tang and M. Zhang, *ACS Appl. Mater. Interfaces*, 2021, **13**, 21040–21050.
- 80 Y. Xing, L. Wang, L. Wang, J. Huang, S. Wang, X. Xie, J. Zhu, T. Ding, K. Cai and J. Zhang, *Adv. Funct. Mater.*, 2022, **32**, 2111171.
- 81 C. Ren, X. Hu and Q. Zhou, *Adv. Sci.*, 2018, **5**, 1700595.
- 82 S. Pansambal, R. Oza, S. Borgave, A. Chauhan, P. Bardapurkar, S. Vyas and S. Ghotekar, *Appl. Nanosci.*, 2023, **13**, 6067–6092.
- 83 W. Gao, J. He, L. Chen, X. Meng, Y. Ma, L. Cheng, K. Tu, X. Gao, C. Liu, M. Zhang, K. Fan, D.-W. Pang and X. Yan, *Nat. Commun.*, 2023, **14**, 160.
- 84 Y. Ren, R. Wang, S. Weng, H. Xu, Y. Zhang, S. Chen, S. Liu, Y. Ba, Z. Zhou, P. Luo, Q. Cheng, Q. Dang, Z. Liu and X. Han, *Mol. Cancer*, 2023, **22**, 130.
- 85 K. Li, H. Shi, B. Zhang, X. Ou, Q. Ma, Y. Chen, P. Shu, D. Li and Y. Wang, *Signal Transduction Targeted Ther.*, 2021, **6**, 362.
- 86 W. Mo, S. Liu, X. Zhao, F. Wei, Y. Li, X. Sheng, W. Cao, M. Ding, W. Zhang, X. Chen, L. Meng, S. Yao, W. Diao, H. Wei and H. Guo, *Adv. Healthcare Mater.*, 2023, **12**, e2300191.
- 87 M. Liang and X. Yan, *Acc. Chem. Res.*, 2019, **52**, 2190–2200.
- 88 P. Yousefpour, K. Ni and D. J. Irvine, *Nat. Rev. Bioeng.*, 2023, **1**, 107–124.
- 89 Y. Guo, Y. Liu, W. Wu, D. Ling, Q. Zhang, P. Zhao and X. Hu, *Biomaterials*, 2021, **276**, 121018.
- 90 Z. Dongye, J. Li and Y. Wu, *Br. J. Cancer*, 2022, **127**, 1584–1594.
- 91 E. J. Hennessy, A. E. Parker and L. A. J. O'Neill, *Nat. Rev. Drug Discovery*, 2010, **9**, 293–307.
- 92 Z. Fan, S. Wu, H. Deng, G. Li, L. Huang and H. Liu, *ACS Nano*, 2024, **18**, 12261–12275.
- 93 M. Yang, J. Li, P. Gu and X. Fan, *Bioact. Mater.*, 2021, **6**, 1973–1987.
- 94 L. Liu, Y. Zhang, S. Zhang and B. Tang, *Adv. Sci.*, 2023, **10**, 2207652.
- 95 T. Zhao, X. Li, H. Li, H. Deng, J. Li, Z. Yang, S. He, S. Jiang, X. Sui, Q. Guo and S. Liu, *Acta Pharm. Sin. B*, 2023, **13**, 4127–4148.
- 96 C. Fu, L. Yu, Y. Miao, X. Liu, Z. Yu and M. Wei, *Acta Pharm. Sin. B*, 2023, **13**, 498–516.
- 97 S. Son, J. H. Kim, X. Wang, C. Zhang, S. A. Yoon, J. Shin, A. Sharma, M. H. Lee, L. Cheng, J. Wu and J. S. Kim, *Chem. Soc. Rev.*, 2020, **49**, 3244–3261.
- 98 Y. Zheng, J. Ye, Z. Li, H. Chen and Y. Gao, *Acta Pharm. Sin. B*, 2021, **11**, 2197–2219.
- 99 M. T. Manzari, Y. Shamay, H. Kiguchi, N. Rosen, M. Scaltriti and D. A. Heller, *Nat. Rev. Mater.*, 2021, **6**, 351–370.
- 100 J. Hou and Y. Xianyu, *Small*, 2023, **19**, e2302640.
- 101 X. Chen, Z. Jia, Y. Wen, Y. Huang, X. Yuan, Y. Chen, Y. Liu and J. Liu, *Acta Biomater.*, 2022, **151**, 537–548.
- 102 J. Yang, A. Griffin, Z. Qiang and J. Ren, *Signal Transduction Targeted Ther.*, 2022, **7**, 379.
- 103 Z. Li, J. Zou and X. Chen, *Adv. Mater.*, 2023, **35**, 2209529.
- 104 Y. Cheng, Z. Qu, Q. Jiang, T. Xu, H. Zheng, P. Ye, M. He, Y. Tong, Y. Ma and A. Bao, *Adv. Mater.*, 2023, **2305095**.
- 105 H. Song, X. Chen, Y. Hao, J. Wang, Q. Xie and X. Wang, *J. Nanobiotechnol.*, 2022, **20**, 431.



- 106 Q. Liang, J. Xi, X. J. Gao, R. Zhang, Y. Yang, X. Gao, X. Yan, L. Gao and K. Fan, *Nano Today*, 2020, **35**, 100935.
- 107 Q. Fu, S. Shen, P. Sun, Z. Gu, Y. Bai, X. Wang and Z. Liu, *Chem. Soc. Rev.*, 2023, **52**, 7737–7772.
- 108 S. Fedeli, J. Im, S. Gopalakrishnan, J. L. Elia, A. Gupta, D. Kim and V. M. Rotello, *Chem. Soc. Rev.*, 2021, **50**, 13467–13480.
- 109 X. Zhang, R. Huang, S. Gopalakrishnan, R. Cao-Milán and V. M. Rotello, *Trends Chem.*, 2019, **1**, 90–98.
- 110 W. Wang, X. Zhang, R. Huang, C. M. Hirschbiegel, H. Wang, Y. Ding and V. M. Rotello, *Adv. Drug Delivery Rev.*, 2021, **176**, 113893.
- 111 Y. Zhang, L. Zhang, W. Wang, Q. Deng, M. Liu, Z. Zhu, H. Liu, J. Ren and X. Qu, *Angew. Chem., Int. Ed.*, 2023, **62**, e202306395.
- 112 X. Zhang, Y. Liu, J. Dounghawee, L. J. Castellanos-García, K. N. Sikora, T. Jeon, R. Goswami, S. Fedeli, A. Gupta, R. Huang, C.-M. Hirschbiegel, R. Cao-Milán, P. K. D. Majhi, Y. A. Cicek, L. Liu, D. J. Jerry, R. W. Vachet and V. M. Rotello, *J. Controlled Release*, 2023, **357**, 31–39.
- 113 X. Zhang, S. Lin, R. Huang, A. Gupta, S. Fedeli, R. Cao-Milán, D. C. Luther, Y. Liu, M. Jiang, G. Li, B. Rondon, H. Wei and V. M. Rotello, *J. Am. Chem. Soc.*, 2022, **144**, 12893–12900.
- 114 Y. Wei, S. Wu, Z. Liu, J. Niu, Y. Zhou, J. Ren and X. Qu, *Mater. Today*, 2022, **56**, 16–28.
- 115 X. Zhang, Y. Liu, M. Jiang, J. A. Mas-Rosario, S. Fedeli, R. Cao-Milán, L. Liu, K. J. Winters, C.-M. Hirschbiegel, A. Nabawy, R. Huang, M. E. Farkas and V. M. Rotello, *Chem. Sci.*, 2024, **15**, 2486–2494.
- 116 W. Zou and D. R. Green, *Cell Metab.*, 2023, **35**, 1101–1113.
- 117 Y. Xiao, T.-J. Yu, Y. Xu, R. Ding, Y.-P. Wang, Y.-Z. Jiang and Z.-M. Shao, *Cell Metab.*, 2023, **35**, 1283–1303.
- 118 I. Elia and M. C. Haigis, *Nat. Metab.*, 2021, **3**, 21–32.
- 119 M. A. Shah and H. A. Rogoff, *Semin. Oncol.*, 2021, **48**, 238–245.
- 120 P. Poprac, K. Jomova, M. Simunkova, V. Kollar, C. J. Rhodes and M. Valko, *Trends Pharmacol. Sci.*, 2017, **38**, 592–607.
- 121 B. Kelly and E. L. Pearce, *Cell Metab.*, 2020, **32**, 154–175.
- 122 M. Zheng, W. Zhang, X. Chen, H. Guo, H. Wu, Y. Xu, Q. He, L. Ding and B. Yang, *Acta Pharm. Sin. B*, 2023, **13**, 1488–1497.
- 123 Z. Wang, Y. Zhang, E. Ju, Z. Liu, F. Cao, Z. Chen, J. Ren and X. Qu, *Nat. Commun.*, 2018, **9**, 3334.
- 124 H. Wang, Z. Gao, X. Liu, P. Agarwal, S. Zhao, D. W. Conroy, G. Ji, J. Yu, C. P. Jaronec, Z. Liu, X. Lu, X. Li and X. He, *Nat. Commun.*, 2018, **9**, 562.
- 125 M. Wang, D. Wang, Q. Chen, C. Li, Z. Li and J. Lin, *Small*, 2019, **15**, 1903895.
- 126 C. Chen, A. Li, P. Sun, J. Xu, W. Du, J. Zhang, Y. Liu, R. Zhang, S. Zhang, Z. Yang, C. Tang and X. Jiang, *J. Controlled Release*, 2020, **324**, 574–585.
- 127 Y. Feng, Z. Liao, H. Zhang, X. Xie, F. You, X. Liao, C. Wu, W. Zhang, H. Yang and Y. Liu, *Chem. Eng. J.*, 2023, **452**, 139506.
- 128 B. Xu, Y. Cui, W. Wang, S. Li, C. Lyu, S. Wang, W. Bao, H. Wang, M. Qin, Z. Liu, W. Wei and H. Liu, *Adv. Mater.*, 2020, **32**, 2003563.
- 129 H. He, Z. Fei, T. Guo, Y. Hou, D. Li, K. Wang, F. Ren, K. Fan, D. Zhou, C. Xie, C. Wang and X. Lu, *Biomaterials*, 2022, **280**, 121272.
- 130 N. Tao, L. Jiao, H. Li, L. Deng, W. Wang, S. Zhao, W. Chen, L. Chen, C. Zhu and Y. N. Liu, *ACS Nano*, 2023, **17**, 22844–22858.
- 131 L. Yao, M. M. Zhao, Q. W. Luo, Y. C. Zhang, T. T. Liu, Z. Yang, M. Liao, P. Tu and K. W. Zeng, *ACS Nano*, 2022, **16**, 9228–9239.
- 132 M. Wang, M. Chang, C. Li, Q. Chen, Z. Hou, B. Xing and J. Lin, *Adv. Mater.*, 2022, **34**, e2106010.
- 133 W.-F. Song, J.-Y. Zeng, P. Ji, Z.-Y. Han, Y.-X. Sun and X.-Z. Zhang, *Small*, 2023, **19**, 2301148.
- 134 W. Zhang, J. Liu, X. Li, Y. Zheng, L. Chen, D. Wang, M. F. Foda, Z. Ma, Y. Zhao and H. Han, *ACS Nano*, 2021, **15**, 19321–19333.
- 135 Y. Zou, B. Jin, H. Li, X. Wu, Y. Liu, H. Zhao, D. Zhong, L. Wang, W. Chen, M. Wen and Y. N. Liu, *ACS Nano*, 2022, **16**, 21491–21504.
- 136 H. Sies, V. V. Belousov, N. S. Chandel, M. J. Davies, D. P. Jones, G. E. Mann, M. P. Murphy, M. Yamamoto and C. Winterbourn, *Nat. Rev. Mol. Cell Biol.*, 2022, **23**, 499–515.
- 137 H. Sies and D. P. Jones, *Nat. Rev. Mol. Cell Biol.*, 2020, **21**, 363–383.
- 138 C. Lennicke and H. M. Cochemé, *Mol. Cell*, 2021, **81**, 3691–3707.
- 139 A. Erez and R. J. DeBerardinis, *Nat. Rev. Cancer*, 2015, **15**, 440–448.
- 140 Q. Zong, K. Wang, X. Xiao, M. Jiang, J. Li, Y. Yuan and J. Wang, *Biomaterials*, 2021, **276**, 121005.
- 141 J. Wan, X. Zhang, Z. Li, F. Mo, D. Tang, H. Xiao, J. Wang, G. Rong and T. Liu, *Adv. Healthcare Mater.*, 2023, **12**, e2202710.
- 142 C. Chen, X. Ni, S. Jia, Y. Liang, X. Wu, D. Kong and D. Ding, *Adv. Mater.*, 2019, **31**, 1904914.
- 143 J. Liu, R. Li and B. Yang, *ACS Cent. Sci.*, 2020, **6**, 2179–2195.
- 144 P. Yu, X. Zhang, N. Liu, L. Tang, C. Peng and X. Chen, *Signal Transduction Targeted Ther.*, 2021, **6**, 128.
- 145 Z. Li, B. Li, C. Yu, H. Wang and Q. Li, *Adv. Sci.*, 2023, **10**, 2206605.
- 146 E. C. Cheung and K. H. Vousden, *Nat. Rev. Cancer*, 2022, **22**, 280–297.
- 147 B. Niu, K. Liao, Y. Zhou, T. Wen, G. Quan, X. Pan and C. Wu, *Biomaterials*, 2021, **277**, 121110.
- 148 D. Tang, X. Chen, R. Kang and G. Kroemer, *Cell Res.*, 2021, **31**, 107–125.
- 149 S. Sun, J. Shen, J. Jiang, F. Wang and J. Min, *Signal Transduction Targeted Ther.*, 2023, **8**, 372.
- 150 X. Jiang, B. R. Stockwell and M. Conrad, *Nat. Rev. Mol. Cell Biol.*, 2021, **22**, 266–282.
- 151 D. Li and Y. Li, *Signal Transduction Targeted Ther.*, 2020, **5**, 108.





- 152 G. Lei, L. Zhuang and B. Gan, *Nat. Rev. Cancer*, 2022, **22**, 381–396.
- 153 X. Chen, R. Kang, G. Kroemer and D. Tang, *Nat. Rev. Clin. Oncol.*, 2021, **18**, 280–296.
- 154 C.-H. Chung, C.-Y. Lin, C.-Y. Chen, C.-W. Hsueh, Y.-W. Chang, C.-C. Wang, P.-Y. Chu, S.-K. Tai and M.-H. Yang, *Adv. Sci.*, 2023, **10**, 2204514.
- 155 K. Nekoueiian, M. Amiri, M. Sillanpää, F. Marken, R. Boukherroub and S. Szunerits, *Chem. Soc. Rev.*, 2019, **48**, 4281–4316.
- 156 A. Truskewycz, H. Yin, N. Halberg, D. T. H. Lai, A. S. Ball, V. K. Truong, A. M. Rybicka and I. Cole, *Small*, 2022, **18**, e2106342.
- 157 J. Muri and M. Kopf, *Nat. Rev. Immunol.*, 2021, **21**, 363–381.
- 158 J. Zhang, E. Ha, D. Li, S. He, L. Wang, S. Kuang and J. Hu, *J. Mater. Chem. B*, 2023, **11**, 4274–4286.
- 159 C. Liu, Y. Cao, Y. Cheng, D. Wang, T. Xu, L. Su, X. Zhang and H. Dong, *Nat. Commun.*, 2020, **11**, 1735.
- 160 S. Wu, P. Wang, J. Qin, Y. Pei and Y. Wang, *Adv. Funct. Mater.*, 2021, **31**, 2102160.
- 161 M. B. Gawande, A. Goswami, F.-X. Felpin, T. Asefa, X. Huang, R. Silva, X. Zou, R. Zboril and R. S. Varma, *Chem. Rev.*, 2016, **116**, 3722–3811.
- 162 Q. Chen, D. Yang, L. Yu, X. Jing and Y. Chen, *Mater. Horiz.*, 2020, **7**, 317–337.
- 163 X. Wang, X. Zhong, Z. Liu and L. Cheng, *Nano Today*, 2020, **35**, 100946.
- 164 Z. Vaseghi, A. Nematollahzadeh and O. Tavakoli, *Rev. Chem. Eng.*, 2018, **34**, 529–559.
- 165 H. Bahrololum, S. Nooraei, N. Javanshir, H. Tarrahimofrad, V. S. Mirbagheri, A. J. Easton and G. Ahmadian, *J. Nanobiotechnol.*, 2021, **19**, 86.
- 166 K. B. Narayanan and N. Sakthivel, *Adv. Colloid Interface Sci.*, 2010, **156**, 1–13.
- 167 X. Chen and F. Alonzo, *Proc. Natl. Acad. Sci. U. S. A.*, 2019, **116**, 3764–3773.
- 168 M. Chang, Z. Hou, M. Wang, C. Yang, R. Wang, F. Li, D. Liu, T. Peng, C. Li and J. Lin, *Angew. Chem., Int. Ed.*, 2021, **60**, 12971–12979.
- 169 J. Zhou, M. Li, Y. Hou, Z. Luo, Q. Chen, H. Cao, R. Huo, C. Xue, L. Sutrisno, L. Hao, Y. Cao, H. Ran, L. Lu, K. Li and K. Cai, *ACS Nano*, 2018, **12**, 2858–2872.
- 170 C. B. Thompson, K. H. Vousden, R. S. Johnson, W. H. Koppenol, H. Sies, Z. Lu, L. W. S. Finley, C. Frezza, J. Kim, Z. Hu and C. R. Bartman, *Nat. Metab.*, 2023, **5**, 1840–1843.
- 171 O. Warburg, *Science*, 1956, **123**, 309–314.
- 172 M. G. Vander Heiden, L. C. Cantley and C. B. Thompson, *Science*, 2009, **324**, 1029–1033.
- 173 W. H. Koppenol, P. L. Bounds and C. V. Dang, *Nat. Rev. Cancer*, 2011, **11**, 325–337.
- 174 N. Hay, *Nat. Rev. Cancer*, 2016, **16**, 635–649.
- 175 Y. Wang, Y. Wang, Y. Ren, Q. Zhang, P. Yi and C. Cheng, *Semin. Cancer Biol.*, 2022, **86**, 542–565.
- 176 H. Yamaguchi, J.-M. Hsu, W.-H. Yang and M.-C. Hung, *Nat. Rev. Clin. Oncol.*, 2022, **19**, 287–305.
- 177 C.-W. Li, S.-O. Lim, W. Xia, H.-H. Lee, L.-C. Chan, C.-W. Kuo, K.-H. Khoo, S.-S. Chang, J.-H. Cha, T. Kim, J. L. Hsu, Y. Wu, J.-M. Hsu, H. Yamaguchi, Q. Ding, Y. Wang, J. Yao, C.-C. Lee, H.-J. Wu, A. A. Sahin, J. P. Allison, D. Yu, G. N. Hortobagyi and M.-C. Hung, *Nat. Commun.*, 2016, **7**, 12632.
- 178 M. J. Watson, P. D. A. Vignali, S. J. Mullett, A. E. Overacre-Delgoffe, R. M. Peralta, S. Grebinoski, A. V. Menk, N. L. Rittenhouse, K. DePeaux, R. D. Whetstone, D. A. A. Vignali, T. W. Hand, A. C. Poholek, B. M. Morrison, J. D. Rothstein, S. G. Wendell and G. M. Delgoffe, *Nature*, 2021, **591**, 645–651.
- 179 D. Guo, Y. Tong, X. Jiang, Y. Meng, H. Jiang, L. Du, Q. Wu, S. Li, S. Luo, M. Li, L. Xiao, H. He, X. He, Q. Yu, J. Fang and Z. Lu, *Cell Metab.*, 2022, **34**, 1312–1324.
- 180 N. Patsoukis, K. Bardhan, P. Chatterjee, D. Sari, B. Liu, L. N. Bell, E. D. Karoly, G. J. Freeman, V. Petkova, P. Seth, L. Li and V. A. Boussiotis, *Nat. Commun.*, 2015, **6**, 6692.
- 181 Y. Gao, N. T. Nihira, X. Bu, C. Chu, J. Zhang, A. Kolodziejczyk, Y. Fan, N. T. Chan, L. Ma, J. Liu, D. Wang, X. Dai, H. Liu, M. Ono, A. Nakanishi, H. Inuzuka, B. J. North, Y. H. Huang, S. Sharma, Y. Geng, W. Xu, X. S. Liu, L. Li, Y. Miki, P. Sicinski, G. J. Freeman and W. Wei, *Nat. Cell Biol.*, 2020, **22**, 1064–1075.
- 182 S. Zhang, Y. Zhang, Y. Feng, J. Wu, Y. Hu, L. Lin, C. Xu, J. Chen, Z. Tang, H. Tian and X. Chen, *Adv. Mater.*, 2022, **34**, e2206851.
- 183 S. Wu, L. Xu, C. He, P. Wang, J. Qin, F. Guo and Y. Wang, *Adv. Sci.*, 2023, **10**, e2300686.
- 184 Y. Xie, M. Wang, Y. Qian, L. Li, Q. Sun, M. Gao and C. Li, *Small*, 2023, 2303596.
- 185 W. Wang, L. Zhang, Z. Liu, Y. Zhang, J. Zhu, M. Liu, J. Ren and X. Qu, *Adv. Mater.*, 2023, **35**, 2211866.
- 186 C. E. Hagberg, *Signal Transduction Targeted Ther.*, 2023, **8**, 314.
- 187 B. I. Reinfeld, M. Z. Madden, M. M. Wolf, A. Chytil, J. E. Bader, A. R. Patterson, A. Sugiura, A. S. Cohen, A. Ali, B. T. Do, A. Muir, C. A. Lewis, R. A. Hongo, K. L. Young, R. E. Brown, V. M. Todd, T. Huffstater, A. Abraham, R. T. O'Neil, M. H. Wilson, F. Xin, M. N. Tantawy, W. D. Merryman, R. W. Johnson, C. S. Williams, E. F. Mason, F. M. Mason, K. E. Beckermann, M. G. Vander Heiden, H. C. Manning, J. C. Rathmell and W. K. Rathmell, *Nature*, 2021, **593**, 282–288.
- 188 Q. Cheng, X. L. Shi, Q. L. Li, L. Wang and Z. Wang, *Adv. Sci.*, 2024, **11**, e2305662.
- 189 S. Chen, A. F. U. H. Saeed, Q. Liu, Q. Jiang, H. Xu, G. G. Xiao, L. Rao and Y. Duo, *Signal Transduction Targeted Ther.*, 2023, **8**, 207.
- 190 B. Kelly and L. A. J. O'Neill, *Cell Res.*, 2015, **25**, 771–784.
- 191 J. Ling, Y. Chang, Z. Yuan, Q. Chen, L. He and T. Chen, *ACS Appl. Mater. Interfaces*, 2022, **14**, 27651–27665.
- 192 M. Singh, J. Afonso, D. Sharma, R. Gupta, V. Kumar, R. Rani, F. Baltazar and V. Kumar, *Semin. Cancer Biol.*, 2023, **90**, 1–14.



- 193 X. Sun, S. Yao, Q. Zhao, Y. Zhao and J. Cheng, *Int. J. Electrochem. Sci.*, 2020, **15**, 651–665.
- 194 D. Benjamin, D. Robay, S. K. Hindupur, J. Pohlmann, M. Colombi, M. Y. El-Shemerly, S.-M. Maira, C. Moroni, H. A. Lane and M. N. Hall, *Cell Rep.*, 2018, **25**, 3047–3058.
- 195 Z. Dong, C. Wang, Y. Gong, Y. Zhang, Q. Fan, Y. Hao, Q. Li, Y. Wu, X. Zhong, K. Yang, L. Feng and Z. Liu, *ACS Nano*, 2022, **16**, 13884–13899.
- 196 K. Xu, N. Yin, M. Peng, E. G. Stamatiades, A. Shyu, P. Li, X. Zhang, M. H. Do, Z. Wang, K. J. Capistrano, C. Chou, A. G. Levine, A. Y. Rudensky and M. O. Li, *Science*, 2021, **371**, 405–410.
- 197 S. Chen, Y. Xu, W. Zhuo and L. Zhang, *Cancer Lett.*, 2024, **590**, 216837.
- 198 L. Ippolito, A. Morandi, E. Giannoni and P. Chiarugi, *Trends Biochem. Sci.*, 2019, **44**, 153–166.
- 199 B. Faubert, K. Y. Li, L. Cai, C. T. Hensley, J. Kim, L. G. Zacharias, C. Yang, Q. N. Do, S. Doucette, D. Burguete, H. Li, G. Huet, Q. Yuan, T. Wigal, Y. Butt, M. Ni, J. Torrealba, D. Oliver, R. E. Lenkinski, C. R. Malloy, J. W. Wachsmann, J. D. Young, K. Kernstine and R. J. DeBerardinis, *Cell*, 2017, **171**, 358–371.
- 200 S. Hui, J. M. Ghergurovich, R. J. Morscher, C. Jang, X. Teng, W. Lu, L. A. Esparza, T. Reya, Z. Le, J. Yanxiang Guo, E. White and J. D. Rabinowitz, *Nature*, 2017, **551**, 115–118.
- 201 Y. Xie, M. Wang, L. Qiao, Y. Qian, W. Xu, Q. Sun, S. Luo and C. Li, *Small Methods*, 2023, 2300945.
- 202 H. Lemos, L. Huang, G. C. Prendergast and A. L. Mellor, *Nat. Rev. Cancer*, 2019, **19**, 162–175.
- 203 C. Han, M. Ge, P.-C. Ho and L. Zhang, *Cancer Immunol. Res.*, 2021, **9**, 1373–1382.
- 204 Y. Zheng, Y. Yao, T. Ge, S. Ge, R. Jia, X. Song and A. Zhuang, *J. Exp. Clin. Cancer Res.*, 2023, **42**, 291.
- 205 M. Liu, X. Wang, L. Wang, X. Ma, Z. Gong, S. Zhang and Y. Li, *J. Hematol. Oncol.*, 2018, **11**, 100.
- 206 M. Platten, E. A. A. Nollen, U. F. Röhrig, F. Fallarino and C. A. Opitz, *Nat. Rev. Drug Discovery*, 2019, **18**, 379–401.
- 207 V. Sunil, J. H. Teoh, B. C. Mohan, A. Mozhi and C. H. Wang, *J. Controlled Release*, 2022, **350**, 215–227.
- 208 Y. Bian, W. Li, D. M. Kremer, P. Sajjakulnukit, S. Li, J. Crespo, Z. C. Nwosu, L. Zhang, A. Czerwonka, A. Pawłowska, H. Xia, J. Li, P. Liao, J. Yu, L. Vatan, W. Szeliga, S. Wei, S. Grove, J. R. Liu, K. McLean, M. Cieslik, A. M. Chinnaiyan, W. Zgodziński, G. Wallner, I. Wertel, K. Okla, I. Kryczek, C. A. Lyssiotis and W. Zou, *Nature*, 2020, **585**, 277–282.
- 209 Z. Wang, L. Y. Yip, J. H. J. Lee, Z. Wu, H. Y. Chew, P. K. W. Chong, C. C. Teo, H. Y.-K. Ang, K. L. E. Peh, J. Yuan, S. Ma, L. S. K. Choo, N. Basri, X. Jiang, Q. Yu, A. M. Hillmer, W. T. Lim, T. K. H. Lim, A. Takano, E. H. Tan, D. S. W. Tan, Y. S. Ho, B. Lim and W. L. Tam, *Nat. Med.*, 2019, **25**, 825–837.
- 210 S. M. Sanderson, X. Gao, Z. Dai and J. W. Locasale, *Nat. Rev. Cancer*, 2019, **19**, 625–637.
- 211 M. H. Hung, J. S. Lee, C. Ma, L. P. Diggs, S. Heinrich, C. W. Chang, L. Ma, M. Forgues, A. Budhu, J. Chaisaingmongkol, M. Ruchirawat, E. Ruppin, T. F. Greten and X. W. Wang, *Nat. Commun.*, 2021, **12**, 1455.
- 212 D. Wang and R. N. Dubois, *Nat. Rev. Cancer*, 2010, **10**, 181–193.
- 213 T. M. Loo, F. Kamachi, Y. Watanabe, S. Yoshimoto, H. Kanda, Y. Arai, Y. Nakajima-Takagi, A. Iwama, T. Koga, Y. Sugimoto, T. Ozawa, M. Nakamura, M. Kumagai, K. Watashi, M. M. Taketo, T. Aoki, S. Narumiya, M. Oshima, M. Arita, E. Hara and N. Ohtani, *Cancer Discovery*, 2017, **7**, 522–538.
- 214 G. Yan, H. Zhao, Q. Zhang, Y. Zhou, L. Wu, J. Lei, X. Wang, J. Zhang, X. Zhang, L. Zheng, G. Du, W. Xiao, B. Tang, H. Miao and Y. Li, *Cancer Res.*, 2018, **78**, 5586–5599.
- 215 D. I. Albu, Z. Wang, K. C. Huang, J. Wu, N. Twine, S. Leacu, C. Ingersoll, L. Parent, W. Lee, D. Liu, R. Wright-Michaud, N. Kumar, G. Kuznetsov, Q. Chen, W. Zheng, K. Nomoto, M. Woodall-Jappe and X. Bao, *Oncoimmunology*, 2017, **6**, 1338239.
- 216 S. Zelenay, A. G. van der Veen, J. P. Böttcher, K. J. Snelgrove, N. Rogers, S. E. Acton, P. Chakravarty, M. R. Girotti, R. Marais, S. A. Quezada, E. Sahai and C. Reis e Sousa, *Cell*, 2015, **162**, 1257–1270.
- 217 K. Sun, J. Hu, X. Meng, Y. Lei, X. Zhang, Z. Lu, L. Zhang and Z. Wang, *Small*, 2021, **17**, 2101897.
- 218 Y. Liu, R. Niu, R. Deng, S. Song, Y. Wang and H. Zhang, *J. Am. Chem. Soc.*, 2023, **145**, 8965–8978.
- 219 G. Luo, X. Li, J. Lin, G. Ge, J. Fang, W. Song, G. G. Xiao, B. Zhang, X. Peng, Y. Duo and B. Z. Tang, *ACS Nano*, 2023, **17**, 15449–15465.
- 220 L. Qiao, G. Zhu, T. Jiang, Y. Qian, Q. Sun, G. Zhao, H. Gao and C. Li, *Adv. Mater.*, 2023, e2308241.
- 221 D. Li and Y. Li, *Signal Transduction Targeted Ther.*, 2020, **5**, 108.
- 222 P. Liao, W. Wang, W. Wang, I. Kryczek, X. Li, Y. Bian, A. Sell, S. Wei, S. Grove, J. K. Johnson, P. D. Kennedy, M. Gijón, Y. M. Shah and W. Zou, *Cancer Cell*, 2022, **40**, 365–378.
- 223 H.-L. Zhang, B.-X. Hu, Z.-L. Li, T. Du, J.-L. Shan, Z.-P. Ye, X.-D. Peng, X. Li, Y. Huang, X.-Y. Zhu, Y.-H. Chen, G.-K. Feng, D. Yang, R. Deng and X.-F. Zhu, *Nat. Cell Biol.*, 2022, **24**, 88–98.
- 224 B. Gan, *Signal Transduction Targeted Ther*, 2022, **7**, 128.
- 225 S. Doll, B. Proneth, Y. Y. Tyurina, E. Panzilius, S. Kobayashi, I. Ingold, M. Irmiler, J. Beckers, M. Aichler, A. Walch, H. Prokisch, D. Trümbach, G. Mao, F. Qu, H. Bayir, J. Füllekrug, C. H. Scheel, W. Wurst, J. A. Schick, V. E. Kagan, J. P. F. Angeli and M. Conrad, *Nat. Chem. Biol.*, 2017, **13**, 91–98.
- 226 L. Xu, M. Peng, T. Gao, D. Wang, X. Lian, H. Sun, J. Shi, Y. Wang and P. Wang, *Adv. Sci.*, 2023, 2306203.
- 227 H. Hu, Q. Xu, Z. Mo, X. Hu, Q. He, Z. Zhang and Z. Xu, *J. Nanobiotechnol.*, 2022, **20**, 457.
- 228 H. Lei, G. Hou, M. Chen, J. Ji and L. Cheng, *Nano Today*, 2023, **53**, 102033.



- 229 G. Li, W. Ma, Y. Yang, C. Zhong, H. Huang, D. Ouyang, Y. He, W. Tian, J. Lin and Z. Lin, *ACS Appl. Mater. Interfaces*, 2021, **13**, 49482–49489.
- 230 C. Giorgi, S. Marchi and P. Pinton, *Nat. Rev. Mol. Cell Biol.*, 2018, **19**, 713–730.
- 231 M. Lv, M. Chen, R. Zhang, W. Zhang, C. Wang, Y. Zhang, X. Wei, Y. Guan, J. Liu, K. Feng, M. Jing, X. Wang, Y.-C. Liu, Q. Mei, W. Han and Z. Jiang, *Cell Res.*, 2020, **30**, 966–979.
- 232 P. Tsvetkov, S. Coy, B. Petrova, M. Dreishpoon, A. Verma, M. Abdusamad, J. Rossen, L. Joesch-Cohen, R. Humeidi, R. D. Spangler, J. K. Eaton, E. Frenkel, M. Kocak, S. M. Corsello, S. Lutsenko, N. Kanarek, S. Santagata and T. R. Golub, *Science*, 2022, **375**, 1254–1261.
- 233 E. J. Ge, A. I. Bush, A. Casini, P. A. Cobine, J. R. Cross, G. M. DeNicola, Q. P. Dou, K. J. Franz, V. M. Gohil, S. Gupta, S. G. Kaler, S. Lutsenko, V. Mittal, M. J. Petris, R. Polishchuk, M. Ralle, M. L. Schilsky, N. K. Tonks, L. T. Vahdat, L. Van Aelst, D. Xi, P. Yuan, D. C. Brady and C. J. Chang, *Nat. Rev. Cancer*, 2022, **22**, 102–113.
- 234 N. Xie, L. Zhang, W. Gao, C. Huang, P. E. Huber, X. Zhou, C. Li, G. Shen and B. Zou, *Signal Transduction Targeted Ther.*, 2020, **5**, 227.
- 235 S. Liu, S. Fu, G. Wang, Y. Cao, L. Li, X. Li, J. Yang, N. Li, Y. Shan, Y. Cao, Y. Ma, M. Dong, Q. Liu and H. Jiang, *Cell Metab.*, 2021, **33**, 1974–1987.
- 236 L. E. Navas and A. Carnero, *Signal Transduction Targeted Ther.*, 2021, **6**, 2.
- 237 X. Yuan, L. Wang, M. Hu, L. Zhang, H. Chen, D. Zhang, Z. Wang, T. Li, M. Zhong, L. Xu, D. Wang, Y. Liu and W. Tan, *Angew. Chem., Int. Ed.*, 2021, **60**, 20943–20951.
- 238 Y. Wu, W. Xu, L. Jiao, Y. Tang, Y. Chen, W. Gu and C. Zhu, *Mater. Today*, 2022, **52**, 327–347.
- 239 D. Jana, B. He, Y. Chen, J. Liu and Y. Zhao, *Adv. Mater.*, 2022, 2206401.
- 240 T. N. Seyfried and L. C. Huysentruyt, *Crit. Rev. Oncog.*, 2013, **18**, 43–73.
- 241 S. Cai, J. Liu, J. Ding, Z. Fu, H. Li, Y. Xiong, Z. Lian, R. Yang and C. Chen, *Angew. Chem., Int. Ed.*, 2022, **61**, e202204502.
- 242 S. Zhu, T. Zhang, L. Zheng, H. Liu, W. Song, D. Liu, Z. Li and C. X. Pan, *J. Hematol. Oncol.*, 2021, **14**, 156.
- 243 J. Yi, L. Liu, W. Gao, J. Zeng, Y. Chen, E. Pang, M. Lan and C. Yu, *J. Mater. Chem. B*, 2024, **12**, 6285–6304.
- 244 X. Li, J. F. Lovell, J. Yoon and X. Chen, *Nat. Rev. Clin. Oncol.*, 2020, **17**, 657–674.
- 245 S. Wang, Z. Wang, Z. Li, X. Zhang, H. Zhang, T. Zhang, X. Meng, F. Sheng and Y. Hou, *Sci. Adv.*, 2022, **8**, eabn3883.
- 246 W. Qin, J. Huang, C. Yang, Q. Yue, S. Chen, M. Wang, S. Gao, X. Zhou, X. Yang and Y. Zhang, *Adv. Funct. Mater.*, 2023, **33**, 2209748.
- 247 M. Wang, M. Chang, P. Zheng, Q. Sun, G. Wang, J. Lin and C. Li, *Adv. Sci.*, 2022, **9**, 2202332.
- 248 C. Hu, R. Man, H. Li, M. Xia, Z. Yu and B. Tang, *Anal. Chem.*, 2023, **95**, 13575–13585.
- 249 X. Cai, R. Liu, H. Yan, L. Jiao, M. Sha, Y. Chen, S. Rong, Z. Liu, L. Deng, L. Shen and C. Zhu, *Adv. Healthcare Mater.*, 2023, **12**, 2300516.
- 250 R. Wang, M. Qiu, L. Zhang, M. Sui, L. Xiao, Q. Yu, C. Ye, S. Chen and X. Zhou, *Adv. Mater.*, 2023, e2306748.
- 251 Y.-C. Chin, L.-X. Yang, F.-T. Hsu, C.-W. Hsu, T.-W. Chang, H.-Y. Chen, L. Y.-C. Chen, Z. C. Chia, C.-H. Hung, W.-C. Su, Y.-C. Chiu, C.-C. Huang and M.-Y. Liao, *J. Nanobiotechnol.*, 2022, **20**, 373.
- 252 A. Zhang, A. Gao, C. Zhou, C. Xue, Q. Zhang, J. M. Fuente and D. Cui, *Adv. Mater.*, 2023, **35**, 2303722.
- 253 Y. Liu, P. Bhattarai, Z. Dai and X. Chen, *Chem. Soc. Rev.*, 2019, **48**, 2053–2108.
- 254 Z. M. Tang, H. L. Zhang, Y. Y. Liu, D. L. Ni, H. Zhang, J. W. Zhang, Z. W. Yao, M. Y. He, J. L. Shi and W. B. Bu, *Adv. Mater.*, 2017, **29**, 1701683.
- 255 L. G. N. de Almeida, H. Thode, Y. Eslambolchi, S. Chopra, D. Young, S. Gill, L. Devel and A. Dufour, *Pharmacol. Res.*, 2022, **74**, 712–768.
- 256 C. Yang, M. R. Younis, J. Zhang, J. Qu, J. Lin and P. Huang, *Small*, 2020, **16**, 2001518.
- 257 G. Gao, Y.-W. Jiang, Y. Guo, H.-R. Jia, X. Cheng, Y. Deng, X.-W. Yu, Y.-X. Zhu, H.-Y. Guo, W. Sun, X. Liu, J. Zhao, S. Yang, Z.-W. Yu, F. M. S. Raya, G. Liang and F.-G. Wu, *Adv. Funct. Mater.*, 2020, **30**, 1909391.
- 258 W. H. Chen, G. F. Luo, Q. Lei, S. Hong, W. X. Qiu, L. H. Liu, S. X. Cheng and X. Z. Zhang, *ACS Nano*, 2017, **11**, 1419–1431.
- 259 S. Nomura, Y. Morimoto, H. Tsujimoto, M. Arake, M. Harada, D. Saitoh, I. Hara, E. Ozeki, A. Satoh, E. Takayama, K. Hase, Y. Kishi and H. Ueno, *Sci. Rep.*, 2020, **10**, 9765.
- 260 T. Wang, D. Wang, H. Yu, B. Feng, F. Zhou, H. Zhang, L. Zhou, S. Jiao and Y. Li, *Nat. Commun.*, 2018, **9**, 1532.
- 261 J. A. Mertz, A. R. Conery, B. M. Bryant, P. Sandy, S. Balasubramanian, D. A. Mele, L. Bergeron and R. J. Sims, *Proc. Natl. Acad. Sci. U. S. A.*, 2011, **108**, 16669–16674.
- 262 J. Wang, Z. Liu, Z. Wang, S. Wang, Z. Chen, Z. Li, M. Zhang, J. Zou, B. Dong, J. Gao and L. Shen, *Cancer Lett.*, 2018, **419**, 64–74.
- 263 F. Zhou, J. Gao, Y. Tang, Z. Zou, S. Jiao, Z. Zhou, H. Xu, Z. P. Xu, H. Yu and Z. Xu, *Adv. Mater.*, 2021, **33**, 2102668.
- 264 S. C. Casey, L. Tong, Y. Li, R. Do, S. Walz, K. N. Fitzgerald, A. M. Gouw, V. Baylot, I. Gütgemann, M. Eilers and D. W. Felsner, *Science*, 2016, **352**, 227–231.
- 265 Z. Liu, Z. Xie, W. Li, X. Wu, X. Jiang, G. Li, L. Cao, D. Zhang, Q. Wang, P. Xue and H. Zhang, *J. Nanobiotechnol.*, 2021, **19**, 160.
- 266 S. Dong, Y. Dong, T. Jia, S. Liu, J. Liu, D. Yang, F. He, S. Gai, P. Yang and J. Lin, *Adv. Mater.*, 2020, **32**, 2002439.
- 267 W. Shen, P. Pei, C. Zhang, J. Li, X. Han, T. Liu, X. Shi, Z. Su, G. Han, L. Hu and K. Yang, *ACS Nano*, 2023, **17**, 23998–24011.
- 268 J. Tang, X. Zhang, L. Cheng, Y. Liu, Y. Chen, Z. Jiang and J. Liu, *Bioact. Mater.*, 2022, **15**, 355–371.
- 269 S. Fu, R. Yang, J. Ren, J. Liu, L. Zhang, Z. Xu, Y. Kang and P. Xue, *ACS Nano*, 2021, **15**, 11953–11969.





- 270 Y. Li, J. Huang, H. Yu, Y. Zhao, Z. Xu, Y. Kang and P. Xue, *Small*, 2022, **18**, 2203080.
- 271 H. Li, X. Yang, Z. Wang, W. She, Y. Liu, L. Huang and P. Jiang, *ACS Nano*, 2023, **17**, 11749–11763.
- 272 L. L. Feng, S. L. Gai, Y. L. Dai, F. He, C. Q. Sun, P. P. Yang, R. C. Lv, N. Niu, G. H. An and J. Lin, *Chem. Mater.*, 2018, **30**, 526–539.
- 273 Z. Zhou, J. Huang, Z. Zhang, L. Zhang, Y. Cao, Z. Xu, Y. Kang and P. Xue, *Chem. Eng. J.*, 2022, **435**, 135085.
- 274 N. Tao, H. Li, L. Deng, S. Zhao, J. Ouyang, M. Wen, W. Chen, K. Zeng, C. Wei and Y. N. Liu, *ACS Nano*, 2022, **16**, 485–501.
- 275 C. H. June, R. S. O'Connor, O. U. Kawalekar, S. Ghassemi and M. C. Milone, *Science*, 2018, **359**, 1361–1365.
- 276 H. E. Barker, J. T. Paget, A. A. Khan and K. J. Harrington, *Nat. Rev. Cancer*, 2015, **15**, 409–425.
- 277 L. Wu, F. Bao, L. Li, X. Yin and Z. Hua, *Adv. Drug Delivery Rev.*, 2022, **187**, 114363.
- 278 S.-R. Kang, D.-H. Nguyen, S. W. Yoo and J.-J. Min, *Adv. Drug Delivery Rev.*, 2022, **181**, 114085.
- 279 H. Li, P. Pei, Q. He, X. Dong, C. Zhang, W. Shen, H. Chen, L. Hu, Y. Tao and K. Yang, *Adv. Mater.*, 2023, 2309332.
- 280 T. Li, Y. Zhang, J. Zhu, F. Zhang, A. A. Xu, T. Zhou, Y. Li, M. Liu, H. Ke, T. Yang, Y. A. Tang, J. Tao, L. Miao, Y. Deng and H. Chen, *Adv. Mater.*, 2023, **35**, 2210201.
- 281 J.-Y. Li, Y.-P. Chen, Y.-Q. Li, N. Liu and J. Ma, *Mol. Cancer*, 2021, **20**, 27.
- 282 J. Wang, L. Fang, P. Li, L. Ma, W. Na, C. Cheng, Y. Gu and D. Deng, *Nano-Micro Lett.*, 2019, **11**, 74.
- 283 L. A. Emens, *Clin. Cancer Res.*, 2018, **24**, 511–520.
- 284 L. Chen, S. F. Zhou, L. Su and J. Song, *ACS Nano*, 2019, **13**, 10887–10917.
- 285 J. Li, J. Huang, Y. Ao, S. Li, Y. Miao, Z. Yu, L. Zhu, X. Lan, Y. Zhu, Y. Zhang and X. Yang, *ACS Appl. Mater. Interfaces*, 2018, **10**, 22985–22996.
- 286 X. Wang, N. Ye, C. Xu, C. Xiao, Z. Zhang, Q. Deng, S. Li, J. Li, Z. Li and X. Yang, *Nano Today*, 2022, **44**, 101458.
- 287 P. Li, Y. Yao, X. Chen, C. Song, M. Wu, J. Huang, D. Wang, X. Li, B. Luo, X. Yang and J. Hu, *Chem. Eng. J.*, 2023, **474**, 145738.
- 288 Y. Zhang, Z. Zhou, Z. Gao, X. Li, X. Wang, Z. Zheng, J. Deng, D. Liu, T. Peng and Z. Hou, *Chem. Eng. J.*, 2023, **474**, 145677.
- 289 M. Lyu, M. Luo, J. Li, O. U. Akakuru, X. Fan, Z. Cao, K. Fan and W. Jiang, *Adv. Funct. Mater.*, 2023, **33**, 2306930.
- 290 S. Wang, L. B. Vong, Z. Heger, Y. Zhou, X. Liang, V. Adam and N. Li, *Nano Today*, 2023, **49**, 101769.
- 291 S. Li, R. Liu, X. Jiang, Y. Qiu, X. Song, G. Huang, N. Fu, L. Lin, J. Song, X. Chen and H. Yang, *ACS Nano*, 2019, **13**, 2103–2113.
- 292 W. Sun, C. Zhu, J. Song, S. C. Ji, B. P. Jiang, H. Liang and X. C. Shen, *Adv. Healthcare Mater.*, 2023, **12**, 2300385.
- 293 X. Chen, Y. Yang, G. Ye, S. Liu and J. Liu, *Small*, 2023, **19**, 2207823.
- 294 Y. Cao, J. Zheng, H. Wan, Y. Sun, S. Fu, S. Liu, B. He, G. Cai, Y. Cao, H. Huang, Q. Li, Y. Ma, S. Chen, F. Wang and H. Jiang, *EMBO J.*, 2023, **42**, e113033.
- 295 Z. Zhou, Z. Gao, W. Chen, X. Wang, Z. Chen, Z. Zheng, Q. Chen, M. Tan, D. Liu, Y. Zhang and Z. Hou, *Acta Biomater.*, 2022, **151**, 600–612.
- 296 Y. Li, J. Dang, Q. Liang and L. Yin, *Biomaterials*, 2019, **209**, 138–151.
- 297 P. Zhao, Y. Han, H. Nguyen, E. Corey and X. Gao, *Adv. Healthcare Mater.*, 2022, **11**, 2101010.
- 298 W. Ying, Y. Zhang, W. Gao, X. Cai, G. Wang, X. Wu, L. Chen, Z. Meng, Y. Zheng, B. Hu and X. Lin, *ACS Nano*, 2020, **14**, 9662–9674.
- 299 J.-u Lee, W. Shin, Y. Lim, J. Kim, W. R. Kim, H. Kim, J.-H. Lee and J. Cheon, *Nat. Mater.*, 2021, **20**, 1029–1036.
- 300 E. S. Ali and I. Ben-Sahra, *Trends Cell Biol.*, 2023, **33**, 950–966.

